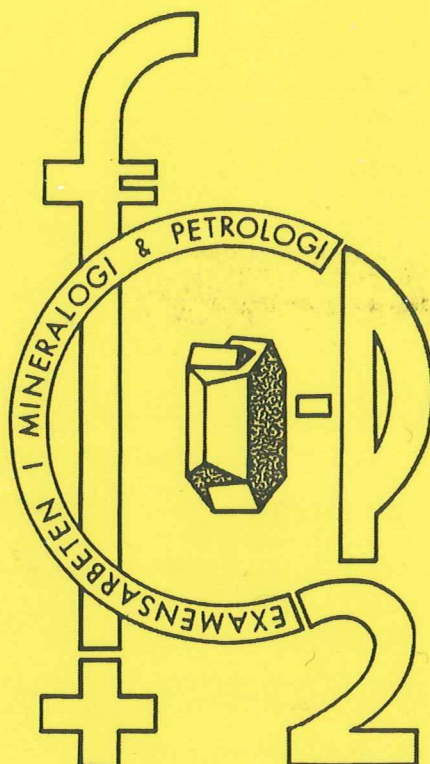


EXAMENSARBETE I GEOLOGI VID LUNDS UNIVERSITET

LUNDS UNIVERSITET
GEOBIBLIOTEKET
PERIODICA

Mineralogi och Petrologi



The geology of the Portobello Peninsula; proposal of
a saturated to oversaturated lineage within the
Dunedin Volcano, New Zealand

Stefan Olsson

Lunds univ. Geobiblioteket



15000

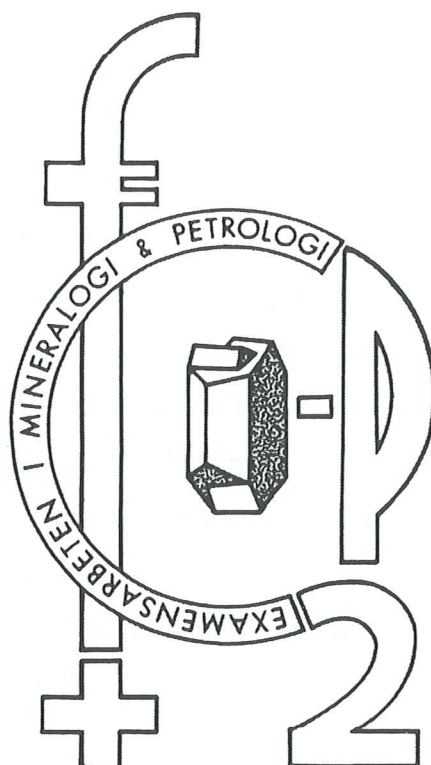
600693641

Examensarbete, 20 p
Institutionen, Lunds Universitet

Nr 148

EXAMENSARBETE I GEOLOGI VID LUNDS UNIVERSITET

Mineralogi och Petrologi



**The geology of the Portobello Peninsula; proposal of
a saturated to oversaturated lineage within the
Dunedin Volcano, New Zealand**

Stefan Olsson

The geology of the Portobello Peninsula; proposal of a saturated to oversaturated lineage within the Dunedin Volcano, New Zealand.

Stefan Olsson

Olsson, S. 2002: The geology of the Portobello Peninsula; proposal of a saturated to oversaturated lineage within the Dunedin Volcano, New Zealand. Master thesis at Lund University, Bedrock Geology, No. 148, p. 105.

The Portobello Peninsula is made up by volcanic sediments, lava flows and numerous dikes. Deposition of sediments and lava flows is thought to be early in the evolution of the Dunedin Volcano.

The lava flows of Portobello Peninsula are silica saturated, belonging to a lineage differing from the two major lineages previously inferred to exist in the volcano (Coombs and Wilkinson, 1969). This new lineage comprises the rock series basalt-potassic trachybasalt-shoshonite-latitude-quartz trachyte following the TAS classification scheme of basaltic rocks by Le Bas et al. (1986). The lineage is mainly separated from the other two by the presence of normative hypersthene and/or quartz. The rocks of intermediate composition also have a lower total alkali content than its undersaturated equivalents.

Oversaturation in magmas from the Dunedin volcano is caused by a process involving fractionation of kaersutite combined with long residence times in the lower crust/ upper mantle.

The potassic nature of the oversaturated lineage originates from crustal/magma interactions as the magmas ascended through the crust.

The possible involvement of kaersutite in the saturated to oversaturated lineage, has implications for magma genesis in the Dunedin Volcano. A model comprising variations in degree of partial melting, fractionation of kaersutite and crustal contamination, can possibly explain the wide range of geochemical behaviour documented within the volcano.

The dikes on Portobello Peninsula are divided into two assemblages with a clear age difference between them. The dike orientations suggest that the extensional tectonic stresses have rotated clockwise from a WSW-ENE orientation into a NW-SE orientation during the later parts of volcanic activity in the area.

Stefan Olsson, Department of Geology, Bedrock Geology, Sölvegatan 13, S-223 62 LUND, Sweden.

Geologin på Portobello halvön; Förslag om en mättad till övermättad bergartsserie i Dunedin Vulkanen.

Stefan Olsson

Olsson, S. 2002: Geologin på Portobello halvön; Förslag om en mättad till övermättad bergartsserie i Dunedin Vulkanen. Examensarbete vid Lunds Universitet, Berggrundsgeologi. 20 poäng, Nr 148, s. 105

Portobello Peninsula utgörs av vulkanoklastiska sediment, lavar och ett stort antal gångar. Depositionen av både sediment och överliggande lavar tros tillhöra de tidigaste stadiet i utvecklingen av Dunedin Volcano.

Lavaflödena i det studerade området är alla mättade till övermättade, och tillhör en bergartsserie skild från de två sedan tidigare kända, undermättade bergartsserierna (Coombs and Wilkinson, 1969). Denna nya bergartsserie innehåller bergarterna basalt-kalitrachybasalt-shoshonit-latit-kvarts trachyt, enligt basalt klassificering (total alkali och kiselhalt) efter Le Bas et al. (1986). Denna bergartsserie skiljer sig från de övriga två främst genom normativ hypersten samt i de mer differentierade bergarterna även normativ kvarts. Dessa mer differentierade bergarter har också en lägre alkali halt jämfört med de undermättade bergarterna.

Mätning till övermätning i Dunedin Volcano kan möjligtvis förklaras genom en process inbegripande differentiering av amfibolen kaersutit kombinerat av lång residenstid i lägre delarna av skorpan eller övre delarna av manteln. Den kaliumrika karaktären hos denna bergartsserie härstammar från kemiska reaktioner mellan magman och sidoberget.

Den möjliga inblandningen av kaersutit i den mättade till övermättade bergartsserien har implikationer för all magma genes i Dunedin Volcano. En modell som består av olika grader av partiell uppsmältning, fraktionering av kaersutit samt kontamination från sidoberget kan möjligtvis förklara den stora variation i geokemisk karaktär som finns dokumenterat i vulkanen.

Gångarna i det undersökta området är av minst två olika åldrar. Orienteringen av dessa indikerar att den extensionella tektoniska stressen har roterat medurs, från en WSW-ENE till en NW-SE riktning under de senare delarna av den vulkaniska aktiviteten i området.

Stefan Olsson, Geologiska Institutionen, Berggrundsgeologi, Sölvegatan 13; 223 62 LUND.

Populärvetenskaplig sammanfattning:

Det var en gång...historien om en vulkan

The Dunedin Volcano är belägen utmed östkusten på Nya Zeelands södra ö. Stora delar av både östkusten och de centrala delarna har under de senaste 40 miljoner åren upplevt perioder med intra platt vulkanism orsakad av en temperatur anomali i övre manteln under både Nya Zeelands Sydö och delar av havet öster om. Vulkanen vid Dunedin är tillsammans med en vulkan på Banks Peninsula (utanför Christchurch) de största enskilda resultaten av den vulkaniska aktiviteten. Båda vulkanerna var aktiva under samma tidsperiod från 13 till 10 miljoner år sedan. Avslutandet av vulkanismen tros vara orsakad av en förändring i den tektoniska stressen, från en extensiv/transensionell till en mer kompressiv. The Southern Alps är resultatet av det kompressiva stresstillstånd som rått i denna region under de senaste 10 miljoner åren.

Dunedin Volcano är resterna av en basaltisk vulkan med förhållandevis låg relief. Höjd skillnaden mellan högsta punkten och vattenytan är idag 700 meter och den var troligtvis inte mycket större då vulkanen var aktiv. Vulkanen var aktiv under mer än tre miljoner år men var speciellt aktiv under fyra olika perioder. Under dessa perioder byggdes det mesta av de avlagringar som idag kringligger staden Dunedin.

Vulkanism har förutsättningar att skapas då den geotermala gradienten korsar mantelns trycksmältpunkt, vilket orsakar partiell uppsmältning av manteln. Smälta är generellt sett lättare and motsvarande fast berg vilket får smältan att börja stiga uppåt genom manteln och in i jordskorpan. Alkali basaltisk smälta kan börja röra sig uppåt vid minst 2 % partiell uppsmältning. För att magman skall kunna nå jordytan måste kriterier såsom extensivt eller transtensionellt stress tillstånd i jordskorpan och/eller negativ densitetskontrast mellan smälta och jordskorpa (d.v.s. lättare smälta än sidoberg) vara uppfyllda.

Magma transporteras i gångar då detta för är det mest gynnsamma transportsättet de flesta smältor. Magma följer generellt sett inte befintliga sprickor utan trycket från magman orsakar berget att spricka upp i den riktning som är svagast, kallad σ_3 . I extensivt och transtensionellt (jordskorpan skjivas) stress tillstånd är σ_3 horisontell vilket medför att berget spricker upp vertikalt och fylls av magma som transporteras uppåt efterhand som sprickan i berget vidgas uppåt och utåt. Vulkaniska bergarter som utgör en gång i en vulkan eller i annan terräng är magma som aldrig nått jordens yta utan "fryst" i

transportsystemet. Gångar kan också skapas utan att det resulterar i ett vulkanutbrott. Ett vulkanutbrott kan definieras som ett tillfälle då magma transport i en gång korsar jordytan.

Det undersökta området är beläget i de centrala delarna av Dunedin Volcano inom vilken tio miljoner års erosion har blottlagt stora delar av vulkanens inänmäte. Portobello Peninsula består av tidiga vulkaniska sediment och överliggande lavar. Stora delar av peninsulan är genomskuren av ett otal senare gångar som har en genomsnittlig tjocklek på lite mer än en meter. De många gångar som skurit igenom området har förstört de depositionsförhållanden som en gång existerat mellan olika vulkaniska sediment i området. Sedimenten kan ej med säkerhet sägas vara avsatta i vatten eller på land, men en miljö i närheten av dåtidens havsvattenyta är trolig. Eftersom gångspridning sker genom att sidoberget vidgas i den riktningen där berget är svagast innebär detta att gångars orientering kan säga något om det tektoniska stresstillståndet som rådde då gången skapades. Om ingen dominerande stressriktning finns skulle detta medföra att gångar i alla riktningar skulle vara lika vanliga. På Portobello Peninsula kan två dominerande riktningar urskiljas, en i NNW-SSE och en i NE-SW riktning, vilket anses visa på att ett anisotropt stressfält har existerat i jordskorpan då vulkanen var aktiv. På fem ställen kan skärnings punkter mellan gångar tillhörande de två riktningarna studeras och i alla fallen skär NE-SW gångarna NNW-SSE gångarna. Detta tolkas som en ålderskillnad mellan gångar av olika riktning. De äldre NNW-SSE gångarna visar på ett stressfält med svagaste riktningen ENE-WSW, medan de yngre NE-SW gångarna visar på ett stressfält där den svagaste riktningen är orienterat i NW-SE. Sedimenten som finns i fältområdet idag utgör halvön har deponerats i slutet av initialfasen vilket måste innebära att gångarna skapats senare i utvecklingen. Troligtvis representerar de två dominerande gångriktningarna två av de tre senaste huvudfaserna då vulkanen var mer aktiv. Att de är orienterade i olika riktning antyder att en förändring i de krafter som drar i och trycker på jordskorpan har skett mellan dessa två perioder. Kanske är detta en första indikation på den förändring i krafterna i jordskorpan som senare (för cirka 10 miljoner år sedan) ledde till att jordskorpan började tryckas ihop och skapandet av the Southern Alps (som än idag fortfarande lyfts upp).

Halvöns övre delar är täckt av ett antal basaltiska lavaflöden, vilka ligger som hattar ovanpå de mer porösa vulkaniska sedimenten. Dessa har utvecklats olika mycket under sin "resa" upp genom övre delen av manteln och jordskorpan. Från det att en smälta bildas till det att den slutligen når jordytan i form av ett vulkanutbrott utsätts smältan för att olika processer såsom olika grader partiell uppsmältning av manteln, upplöckning av material från sidoberget och separation av vissa delar av smältan. Dessa processer får till följd att

totalkemin förändras i flera etapper under resans gång. Olika magmor har utvecklats olika mycket. De mycket utvecklade lavorna är ljusa i färgen och de lite utvecklade lavorna är mörka i färgen. Bergarterna på Portobello Peninsula skiljer sig från de flesta bergarter som sedan tidigare är kända från Dunedin Volcano. Skillnaderna kan möjligtvis förklaras med att dessa bergarter har tappat en komponent, kaersutit (ett tungt mineral som har blivit separerat från smältan) tidigt i utvecklingen (långt nere i jordskorpan) samt att de har varit med om en hög grad av inblanding av material från övre delen av jordskorpan. Detta har fått till följd att dessa bergarter har en högre kisel halt samt en alkalihalt (natrium plus kalium) som är något lägre och har en annan fördelning jämfört med de tidigare kända bergarterna.

Table of contents

Chapter 1. Introduction	1
1.1. General	1
1.1.1. Regional setting	1
1.1.2. Basement	3
1.1.3. Tectonic setting	3
1.2. Dunedin Volcano	3
1.2.1. Age of volcanism	4
1.3. Portobello Peninsula	4
Chapter 2. Sediments	7
2.1 Introduction	7
2.2 Outcrop descriptions	7
2.3 Discussion	16
Chapter 3. Lava flows; field occurrence and petrography	18
3.1 Introduction	18
3.2. Mafic lava flows	18
3.2.1 Hatchery basalt	18
3.2.1.1. Field occurrence	18
3.2.1.2. Petrography	19
3.2.2. Hatchery shoshonite and latite	21
3.2.2.1. Field occurrence	21
3.2.2.2. Petrography	22
3.2.3. Portobello potassic trachybasalt	24
3.2.3.1. Field occurrence	24
3.2.3.2. Petrography	25

3.2.4. Quarantine Point trachyte	27
3.2.4.1. Field occurrence	27
3.2.4.2. Petrography	28
Chapter 4. Planar features	29
4.1. Introduction	29
4.2. Distinction dike/intrusion	29
4.3. Planar structures; field relations and petrography	30
4.3.1. Alkali basalt intrusive	30
4.3.1.1. Field occurrence	30
4.3.1.2. Petrography	32
4.3.2. Nepheline benmoreite (“ulrichite”) dike	34
4.3.2.1. Field occurrence	34
4.3.2.2. Petrography	34
4.3.3. Phonolite dikes	36
4.3.3.1. Field occurrence	36
4.3.3.2. Petrography	37
4.3.4. Trachyte dikes	39
4.3.4.1. Field occurrence	39
4.3.4.2. Petrography	39
4.4. Dike geometry	40
4.4.1. Description	40
4.4.2. Discussion	43
Chapter 5. Classification from major elements	47
5.1. Introduction	47

5.2. Classification of rocks in the Dunedin volcanic complex	47
5.2.1. Classification by Coombs and Wilkinson (1969)	47
5.2.2. TAS classification	48
5.3. Whole rock analyses of the Portobello Peninsula	52
5.4. Classification of hy/qz normative rocks	55
5.5. Oxidation state	57
5.6. Conclusion; proposal of new lineage within the Dunedin Volcano	59
Chapter 6 Geochemistry of the oversaturated lineage	60
6.1. Oversaturated lineage (basalt-potassic trachybasalt- shoshonite- latite-qz trachyte)	60
6.2. Analyzing techniques	60
6.3. Field relationship/aerial distribution	60
6.4. Major elements	61
6.4.1. Oversaturated lineage	61
6.4.2. Comparison to undersaturated lineages	61
6.5. Trace elements	64
6.5.1. Oversaturated lineage	64
6.5.2. Comparison to the undersaturated lineages	75
6.6. Discussion	77
6.7. Genesis of hypersthene normative melts	80
6.8 Implications for magma generation in the Dunedin Volcano	82
Chapter 7 Conclusions	83
7.1. Conclusions	83
7.2. Future research	84
Bibliography	86

Appendices	91
Appendix I – Strike/dip measurements	91
Appendix II – Geochemical data	93
Appendix III – Geological map	107

Table of figures

Fig. 1.1 Regional map showing Cenozoic volcanic products in Otago.	2
Fig. 1.2. Map showing location of the Portobello Peninsula	5
Fig. 1.3. Photo overlooking Portobello Peninsula	5
Fig. 2.1. Classification scheme of pyroclastic rocks	8
Fig. 2.2. Map showing outcrops of volcanic sediments	8
Fig. 2.3. Planar bedding in tuffs and lapilli tuffs, unit A1	10
Fig. 2.4. Cross bedding in lapilli tuffs, unit A1	10
Fig. 2.5. photo of rimmed felsic clast, unit A2	11
Fig. 4.1. Columnar jointing in basalt intrusive	31
Fig. 4.2. Stereoplot showing cooling surface of basalt intrusive	31
Fig. 4.3. Spherulitic analcime within phonolite	38
Fig. 4.3. Chilled contact of phonolitic dike cutting through basalt	38
Fig. 4.5. Cumulative dike thickness of the Portobello Peninsula	40
Fig. 4.6. Stereoplots of the dikes of Portobello Peninsula	42
Fig. 4.7 Dips of dike assemblages	42
Fig. 4.8 Changes in tectonic stress field	46
Fig. 5.1. Classification schemes of Price (1973)	49
Fig. 5.2. TAS classification system	51
Fig. 5.3. Representative rocks from the Dunedin volcano	51
Fig. 5.4. Distribution of the rocks of Portobello Peninsula compared	53

to other rocks from the Dunedin Volcano

Fig. 5.5. TAS diagram showing the Portobello volcanic rocks	54
Fig. 5.6. Diagram showing the degree of saturation in rocks from Portobello Peninsula	56
Fig. 5.7. Diagram showing DI versus either $qz+hy/2$ or ne	56
Fig. 5.8. Diagram showing effect of saturation on changes in oxidation	58
Fig. 5.9. TAS diagram showing the diversity of rocks from the Dunedin Volcano	58
Fig. 6.1. Harker diagram for the oversaturated lineage	62
Fig. 6.2. MgO variation diagram for the oversaturated lineage	63
Fig. 6.3. HFSE elements (Nb, Zr)	66
Fig. 6.4. LILE elements (Ba, Rb, Sr, U, Th)	67
Fig. 6.5. Chalcophile elements (Zn, Cu, Ga)	69
Fig. 6.6. Transition elements (Sc, Cr, Ni, V)	71
Fig. 6.7. Spidergrams of rocks from the oversaturated lineage normalized to primitive mantle and to chondrite	73
Fig. 6.8. Spidergram showing traceelement distribution between different members normalized to hy-norm. basalt	74
Fig. 6.9. Spidergrams comparing the oversaturated lineage to the undersaturated lineages	76
Fig. 6.10. Schematic model of magma generation in the Dunedin volcano	81

1. Introduction

1.1. General

Widespread intraplate volcanism has occurred in the South Island of New Zealand. Activity related to this has occurred during greater parts of the Cenozoic. Major episodes of activity were in the Paleocene to lower Eocene, the Upper Eocene to Lower Oligocene, the Miocene and in minor amounts in the Pliocene (Johnson, 1989). The youngest volcanism occurs in the east of the Campbell Plateau with inferred migration from west to east (Adams, 1981; Farrar and Dixon, 1984). The westernmost volcanic rocks can be found in the central parts of the South Island as numerous lamprophyre dikes (Adams and Cooper, 1996) of late Oligocene to early Miocene age. The easternmost parts affected by volcanism can be found to east of the South Island, on the Campbell plateau, as a number of oceanic islands and seamounts (Adams, 1981). The products from the volcanic activity are with a few exceptions alkaline basalts. The model suggesting eastern movement of volcanism ignores alkalic occurrences as Deborah volcanics (section 1.1.2.) which don't fall onto the inferred eastward migrating line and clearly does not fit in to the model. This makes the model somewhat suspect, and it should be handled carefully.

1.1.1. Regional setting

Cenozoic volcanism in the Otago region is divided into three major phases (Coombs et al., 1986). The first phase occurred in the Paleocene, and is only recorded in an exploration well off the coast of North Otago. The second major phase, the Waireka Deborah volcanics were deposited in late Eocene-early Oligocene ($40 \pm 2 - 32$ M.a.). The area affected by this phase was a 1800 km^2 area situated on the shallow continental shelf at that time. The products of the volcanic activity are both tholeiitic and alkalic. The third major phase was more widespread and affected large parts of Otago. This phase is of Miocene age (13-10 Ma.), but older volcanism has been recognized in the area (Coombs et al., 1986; Martin, 2000). The third phase mainly consists of a large shield volcano (the Dunedin Volcano) and its peripheral volcanics, which are present up to distances of 95 km from the centre of the volcano (see figure 1.1). This phase was virtually totally subaerial (Johnson, 1989).

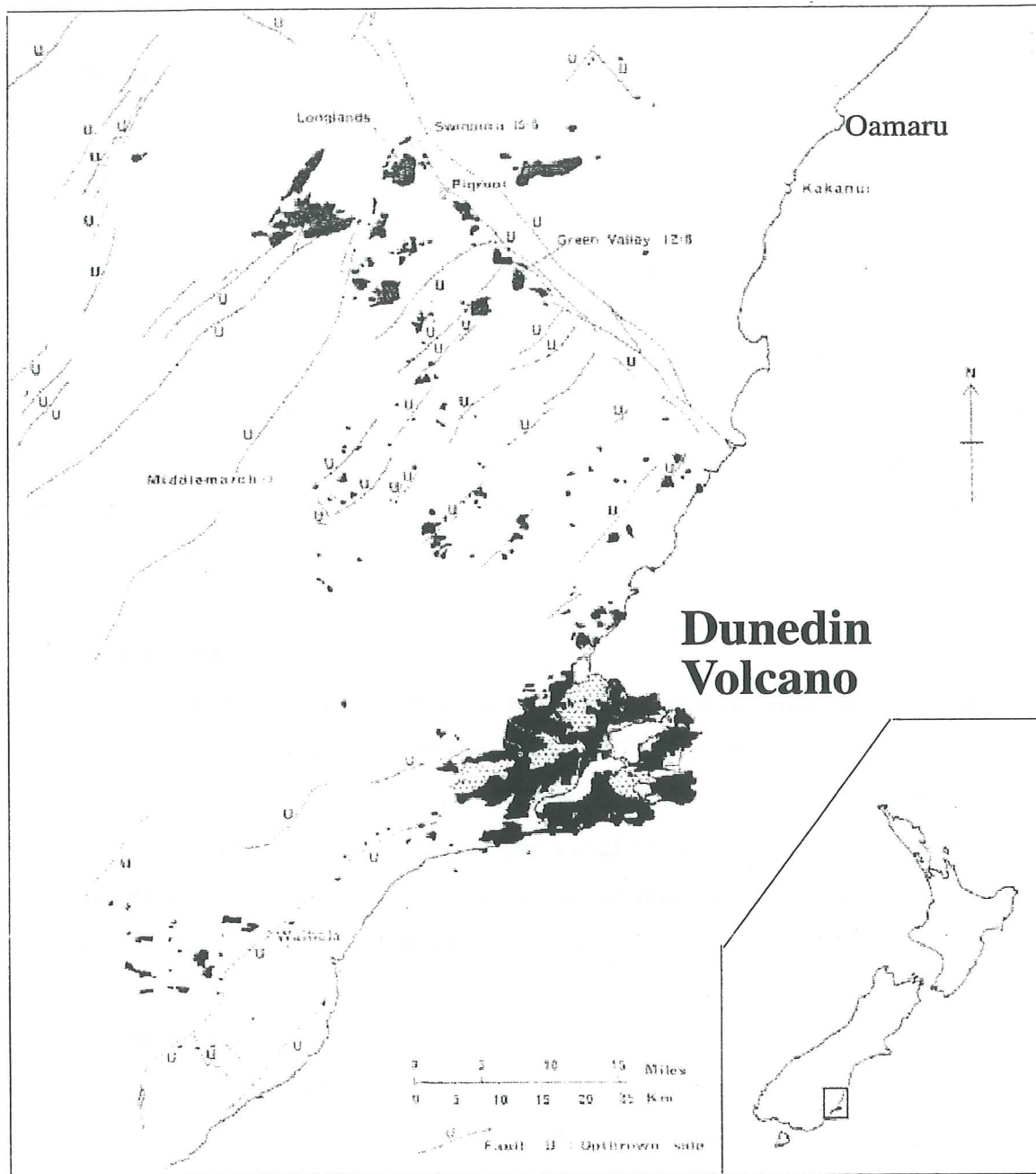


Fig 1.1. Map showing distribution of volcanics of the Miocene alkalic province of east Otago, South Island, New Zealand. Mafic igneous rocks are black and phonolites and trachytes are stippled. Dunedin Volcano is the largest volcanic feature in the region occupying an area of 25 km in diameter. Also shown are the reverse faults last active during the Kaikoura orogeny.

1.1.2. Basement

The Dunedin volcanic complex is underlain by the older Torlesse, a terrane which underlies large parts of the South Island. The basement rocks consist of quartzofeldspathic greywackes and some volcanogenic sediments. They are predominantly of Permian and Middle and Upper Triassic age. The age of the rocks generally decrease in age westwards. The metamorphic grades increase to the west of the terrane from zeolite, through prehnite-pumpellyite, pumpellyite-actinolite and into greenschist facies. In the Dunedin area these rocks are overlain by a terrestrial and transgressive marine sequence comprising upper Cretaceous, Paleocene and Eocene sedimentary rocks (McDougall and Coombs, 1973). The sequence is about 500 m thick in the Dunedin district.

1.1.3. Tectonic setting

Otago is dominated by roughly orthogonal northeasterly and east-southeasterly striking, steeply dipping reverse faults (Carter and Norris, 1976) (Fig. 1.1). These are thought to be older (Cretaceous) extensional faults (Mutch and Wilson, 1952; Bishop and Laird, 1976) that have been reactivated in the compressional regime leading to the formation of the Southern Alps (10 Ma to present). During the volcanism the region was experiencing northwest-southeast extensional stresses (Coombs et al., 1986).

1.2. Dunedin volcano

Dunedin volcano is the remnants of a shield volcano with a diameter of 25 km. The volcano is situated at the northeastern end of the Taieri graben, an extensional feature having a strike northeast to southwest (Coombs et al., 1986). The faults making up the graben are thought to have been active during the volcanism (Sherwood, 1988). The centre of the volcano is located in the middle reaches of the Dunedin Harbour, around Portobello and Port Chalmers. Benson postulated this area to be where the initial phase consisting of trachytic volcanism was erupted. Subsequent activity he divided into three major phases of basaltic volcanism. The initial phase has, by later workers (Allen 1974, Martin 2000), been proven to be much more diversified than Benson first thought, but the later three main phases are still thought to be the major episodes of basaltic volcanism

during the volcano's active period. The petrology of the volcano, containing two undersaturated lineages (see chapter 5), was thoroughly described by Coombs and Wilkinson (1969), and extended to include potassic varieties of both the lineages by Price (1973) (see Chapter 5).

Reilly (1972) postulated the volcano to be centred on the Portobello peninsula, based on a gravitational anomaly.

1.2.1. Age of volcanism

The Dunedin volcano is of middle Miocene age (Price and Compston, 1973; McDougall and Coombs, 1973; Sherwood, 1988). Rb-Sr dating of the volcanics gave ages between 14.4-12 Ma (Price and Compston, 1973), however with rather large errors. The KAr dating method has been applied on nine rocks in the Dunedin volcano (McDougall and Coombs, 1973) and later correlated with paleomagnetic studies (Sherwood, 1988). Two initial phase trachytes have been dated at 13.4 ± 0.3 Ma and 13.3 ± 0.4 Ma. No ages have been recorded on rocks from the first main eruptive phase, but the magnetic field shows normal polarity. The second main phase has ages between 12.4 ± 0.4 Ma and 11.6 ± 0.4 Ma, with normal polarity in the beginning and reversed polarity towards the end of the phase. The third main phase have been dated to 11.2 ± 0.2 Ma to 10.0 ± 0.2 Ma, and consist of rocks which are normal or anomalously magnetised.

1.3. Portobello Peninsula

The Portobello Peninsula is situated in the middle reaches of the Dunedin Harbour (Fig. 1.2 and 1.3). The area around Port Chalmers and Portobello has long since been recognized to represent the central parts the of the Dunedin Volcano (Benson, 1942; Reilly, 1972; Price, 1973; Coombs et al., 1986). Portobello Peninsula comprises volcanogenic sediments, lava flows and numerous dikes. The Peninsula is made up of two major hills (I44,J44/274-835 and I44,J44/269-841), the northernmost one reaching a height of 94 m. Most of the outcrops are situated along the shores and on the eastern slopes. A number of outcrops are also present along the road leading out to the aquarium. After gravitational studies Reilly (1972) postulated the very centre to be situated on Portobello Peninsula.

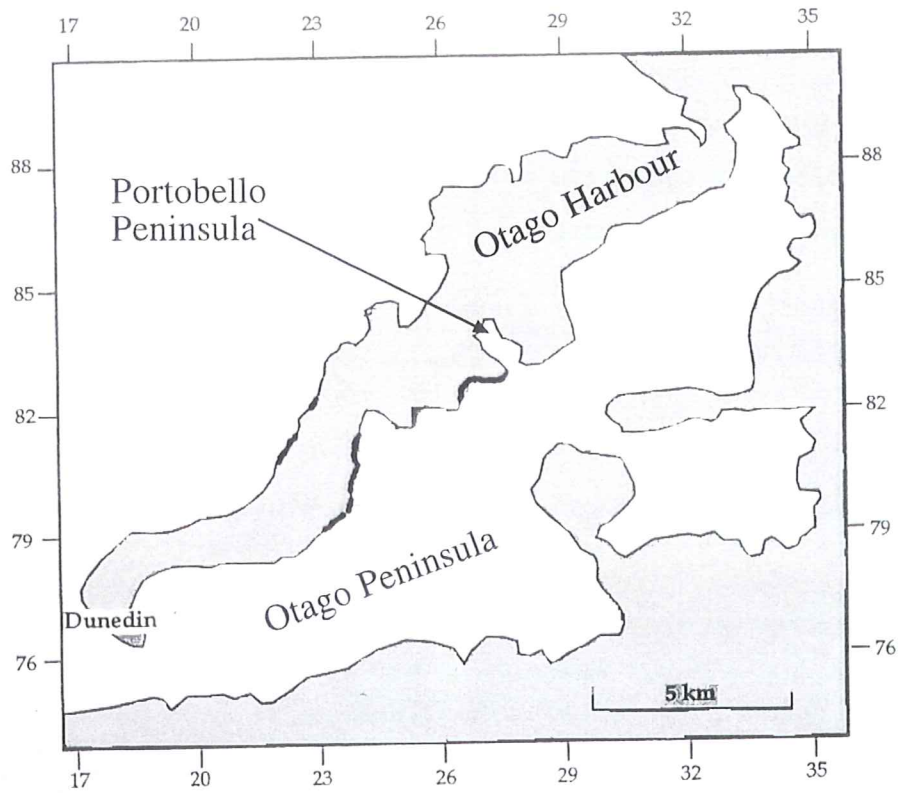


Fig. 1.2 Map showing location of Portobello Peninsula within the Otago Harbour

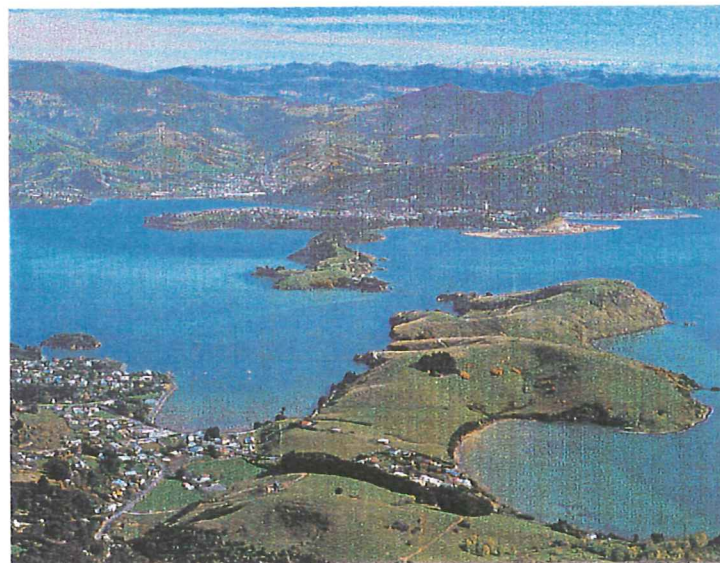


Fig. 1.3 Photo overlooking the Portobello Peninsula, as seen from the southeast.

Previously the volcanics of the Portobello Peninsula have been mapped as flows and sediments (tuffs and breccias) from the initial phase and the first main phase (basaltic agglomerates and bedded tuffs). Only a small flow is present on the map, lying on top of the northern hill mapped as a plagioclase-augite-olivine basalt (Benson, 1968).

2. Sediments

2.1 Introduction

The sediments of Portobello Peninsula are divided into two groups; mafic (basaltic) sediments and felsic (trachytic) sediments. Within these two groups there are several different kinds of sediment mainly classified on average grain size of the sediment according to the classification scheme of volcanoclastic rocks by Schmincke and Fischer (1984), and Fischer (1984) (Fig. 2.1).

The sediments occupy the lower terrain of the peninsula. The bigger outcrops are all but one situated down on the beaches or on the lower parts of the adjacent slopes around the peninsula.

Six major outcrops are described. Within these localities all the different clastic rock types that can be found on the peninsula, are described.

2.2 Outcrop descriptions

The six outcrops are (see map 2.2) for locality;

- A. Latham Bay
- B. Aquarium south
- C. Aquarium north
- D. East of Quarantine Point
- E. Lamlash Bay
- F. Hatchery Road
- G. Portobello Bay

A general feature of all the rocks is the number of secondary processes (leaching, limonitization, interaction with seawater during high tide) which have altered the rocks. Primary structures are, consequently, difficult to identify. Along with this many of the localities are also affected by recent mass movements which either cover up or (in a few cases) denude sediments. Field relations (contacts) between different units are only visible in a few places, making stratigraphy studies an impossible task.

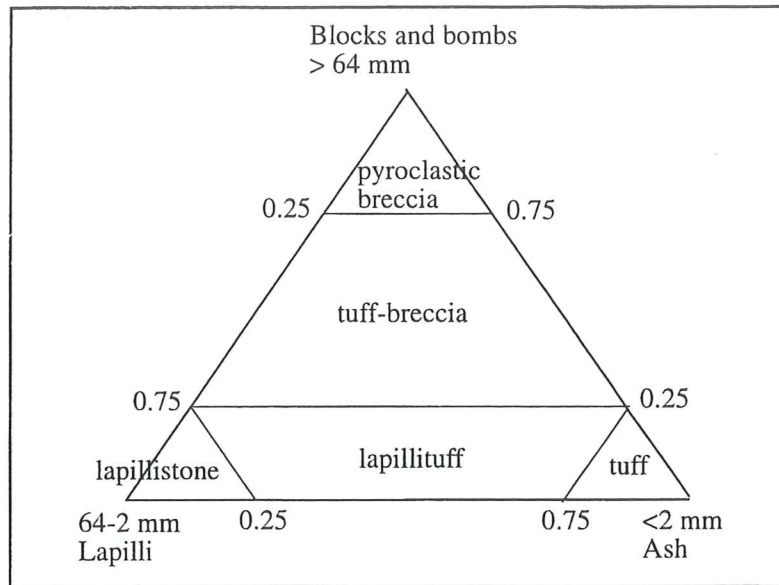


Fig. 2.1. Classification scheme of pyroclastic rock by Fisher and Schmincke (1984) and Fisher (1984).

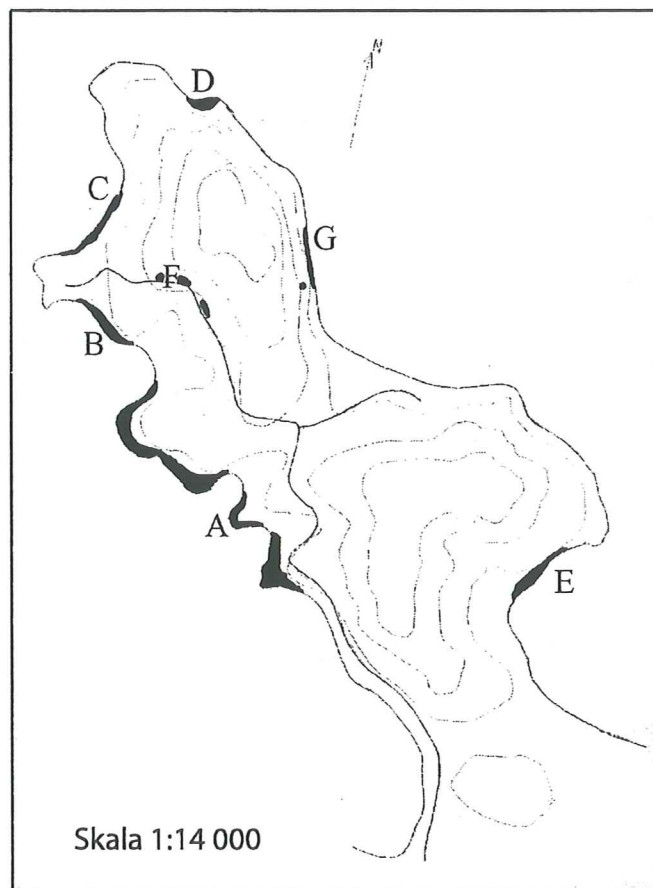


Fig. 2.2 Map showing the six outcrops described in this chapter.

A. Latham Bay

This outcrop is by far the biggest on the peninsula. In total it consists of sedimentary, volcanoclastic rocks along a 400 m long section of the western beaches of the peninsula. The outcrop is cut by numerous dikes. The dikes strike in many different directions, and are dealt with in detail chapter 4. The outcrop is divided into four units from south to north (Fig. 2.2).

Unit A.1 Felsic tuffs and lapilli tuffs

This unit outcrops along a 2 m high, and 50 m long wall (I44,J44/270834) which consists of thin massive layers of unwelded, stratified, beige-reddish, felsic material, a lot of it being rounded pumice fragments (Fig. 2.4). The thickness of the layers in the sequence varies from 1-3 cms. The clast size of the layers range from ash (<2mm) to the lower part of the lapilli fraction (max. 5 mm) with the vast amount of layers being in the ash fraction (Fig. 2.3). The sequence in the southern area dips to the southeast ($39/10^{\circ}$ SE and $70/10^{\circ}$ SE). To the north of the area the bedding rotates into a more easterly dip ($357/12^{\circ}$ E). This part of the unit also shows some cross bedding (Fig. 2.4). In the very north of the unit, on top of the tuffs a magmatic body (lava flow or sill) occurs. The body consists of a pale greyish, fairly evolved basaltic rock, with phenocrysts of feldspar, pyroxene and nepheline. The contact between the tuffs and the lava/sill is poorly exposed due to intrusion by a number of dykes (trachytic and phonolitic). Measurements on the top of the body (326/10 N) suggests that it is emplaced concordant to the bedding of the tuff but no clue resolving the possible origin of the body could be found.

Unit A.2 Mafic lapilli tuff

This outcrops along a 100 m long section (I44,J44/270-835). The unit consists of a massive, poorly sorted, matrix supported lapilli tuff with felsic clasts (max 10 cm) dispersed randomly throughout the grey matrix. The average clast size is approximately 1 centimeter. The shape of the clasts are subangular to subrounded. The whole unit is

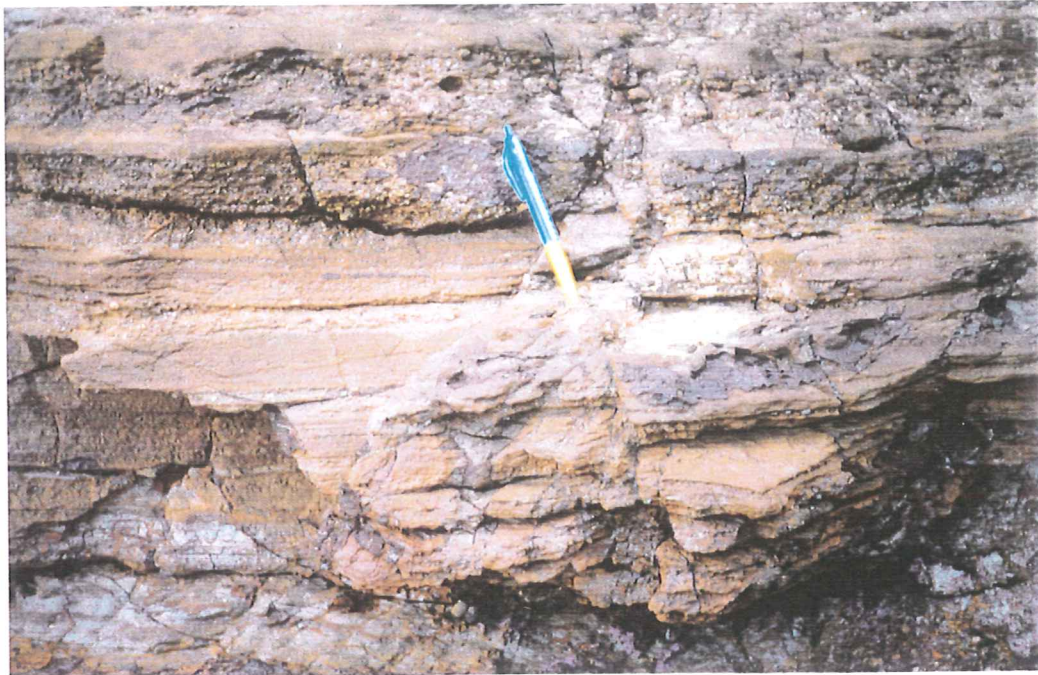


Fig. 2.3 Planar bedding in tuffs and lapilli tuffs belonging to unit A.1.
Pen (10 cm) for scale



Fig. 2.4 Crossbedding of lapilli tuffs in unit A1. Bottom bed is massive, overlain by at least two inverse graded beds dipping to the left in the picture. Clasts are felsic lithics, subrounded to rounded. The top layers are subhorizontal, clearly cutting the others. Pen for scale (10 cm).

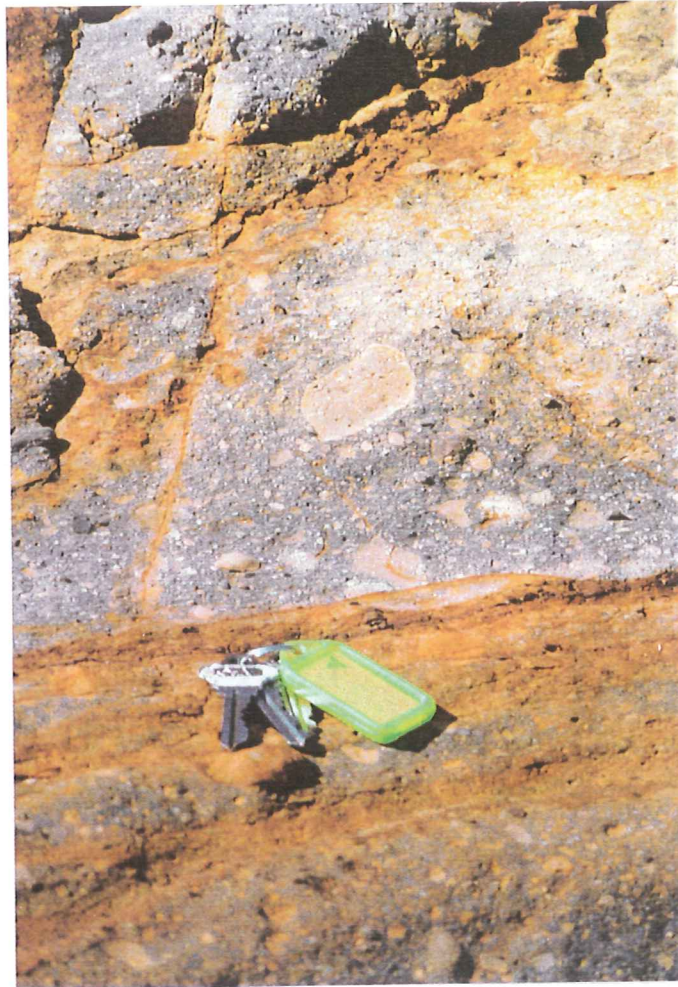


Fig. 2.5 Subangular, felsic clast showing pale rims within lapilli tuff belonging to unit A2. Keys (3 cm) for scale.

massive without any internal, measurable structures. Some of the bigger clasts show a pale rim, which might indicate a hot environment during emplacement (Fig. 2.5). Apart from these clasts no other indications of likely temperature regime can be found.

Unit A.3 Mafic lapilli tuffs

The tuff breccia outcrops along a 200 meter long section (I44,J44/268-836). However a part of the section is inaccessible which makes any studies impossible.

This unit might consist of a number of sub units, but the lack of any clearcut boundaries, only gradational changes makes me map this as one unit. The outcrop is made up of a massive mafic lapilli tuff with clasts ranging up to 10 centimetres. The clasts are all of mafic origin and have an angular to subrounded shape. The clasts are randomly dispersed throughout the matrix, not showing any internal structures. The southernmost part has in average bigger clast sizes, with maximum clasts up to 30 cm big. These big clasts are both felsic (pumice) and more mafic lithics. The middle part show some stratification, while the northern part have more angular clasts with a maximum clast size of 20 centimeters.

Unit A.4 Trachytic lapilli tuff (brecciated appearance)

This unit outcrops to the north of unit A.4 (I44,J44/268-837). The rock consists of beige clasts with a small amount of reddish matrix in between the grains. The clast-matrix ratio is approximately 1:1, which is by far the greatest ratio in the area. The clasts have a size range from a couple of mm to a couple of cm. The shape of the clasts are very angular to angular. The unit is totally massive without any structures. Some of the larger clasts have a darker core and a pale outer rim. If this feature is primary it suggests a hot environment during emplacement. If it is secondary feature (which probably is more likely since only a few have pale rims) it might be a result of weathering.

B. Aquarium south

This outcrop is about 75 m long and in average about 2.5 m high. It is situated just south of the aquarium (I44,J44/267-838). The locality consists of two different units, both of a felsic character. The locality is cut by a great number of dikes striking mainly in a NS direction.

B.1 Trachytic tuff with interbedded mafic layers of lapilli

This unit, making up the southern part of the outcrop, is a stratified tuff consisting of layers of different clast size. The unit consists dominantly of massive layers of fine grained trachytic tuff with a number of thin (approx 1 cm) layers of coarser grained mafic material. The maximum size of the coarser grained clasts is 3 centimeters in diameter. The unit also holds occasional larger clasts with a diameter of 10 cm. The shape of these clasts are subrounded to rounded and they are often filled with vesicles. Measurements were made on two of these layers, one in the southern part ($27^{\circ}/16^{\circ}$ N), and one in the northern part ($40^{\circ}/12^{\circ}$ NW).

B.2 Trachytic tuff breccia

This rock, situated to the north of unit B.1 consists of a massive tuff breccia with a high concentration of clasts per unit area. The size of the clasts ranges from 0.1-30 cm in diameter and have shapes from very angular to rounded. The clasts were derived from a number of sources. Among the clasts, there are a range of volcanoclastic rocks, felsic porphyritic rocks, mafic porphyritic and aphyric rocks and mafic vesicular rocks. Among the lithics you can see occasional rimmed clasts.

C. Aquarium north

This locality is situated along the shoreline just north of the aquarium (I44,J44/267841) and consists of a 30 m long outcrop, which to the south is cut by a number of dikes and to the north by later mass movement deposits.

C.1 Trachytic lapilli tuff

This outcrop consists of a massive lapilli tuff containing clasts ranging from mm size up to dm size (max clast measured 10 cm). The clasts are all of felsic composition giving the rock an overall beige colour.

D. East of Quarantine point

The northernmost point, Quarantine point, consists of trachytic lavas and will be dealt with in chapter 3. About 200 m to the east of this (I44,J44/268844), a number of

outcrops containing volcanoclastic rocks, make up a sequence of three units. The fourth unit also described is situated in the tidal zone to the east of the other three units. This unit might have a somewhat different origin.

D.1 Trachytic lapilli tuff

This unit make up the basal part of the locality and consists of a pale beige matrix without any larger clasts. The unit seems to exhibit weak stratification, however, the poor outcrop makes it impossible to make any strike/dip estimations of the strata.

D.2 Trachytic Lapilli tuff

This unit is made of a grey-brownish sediment, containing large rounded boulders of mafic origin in a matrix of felsic particles. The unit is massive and matrix supported with larger boulders evenly distributed throughout the matrix. The boulders are from a number of sources. Among them there are both porphyritic and aphyric, dense rocks and rocks containing lots of vesicles. The particles making up the matrix are dominantly of the lapilli fraction but occasional larger clasts can be found.

D.3 Trachytic lapilli tuff

This sediment contains a pale beige matrix of small spheroidal particles, 1-2 cm in diameter. The unit is massive except for a couple of thin purple lenses, probably of more mafic composition. This unit overlies unit D.2 and the contact is smeared out into a transition zone, a couple of meters thick.

D.4 Lithified tuff breccia

This unit differs from the other unit making up the locality, both in its placing and its characteristics. The outcrop is mainly situated in the lower parts of the tidal zone which makes it accessible only at very low tide. This rock consists of clasts ranging up to 0.4 m in diameter, lying within a dark grey, finegrained matrix. There is no preferential clast size but an evenly distributed spectrum of clast sizes. The clasts are subrounded to rounded and mainly of mafic composition.

E. Lamlash Bay

This locality located along the shoreline of Lamlash bay (I44,J44/276834), on the eastern side of the peninsula, is about 100 m long and is cut by a few dikes, mainly of phonolitic composition.

E.1 Lapilli tuff breccia with inter-layered lapilli tuffs

The outcrop contains a sequence of lapilli tuff breccias with thin layers of intermixed finer-grained lapilli tuff. The coarser grained sediment is made up of a trachytic matrix with large subrounded clasts of mafic composition. The maximum clast size measured is about 40 cm. The clasts are from several different sources. Measurements made in one of the thin lapilli layers, show an E-W striking bedding surface with a dip towards the NE ($290^{\circ}/29^{\circ}$ NE).

The appearance of the locality changes somewhat from NE to SW. Towards the southern end the frequency of clasts increases and the clasts shape becomes more rounded. The appearance of the matrix stays the same throughout the locality.

F Hatchery Road

This locality is a road cut about 100 m to the east of the aquarium (I44,J44/267840). The outcrop follows the side of the road for approximately 50 m.

F.1 Mafic lapilli tuff

The sediment consists of trachytic particles in the lapilli fraction within a mafic, purple matrix. The felsic clasts are very angular to angular and lack inner structures (alteration rims, stratification). The whole unit shows well developed bedding, but secondary alteration mask the primary structures making determination of paleoslope difficult. One measurement was made, $004^{\circ}/18^{\circ}$ E.

G Portobello Bay

This locality is made up of a number of small outcrops along a 200 m long portion of the beach and adjacent slope (I44,J44/271-840). Recent mass movement deposits cover most

of the slope, but in a few "windows" the underlying sediments are exposed, mainly along the beach.

G.1 Intermixed mafic tuff breccias and lapilli tuffs

The unit is made up of mafic tuff breccias and lapilli tuffs which occur in approximately equal ratio. The thickness of the layers differs from cm to m size, with the coarser grained layers generally having the greatest thickness. The fine grained lapilli layers often show well developed bedding. The clasts are all of mafic origin. Unfortunately most of the sediments are not in situ. Most of these are redeposited rocks from the upper parts of the slope. One measurement was made ($008^{\circ}/5^{\circ}$ W) down on the beach, indicating a westerly facing paleoslope.

The outcrops occur from the beach and on the lower parts of the slope. Further up, a couple of poorly exposed outcrops indicate a more trachytic composition of the sediments.

2.3 Discussion

The major part of the peninsula is made up of sediments. The goal with the mapping of these was to determine the volcanogenic, sedimentary environment in which they have been created. Most of the outcrops only holds one or two different units, and the boundary between them is often not exposed. Therefore it is impossible to establish the field relations between different units on the peninsula. The poor state of the rocks and the lack of structure within the different units makes it impossible to determine with certainty in what environment the deposition has occurred. However, some general details are worth discussing. The following discussion will mainly deal with the lapilli tuffs and lapilli tuff breccias since these make up the dominant component of exposed sediments.

No signs of any marine strata are found in the area. Aqueous environments can be indicated by the bedding in some layers, but this is by no mean enough to make any estimation as to whether these units are deposited in a marine environment other aqueous

environment, such as debris flow, or wet pyroclastic flow/surge. The layers are mostly massive, without any grading and could just as easily develop on land.

The dominating grain fraction on the peninsula seems to be in the lower to middle regions of the lapilli range. Most units found are totally structureless and homogeneous.

The maximum clast size is commonly about 30-40 cm which can be interpreted in two ways. Either the source of the mass movement didn't have particles bigger than this or the flow regime didn't allow bigger particles to be picked up. There is of course also the possibility that bigger particles had already been deposited before the sediment reached the area. This possibility is by the author regarded to be the least likely explanation.

Many units have a bimodal composition. Beds containing trachytic matrix with mafic clasts and mafic matrix with trachytic clasts are present. A number of units also display clasts from several sources. In one locality (locality A) they share a contact. The implication of this is that the juvenile material in massflow eroded into older sediments of different composition.

In a few places it was possible to measure paleosurfaces. The measurements are very inconsistent and show dips in a number of directions. This would indicate distribution from a number of different sources, something that is supported by the notion of the great number of inferred vent sites in the Dunedin volcano (Price and Coombs, 1975).

The lack of structures and the composition variation within each unit is suggestive of quite rapid movement of debris, which therefore has not been sorted. The suggestion for the sediments must be some form of debris flow or pyroclastic flow. Martin (2000) has, on the northern slopes of Harbour cone, described units similar in appearance to the units on Portobello peninsula. She interprets these to represent pyroclastic flow deposits. An important difference is that in many of Martin's sediments there are a lot of schist and quartz fragments, a feature which seems to be lacking on the Portobello peninsula.

3. Lava flows; field relations and petrography

3.1 Introduction

The lava flows occupy the higher parts of the Portobello Peninsula, i.e. on the tops of the two major hills, and at two different places along the shoreline. The flows are both of mafic and felsic composition. The mafic lavas occur on the top of the hills and the felsic ones occur along the shoreline, and on the lower slopes.

3.2 Mafic lava flows

The mafic lava flows consist of four separate flows, one (Potassic Trachybasalt) outcropping on the inner hill, and three (Latite, Shoshonite and Basalt) outcropping on the outer hill. No correlation between the two hills can be made, but the geochemical similarity between the Potassic trachybasalt and the others, might suggest a common source. No direct evidence of the paleoflow direction can be determined in the field. Weak indications might point to a westerly flow direction, at least on the outermost hill.

3.2.1. Hatchery Basalt (hypersthene normative) (OU 63905)

3.2.1.1. Field occurrence

The Hatchery Basalt outcrops at the very top of the outer hill (I44,J44/269281), and is overlying a shoshonitic and a latitic flow. The outcrops consist of a number of small areas of exposed in situ basalt, and a lot of scattered boulders on the ground surface. The basalt occurs on the western hill side, but can not be found on the eastern side. This is taken to be an indirect evidence of a westerly dipping base of the flow, which means that the source most likely had to have been somewhere to the east.

The rock is dark grey, and contains feldspar, olivine and pyroxene phenocrysts sparsely scattered throughout the fine grained groundmass. The feldspar has milky white, tabular prisms with a maximum diameter of 0.5 cm. The olivine is made of small green to yellow, rounded crystals with a diameter of up to 0.3 cm. The pyroxenes are euhedral and black with a maximum size of 0.5 cm. No preferential orientation of the phenocrysts can be seen in any of the outcrops.

3.2.1.2. Petrography

Hachery Basalt is a holocrystalline rock with phenocrysts of plagioclase, olivine, titanite and magnetite. The latter only occurs in minor amounts. Calcite occurs as vesicle fillings. The phenocrysts lie within a groundmass consisting of microlites of plagioclase, titanite, olivine and tiny euhedral magnetite crystals. It possibly also holds small needles of apatite.

Throughout the thin sections there are glomeroporphyritic assemblages of phenocrysts, which are interpreted as being crystals stuck together during the transport of the magma, either during the ascent to the surface or during the later phase after the extrusion.

Plagioclase (Labradorite) occur as tabular grains (phenocrysts) and laths (microlites) without any preferred orientation. The phenocrysts show both simple (Carlsbad) and multiple (Albite) twinning. Some of the crystals show concentric zonation which indicates layers of different composition. Phenocrysts cut normal to (010) show oblique extinction angles between 28° and 33° ($An_{50}-An_{60}$), using the Michel-Levy statistical method. The microlites have a slightly more albite rich composition with extinction angles between 25° and 30° ($An_{45}-An_{50}$). These values are consistent with the normalized plagioclase composition of An_{54} , which indicates a basaltic composition. Some of the phenocrysts (mostly the larger ones) show sieve textures with inclusion-rich cores and clean, inclusion-free rims. This texture is thought to be the result of the magma picking up a crystal from the wall rock it is passing through during its ascent, mixing it into the magma. When in the magma, it starts to crystallize new, fresh plagioclase on the rims of the old one. This scenario raises the question whether you should call a crystal like this a pheno- or a xenocryst. Since it has parts crystallized within one magma and other parts crystallizing in another magma neither of the two terms are incorrect.

Among the larger crystals there are crystals with inclusions arranged parallel to the twinning. Within these crystals you find microlites of dendritic ilmenite, euhedral magnetite, apatite, titanite and mica.

Olivine occurs as colourless, rounded or euhedral phenocrysts. The maximum birefringence is high second order. The birefringence, the lack of colour and the nature of

the Dunedin volcanic basalts (Price and Chappel, 1975) indicate that the major olivine component is forsterite. The normalized value for the forsterite component is about 57%, a rather low forsterite content compared to the normative values of Price (1973), basalts who reports olivines of F_{080} from Dunedin. Secondary processes like weathering alter the olivines. The oxidisation that occurs during weathering would, however, reduce the normative amount of ferrous iron, and can therefore not be used as a process to explain the normative, relatively Mg-poor olivine.

The olivine often shows different degrees of alteration. The alteration product cuts through the olivine in an uneven, irregular pattern, creating a vein system of a pale green mica. The mica shows a weak pleochroism on some surfaces and has a birefringence minimum of the third order.

Titanaugite is euhedral and often has a pale pinkish appearance. The crystals often show zoning with a more intense pinkish rim. The colour difference is due to the transition element Ti. This element is strongly partitioned in the melt. As the magma cooles the Ti concentration in the restite melt increases. The increased concentration makes it possible for more Ti to enter the titanaugite in this later stage, subsequently making the rims more pinkish. Both simple and multiple twinning is common among the phenocrysts. The more pinkish rims often show a pale pleochroism. The microlites are often clearly pinkish, just like the rims, indicating creation at a late stage.

The phenocrysts are often rich in inclusions and contain embayments of plagioclase, magnetite and olivine. Plagioclase is the most common inclusion phase, often being the only inclusion type. Overgrowth of plagioclase into titanaugite is common which also may indicate that the presence of plagioclase within pyroxenes maybe isn't an embayment but an overgrowth phenomena, i.e. the plagioclase existed prior to the growth of pyroxene phenocrysts. This may explain the large population of plagioclase inclusions.

Magnetite occurs as a minor phenocryst phase. It is either euhedral or skeletal in shape. Within the groundmass magnetite occurs as abundant, small, euhedral grains.

Calcite can be found as an accessory phase, filling vesicles within. It occurs as radially arranged needles.

Xenoliths/Xenocrysts are uncommon within the thin sections. Rarely you find small assemblages of quartz, belonging to the underlying schist. These show thick alteration rims consisting of microlitic granular clinopyroxene. This pyroxene is the result of the quartz-magma reaction occurring when the schist fragment comes in contact with the silica poor magma. As mentioned above, the large plagioclase crystals showing sieve textured cores may also be xenocrysts.

3.2.2. Hatchery shoshonite (OU 63910) and latite (OU 63902, 63903, 63913)

3.2.2.1. Field occurrence

Hatchery shoshonite and Hatchery latite are situated just below the basaltic lava flow on the upper parts of the outer hill. The estimated thicknesses of the lava flows are between 15 and 20 m. The latite outcrops at a number of places around the hill, while the shoshonite only has been found at one place, on the south side of the hill.

The largest latite outcrop occurs along the eastern side (I44,J44/270-842) where it makes up an approximately 10 m high vertical outcrop extending some 100 m along the hillside. Large portions of this outcrop are inaccessible, but no indication of the outcrop being made up of more than one flow exists along the outcrop. The bottom of the latite flow can be seen in two different outcrops along the hillside, masked by a line of springs. Along the other three sides the contacts are not exposed but can be narrowed down to a zone of about ten meters, given the existing outcrops. The contact with the underlying sediment is subhorizontal along the eastern side and seems to be subhorizontal along the western side as well. Correlation between the two sides is however hard to make.

This rock shows a very characteristic weathering. When fresh, the rock is grey (OU 63903), but when weathered it changes from grey through pale beige (OU 63902) into dark brown. The less weathered rock occurs as sharply bounded nodules within a more weathered matrix. The fresh grey and the weathered pale beige variants often occur juxtaposed, with only a thin mm-thick joint in between them.

The rock is relatively poor in phenocrysts. No macroscopic orientation of the phenocrysts. In the field you can recognise a milky, white rectangular feldspar and a dark pyroxene.

3.2.2.2. Petrography

Compared to the others Hactchery shoshonite and Hatchery latite are fairly phenocryst poor. The two flows are very similar (the only difference is the composition of normative plagioclase), and their petrography and field characteristics are described together. In later, geochemical descriptions they are treated separately.

The rocks are holocrystalline, and are dominated by the flow textured groundmass containing microlites of alkali feldspar, green clinopyroxene, magnetite, olivine and minor amounts of plagioclase and apatite. The scattered phenocrysts are mainly made of plagioclase, titanite, magnetite and olivine. Minor amounts of alkali feldspar and green clinopyroxene are also encountered.

Plagioclase (andesine in shoshonite and oligoclase in latite) is the most common phenocryst. It is euhedral to subhedral and occurs as laths without any preferred orientation. No modal distinction between the shoshonite and the latite can be made (in thin sections). Plagioclase predominantly has clean phenocrysts without any alteration or inclusions. The extinction angle normal to (010) is between 15° and 25° suggesting the plagioclase to be an andesine. However, some crystals (2 found) have an extinction angle of 35°, also suggesting labradorite, to be in the rock. The extinction angles determined optically do not correlate well with the values obtained from the chemical analysis of the rock. The freshest analysed samples yield normative oligoclase (An₂₃) and andesine (An₃₄), more sodic than compositions determined optically. This is probably caused by the partition of albite into both alkali feldspar and plagioclase in the optic determination, something which is lacking in the normative composition. Hence the normative composition will be more sodic than the optic composition. Both albite and carlsbad twinning exist. Sometimes both occur in the same crystal, and in some only one is present. A minor number of phenocrysts has a corroded rim, but the compositions of the rims are not easily determined.

Alkali feldspar is the dominating feldspar microlite, making up the groundmass. The geochemical analysis show 21% normalized orthoclase, or just below 30% of the total feldspar content. The microlites occur as colourless (patchy, greyish in crossed polars) subhedral laths throughout the matrix.

Some of them are big enough to be regarded as phenocrysts, occurring as subhedral to anhedral grains.

Clinopyroxene phenocrysts are titanite which occur as euhedral to subhedral grains. The rims of the phenocrysts often show signs of corrosion, i.e. a blurry rim containing much small euhedral magnetite grains. Others have a reaction rim within the phenocrysts. This texture is interpreted as being a result of temporary corrosion of the pyroxene, in between two periods of phenocryst growth. The pyroxene show both simple and multiple twinning, most commonly in euhedral, non altered crystals. The color of the phenocrysts is pale pink and these often are faintly pleochroistic. Some show zoning (difference in extinction angle) under crossed polars, but no crystals show any signs of zonation, i.e. concentric arrangement of more intense pinkish shades (Ti-rich rims) under plane polarised polars. Instead the groundmass contains a greenish clinopyroxene, probably an aegirine-augite (Price, 1973), which occurs throughout the groundmass as small laths.

As the rock weathers, the clinopyroxene changes in appearance. The color seems to change from its original pinkish tone, first into a clear greenish (pale beige alteration phase) and as weathering proceeds, into a reddish color (brown alteration phase, see above). The processes behind this behaviour are not further investigated in this work, only noted as a peculiar characteristic.

Magnetite occurs as a minor phenocryst phase and as a major constituent in the groundmass. As a phenocryst, the magnetite is skeletal, often associated with other phenocrysts. In the groundmass, it is in general more euhedral. This mineral also seems to play a part in the alteration of the rock. The ratio of magnetite in the matrix seems to fluctuate throughout the weathering. It seems to first increase and then decrease during the alteration process.

Olivine is partially to totally resorbed throughout the rock, both in the groundmass and in the phenocryst phase. The olivine is replaced by a dark brown, non pleochroic mineral, probably a phyllosilicate (serpentine). In a few phenocrysts, some remnants of the olivine still exist, but most commonly the only trace of the former olivine is the crystal shape and the characteristic cracks within it. Within the pseudomorphs inclusions of apatite and clinopyroxene occur.

Apatite is an accessory phase, occurring both as inclusions and as a free phase in the groundmass. It is easiest seen as inclusions, where it occurs as hexagonal, isotropic crystals associated with the resorbed olivine.

Calcite occurs as a vesicle filling throughout the flow. The amygdules are made up of radiating needles of calcite which, under crossed polars, give the calcite an undulose extinction.

3.2.3. Portobello potassic trachybasalt (OU 63905)

3.2.3.1. Field occurrence

The Portobello potassic trachybasalt is slightly hypersthene normative. The affinity of this rock is difficult to determine. A small alteration of oxidation state tips it over into the nepheline normative field. This would make it a potassic member of the mildly undersaturated lineage of the Dunedin volcanic complex, defined by Price (1973). If, however, the calculated oxidation state is the true one, the rock would plot with the rest of the saturated to oversaturated flows.

This flow seems to be the only one making up the top of the inner hill (I44,J44/274-834). It outcrops mainly as boulders on the top surface and as small "windows", less than a square meter in size at the western and eastern ends of the hill. The top surface of the hill is horizontal and no contact with the underlying sediments is exposed. This poor exposure makes any attempt of determining the flow direction impossible.

The rock making up the flow is dark grey, fine grained and contain phenocrysts without any preferential macroscopic orientation. Three phenocryst phases, plagioclase, pyroxene and olivine, are present. The plagioclases are milky white and prismatic, with a maximum observed crystal length of 1 cm. The pyroxene is a dark, box shaped augite with characteristic 87° cleavage. The crystals are millimeter sized, sometimes clustering together forming glomeroporphyritic aggregates. This phenomena is especially visible on weathered surfaces. The olivine is green on fresh surfaces and more yellow to brown on weathered surfaces. The crystals are rounded lacking any distinct cleavage.

3.2.3.2. Petrography

The mineral assemblage making up this rock is composed of plagioclase, olivine, titanite and magnetite. These phases occur both as phenocrysts and make up the groundmass. The matrix has a distinct, dark appearance, which is caused by a great abundance of small, euhedral magnetite. All the opaque grains give the groundmass (in thin section) a very dark and blurry appearance.

Plagioclase (norm. andesine (An_{41})) occurs as subhedral laths, both as phenocrysts and microlites. The phenocrysts have an extinction angle normal to (010) between 28 & 35° , indicating an anorthite component between An_{50} and An_{65} . This optical observation indicates that the plagioclase is a labradorite. The microlites using, the Michel-Levy statistical method, give compositions between An_{45} - An_{55} (andesine and labradorite). This indicates a groundmass phase that is more albite rich in composition than the phenocrysts, consistent with Price's (1973) observation of the hawaiites (sodic equivalents) of the Dunedin volcano. However, the total composition of the plagioclase being mostly labradorite is not in accordance with the observation of Price (1973). According to Price, the hawaiite consists of andesine phenocrysts, not as indicated by my optical observations, labradorite. In fact, it is mainly the differences in plagioclase composition that defines the boundary between hawaiite and basalt (and subsequently also between basalt and potassic trachybasalt). The boundary is defined from normative compositions, but a general correlation between chemical data and optical observations should exist (Coombs and Wilkinson, 1969).

Crystals show both Carlsbad and albite twinning, often occurring in the same crystal. The albite twinning consists of very closely spaced lamellae, a feature known to occur in labradorite. A few of the phenocrysts show a reaction rim within the phenocryst, indicating a temporal exsolution of the feldspar.

Another significant feature of this flow is the invasion of groundmass into the plagioclase. The inflow of magma has probably occurred along cracks in the crystals and later crystalized there.

Titanaugite in the potassic trachybasalt is pale pinkish and show shapes all the way from anhedral to euhedral but it occurs most frequently as subhedral, slightly rounded crystals. No color difference between the rim and the interior of the crystals can be observed. The phenocrysts show both simple and multiple twinning. Invasion of groundmass, like in the plagioclase (see above), occurs in some crystals. The crystals show a dark, corroded rim, consisting of numerous euhedral magnetite crystals. Only a few euhedral crystals do not have corroded rims. Both clean and corroded crystals occur as a free phase and as overgrowth onto olivine. The clean, non corroded crystals being are associated with dendritic ilmenite.

The pyroxene assemblage in the rock may be interpreted as consisting of both phenø and xenocrysts, the xenocrysts being the ones with corroded rims. Xenocrysts are generally thought to be deep seated, and hence older than the phenocrysts. If the magma isn't favouring pyroxene growth at the time of entrapment the xenocryst starts to react with the magma, creating the observed rims.

Olivine occurs as rounded (subhedral) phenocrysts. The olivine is showing the full spectrum from almost unaltered to totally altered. The alteration of olivine have produced a green mica (probably serpentine) with only small portions remaining within the altered crystals. Invasion of groundmass occurs among crystals of this mineral as well.

Magnetite occurs both as phenocrysts and as a groundmass phase. The phenocrysts are skeletal forming anhedral grain assemblages often with tiny inclusions of feldspar. The

groundmass material is abundant and consists of small euhedral microlites, as mentioned before contributing to the matrix the very dark appearance of the thin sections.

The inflow of groundmass into the crystals (observed in plagioclase, olivine and pyroxene) is anomalous compared to the other flows in the area. This behaviour may have something to do with difference in extrusion rates, causing the turbulence in the flow to break the crystals and subsequent fluid (magma) to penetrate into the crystals. Many pyroxenes seem to be broken in half, also indicating a more violent eruption.

3.2.4. Quarantine Point trachyte (OU 63904)

3.2.4.1. Field relations

Quartz normative, trachytic units outcrop of two different places on the peninsula, one at Quarantine Point (I44,J44/266-845) and one along the outer eastern side of the peninsula (I44,J44/271-842). These belong to the numerous trachytes of similar geochemical affinity that are found in Otago Harbour (Allen, 1973).

At Quarantine Point the unit consists of a 150 m long section, making up the outermost part of the peninsula. The outcrop consists of the beach and the hillside adjacent to it. The locality seems to be made up of intermixed layers of lava flows and tuffs, but the distinction between the two is very hard to make, due to the extensive weathering and alteration. The locality is cut by a few trachytic dikes (3 measured), but some might have been overlooked due to the similarity of the dikes with the surrounding rocks. No signs of any phonolitic or more mafic rocks have been found.

On the eastern side of the peninsula, trachytic igneous material make up a 30 m long section of the beach and three small islands (accessible at low tide) just off shore. No relation to surrounding units can be distinguished. The unit is totally homogeneous and lacks any sign of internal structure.

The two outcrops contain a pale beige rock with only a small fraction of phenocrysts. These all seem to be feldspars, being milky white and with an elongated prismatic shape.

3.2.4.2. Petrography

In thin section the trachyte consists of phenocrysts of feldspar within a flow textured groundmass of feldspar microlites. The phenocrysts are most commonly dispersed throughout the matrix but occur in a few instances as glomeroporphyritic aggregates. Some of these have a rimmed edge which may indicate an origin from another rock.

Feldspar (sanidine) occurs as grey, euhedral laths without any preferred orientation. The feldspar has a negative optic sign, $r > v$ and a $2V$ of 20° , which suggests it is a sanidine. The phenocrysts are to a certain extent altered, having spherical natrolite within the crystals and a brown, pleochroistic mica along rims and as lining along cracks. The only other phase is magnetite, which occurs as a small number of skeletal grains enclosing feldspar microlites.

4. Planar structures

4.1 Introduction

The planar structures of the peninsula are made up of a great number of dikes and one larger intrusive. The composition of these lineaments spans from basaltic to phonolitic/trachytic with the basaltic ones belonging both to the sodic series (alkali basalt-hawaiite-mugearite-benmoreite) and the more undersaturated sodic series (basanite-nepheline hawaiite-nepheline mugearite-nepheline benmoreite) as defined by Coombs et al. (1968). To show the diversity among the dikes, four are described more closely, both their field relations and their petrographic properties.

These are two mafic (alkali basalt and nepheline benmoreite), one trachytic and one phonolitic.

4.2 Distinction dike/intrusion

As mentioned above the peninsula is intruded by a large number of dikes and one intrusive. The distinction between the two are floating and different workers use the terms differently. To make the distinction clear the two are compared.

Dikes and intrusives have many features in common. They both often occur in a planar fashion with a clear strike and dip. Emerman and Marrett (1990) define dikes as "sheetlike intrusions of magma that cut at a high angle across bedding or foliation in the country rock". This definition is to the greatest extent also valid for an intrusive. However the author questions the possibility of having a magma body of comparative big volume, moving as a sheetlike flow. The distinction between intrusive and dike are made only upon the thickness of the body. Shelley (1987) in his examination of dikes in the Lyttleton volcano, Banks peninsula, sets the limit to 20 meters, as a boundary between the two. Other workers, like Fialko and Rubin (1999) use the term dike for structures with a thickness greater than 100 meters, and does not seem to put any restriction on the thickness of these. Clearly sheetlike structures of great thickness do exist. However these numbers are mentioned in relation to feeder dikes in large igneous provinces (flood basalts), and not in association with a normal basaltic volcanoes. In this thesis the term is used as definition of a structure greater than 20 meter in thickness.

The different properties of the dikes in terms of composition gives rise to difference in weathering patterns. The basaltic ones are much more resistant to alteration than the easily weathered phonolites and trachytes. This alteration makes microscopic studies of the latter somewhat limited.

4.3 planar structures; field relations and petrography

4.3.1. Alkali basalt intrusive (OU 63906, 63907, 63908, 63912)

4.3.1.1. Field occurrence

This rock outcrops along a 200 m long section of the beach (I44,J44/276837 to I44,J44/274-837), on the saddle between the two hills of the peninsula (I44,J44/276837) and on the southern side of the inner hill (I44/J44/277-835). Along the beach the outcrop (OU 63907, 63908) is more or less continuous with only a few small gaps covered by quaternary sediments. The basalt is mostly massive, but at two places along the outcrops, the basalt show columnar jointing, with the columns plunging to the southwest (Fig. 4.1). At this locality, the basalt is cross cut by a number of dikes, a couple of trachyte dikes and one phonolite dike, all striking crudely NW-SE.

Up on the hill, approximately 150 m to the west of the beach exposure, the outcrops are not good. Exposed rocks is mainly composed of a number of boulders (OU 63912) which gives the ridge a slightly convex (upwards) surface. The trachytic material constrains the thickness of the dike to the south, being present just below the summit of the hill and along the northern hill side of the southern hill. The northern contact is not as easy as the southern contact to constrain, but an attempt was made to estimate the strike and dip using the columnar jointed basalt (from the beach outcrop). The columnar jointing is created when the lava contracts as it is being cooled. The orientation of the columns indicate (see Fig. 4.2) a cooling surface with a strike/dip of $109/60^{\circ}$ N. The high dip of this plane rules out the possibility of it being a lava flow and strengthens the idea of it being an intrusive structure. The 200 m long beach exposure transverse to the inferred strike of the body, implies that the body is more than 100 meters thick, being *senso stricto* an intrusive.



Fig. 4.1 Columnar jointing in the basaltic intrusive. Compass (10 cm) for scale.

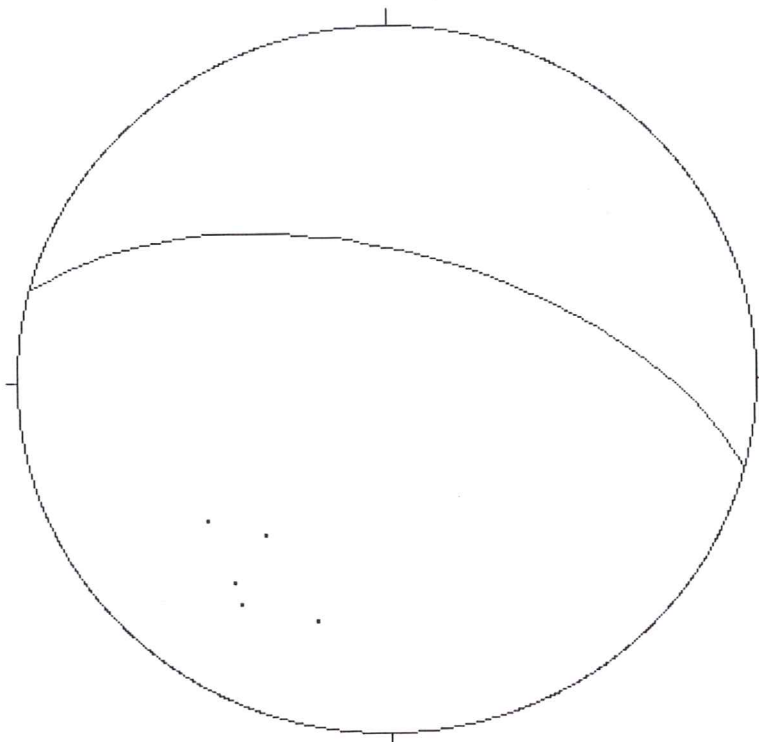


Fig. 4.2 Stereoplot showing the cooling surface for the basalt intrusive.

basalt may be found higher up on the hill, but the poor state of the rocks on top of the hill, made any attempts of geochemical confirmation impossible. Much of the eastern part of

The intrusive unit also outcrops on the southern slopes of the inner hill (OU 63906). However, in these outcrops, the rocks only occur only as boulders, within what probably is a mass wasting deposit. The slope of the hillside suggest that the hillside is made of trachytic material which also complicates the determination of the extent of the intrusive.

The rock is dark grey with an abundance of phenocrysts within it. The phenocryst phases distinguishable in the field are feldspar, pyroxene and olivine. The feldspar is white to beige with a maximum a-axis of 1 cm. The pyroxene is of mm-size, is dark and shows characteristic 87° cleavage. The olivine is greenish on fresh surfaces but most commonly yellow on more weathered surfaces. It is of mm-size and has a rounded crystal shape.

4.3.1.2. Petrography

The basalt is a traditional olivine-augite-plagioclase basalt made up of phenocrysts of plagioclase, titanaugite, magnetite and olivine. The groundmass consists of microlites of the same minerals plus ilmenite and volcanic glass, the latter only as an accessory phase. Within the matrix there occurs a small number of glomeroporphyritic aggregates consisting of a number of phenocrysts packed close together. Groundmass exists between some of the crystals. This together with the lack of an alteration rim around the aggregates indicates that it is a clot of phenocrysts and not a xenolith.

Plagioclase(Labradorite) occurs as euhedral to subhedral laths, which almost all show either Carlsbad twinning, albite twinning or both combined. The extinction angle being consistently greater than 30° is compatible with the expected value of plagioclase composition which on the three analysed samples lies between normative An_{63-67} . The plagioclase crystals sometimes show a sieve textured core and a clean rim. This often occurs in the bigger crystals, interpreted as xenocrysts that have been incorporated into the melt, maybe torn from the wall as the magma has ascended through the crust. Some

of the crystals show a faint zoning which might indicate concentric layers of different composition.

In the groundmass plagioclase occurs as microlites, often showing albite twinning. This phase makes up the greatest part of the groundmass.

Titanaugite occurs as large and small, subhedral, pinkish phenocrysts. These often show a weak pleochroism, especially the ones which have a more pinkish rim. The more intense pinkish rim, as suggested before, indicates a more titanium rich magma towards the end of crystallization. Among the larger phenocrysts, poikilitic texture is common, with inclusions of mainly plagioclase and magnetite. A few crystals show simple twinning but most of the phenocrysts are untwinned. As a groundmass phase titanaugite occurs as pinkish prisms.

Olivine occurs as subhedral, rounded phenocrysts. The crystals show some alteration of the rims and around cracks. In some of the crystals only a very small core of unaltered olivine is left. The altered zones consist of several minerals, probably various phyllosilicates, with green or brown color, the brown varieties sometimes showing pleochroism.

The normative olivine has a forsterite content of 58%, being much too low to be a basalt, according to the classification scheme made by Price (1973). In his scheme the basalt olivine has a somewhat greater forsterite content of 80%. No solution for this anomalous behaviour has been found.

Magnetite is scattered throughout the rock, both as larger phenocrysts and smaller microlites in the groundmass. As a phenocryst phase it only occurs as a small number of skeletal grains, with inclusions of plagioclase. As a groundmass phase magnetite is euhedral with a characteristic orboid shape.

Ilmenite is a common groundmass phase in this basalt, showing acicular shaped microlites. In a few places you can see how the acicular needles are connected to a larger, dendritic structure of ilmenite microlites.

Volcanic glass fills small anhedral spacings between crystals or in the groundmass. The glass is pinkish and has some quench crystals within it. Part of it is often altered into a whitish phase often circular, with low birefringance. This alteration is probably one or a few zeolites.

4.3.2. Nepheline benmoreite (“ulrichite”) dike (OU 63901)

4.3.2.1. Field occurrence

This dike is very exotic to the peninsula in the sense that it only occurs as a single dike having a strike of 348° . It crops out at two localities on the peninsula, one about 100 m to the south of the aquarium (I44,J44/267-838) and the other at an equal distance to the north (I44,J44/267-841). The dike is 3-4 m wide cutting through volcanoclastic sediments, a tuff breccia to the south, and a lapilli tuff to the north. Despite the strike of the dike being approximately parallel to the beach (see geological map) it doesn't outcrop anywhere to the south of the peninsula. This can probably be explained by the emplacement of this dike early on in the evolution of the peninsula, and the subsequent crosscutting of a great number of dikes during a later stage. The contacts show remnants of being chilled. All that is left of the rocks in the contact now is a thin layer of grey clay.

The dike rock is phenocryst rich, with a grey appearance (green on weathered surfaces). The concentration of phenocrysts increases towards the middle of the dike. The feldspars show a parallel alignment, having their direction of long axis parallel to the strike of the dike. In the field four different phenocryst phases can be recognized; feldspar, nepheline, pyroxene and magnetite. The feldspar occurs as white to grey laths having a maximum size of 1 cm. The nepheline is reddish and more columnar and easily recognizable by its greasy luster. The size of the crystals is similar to that of the feldspars. The other two mineral phases are smaller in size, the pyroxene being dark green and the magnetite being dark silver grey.

4.3.2.2. Petrography

This porphyritic dike consists of the phenocryst phases alkalifeldspar, nepheline, kaersutite, olivine, sodalite plus smaller amounts of titanite, apatite, magnetite and

calcite. In addition to this large, green aegirine crystals occur. Occurrence of two pyroxenes might indicate some degree of magma mixing. The greyish groundmass is made up of feldspar, nepheline, green clinopyroxene and magnetite.

Alkali feldspar is the dominant feldspar in the rock. A few grains of plagioclase occur but these are considered to be xenocrysts, as they are rimmed by alkali feldspar. The phenocrysts occur as laths of elongate, subhedral crystals. Some of the crystals show Carlsbad twinning. The optic sign of the feldspar was determined to be negative, with a $2V$ of 30° . This together with the normative composition of equal amounts of both orthoclase and albite suggests that the alkali feldspar is a sanidine.

Nepheline make up 16% of the normative composition of the nepheline benmoreite, being well above the boundary between the sodic and the more undersaturated sodic rock series. The rocks of the more undersaturated sodic rock series have a normative nepheline which exceeds 5% (Coombs et al., 1968).

The phenocrysts occur as short prismatic, euhedral columns. In more weathered thin sections they are easily distinguished from the alkali feldspar by the different degree of alteration. In these thin sections the nepheline is often fully or almost fully altered leaving a greyish assemblage of alteration phases behind. In these pseudomorphs of nepheline a very distinct zonation occurs. This zonation doesn't occur in the fresh nepheline crystals. The zonation is interpreted as being caused by precipitation of several alteration minerals in a concentric fashion.

Clinopyroxene consists mainly of deep green, pleochroic (green-yellow) phenocrysts. These are euhedral (eight sided) to subhedral (rounded) often elongated, in shape. The small extinction angle (7° measured) suggests an aegirine composition of the pyroxenes. The pyroxenes in the groundmass have the same features as the phenocrysts, occurring as greenish prisms, scattered throughout the groundmass. A few of the phenocrysts show thin, pinkish rims. Some of the pyroxenes are totally pinkish (titanaugites), and one displays a more intensely pinkish rim. These pinkish titanaugites also occur in a small number throughout the groundmass in the shape of euhedral columns, a bit larger than the

average green clinopyroxene microlite. One phenocryst show a faint zoning with a green core and a pink rim. From the rim the colour gradually change through the mantle. None of these titanagites show any signs of being out of equilibrium with the melt (reaction rims). This complex behaviour, involving two different pyroxenes, none of them showing any signs of being out of equilibrium, might suggest some degree of magma mixing to have occurred.

Olivine occurs as relatively small rounded crystals, often with a thick reaction rim of euhedral magnetite around the crystals. The reaction rim indicates disequilibrium with the surrounding material.

Sodalite occurs as minor amounts of colourless, subhedral phenocrysts. The crystals are shortprismatic and contain numerous tiny round inclusions of an undetermined phase.

Kaersutite occur as brown, shortprismatic crystals throughout the rock. Often the crystals show strong pleochroism and have a typical eight sided shape. The cleavage is well developed, showing characteristic 124° cleavage.

Calcite is present as vesicle fillings, in some thin section in high abundancy. The calcite show radially arranged needles giving the calcite undulose extinction with crossed polars. Under parallel polars the mineral is colourless to pale beige.

Apatite only occur in minor amounts. The crystals appear longprismatic or hexagonal, depending on how the crystal is cut.

4.3.3. Phonolite dikes

4.3.3.1. Field occurrence

Phonolite dikes are numerous on the peninsula. Most of the dikes are severely weathered and are only made up of greenish clays, lacking any signs of internal structure or crystal phases. Some of the dikes show alteration into spherical analcime. These can be seen as nodules of whitish or pale green material within the more green phonolite (Fig 4.3).

The dike studied was the only phonolite that was reasonably well preserved. The reason for this is that it cuts through the basalt intrusive described earlier, and this has acted as a container of the dike. However some alteration features can be found within the dike, especially close to the contacts. Along the contacts, the rock consists of numerous spherical analcime crystals, which have altered it totally. Towards the center of the dike the spheroids decrease in size and volume, and the center is totally free from these. The dike only outcrops along a five meter long section on the eastern beach, and possibly in a small outcrop about 100 meters to the west, along the hillside.

The dyke has chilled margins a couple of centimeters thick. The contacts are black and has a greasy luster (Fig 4.4).

4.3.3.2. Petrography

In thin section the phonolite shows proof of being strongly altered. The groundmass of the rock is totally altered and now consists of a number of alteration phases. The alteration in the pale coloured spherulites is generally more severe than in the surrounding volume. Among identified replacement minerals three different zeolites (analcime, natrolite and phillipsite), calcite and a mica were identified.

Interstitial to the spherulites remnants of glass shards can be seen as erratically arranged, slightly bent needles.

Most of the phenocryst phases are completely altered. The ones still recognizable are alkali feldspar, albite and magnetite. Phenocrysts of both feldspars show partial or total alteration into mica and zeolite, and they very often contain a large portion of calcite. The calcite appears to occur not only as vesicle filling but also as an alteration phase.

The magnetite occurs as a minor phase, in the form of skeletal grains enclosing alteration phases.



Fig. 4.3 Spherulitic analcime (pale green) with a diameter of 1 cm within green phonolitic dike. The photo is not from the described dike.



Fig. 4.4 Chilled contact of phonolitic dike intruding into basalt. Hand lens (3 cm) for scale.

4.3.4. Trachyte dikes

4.3.4.1. Field occurrence

Similar to the phonolites, the trachyte dikes are often severely altered. In some cases, nothing is left but a gaping hole. The alteration turns the dikes into a whitish clay without any recognizable structures. The dike described more thoroughly is one of four dikes which similarly to the phonolitic dike described in the previous subsection cut through basalt making preserving the dikes. The dike crops out at one place on the eastern side on the peninsula (I44,J44/276-837). It is beige and has small prisms of feldspar (≥ 5 mm) throughout the fine-grained matrix. No preferential orientation of the feldspar crystals exists. The contacts are sharp without any glass or clay (=remnants of glass). It is likely that this rock does not represent the whole trachyte assemblage of the Peninsula. The presence of ne-normative trachytes in addition to the qz-normative trachytes described seems likely due to the existence of both varieties within the volcano. In the field it is, however impossible to make any distinction between the two.

4.3.4.2. Petrography

The petrography of the qz-normative trachyte is, as expected, very similar to the petrography of the of the trachytic lava flow (section 3.2.4.2.). In thin section the only phenocryst phase is alkali feldspar. The groundmass consists of microlites of alkali feldspars, believed to be sanidine. The rock shows a distinct flow texture with a well developed alignment of the microlites.

4.4. Dike geometry

4.4.1 Description

62 dikes on Portobello Peninsula were measured (strike/dip and thickness) and divided into three groups; trachytic, phonolitic and basaltic. The dike assemblage is made up by 28 trachytes, 27 phonolite and 7 basalts. The nepheline benmoreite dike (“ulrichite”) was grouped together with the phonolitic class since these are thought to represent members of the same rock series (Price, 1973). The properties of the dikes will be compared to the dikes of the Lyttleton volcano, Banks peninsula studied by Shelley (1987 & 1988). The major phase of the Lyttleton volcano is estimated to have been erupted between 12.0-9.7 m.y. (Price and Taylor, 1980). This seems to be roughly contemporaneous with the Dunedin volcano (13-10 m.y. according to Coombs et al., (1986)). The volcanoes are both basaltic and are believed to be products of the same inferred belt of eastward volcanic progression (??) in Cenozoic time (Adams, 1981; Farrar and Dixon, 1984). The similarities and the differences will be pointed out. The very limited areal extent of my field area will, of course, bias the dike assemblage and most likely doesn't reflect the total composition of the dikes in the volcano.

As can be seen from fig. 4.5 the largest amount (>60%) of the dikes have a thickness of less than 1.5 m. This observation is in accordance with the observations made by Shelley (1988) in his study of dikes in the Lyttleton Volcano, Banks Peninsula. In this article he also states that this pattern is consistent throughout the whole of the volcano.

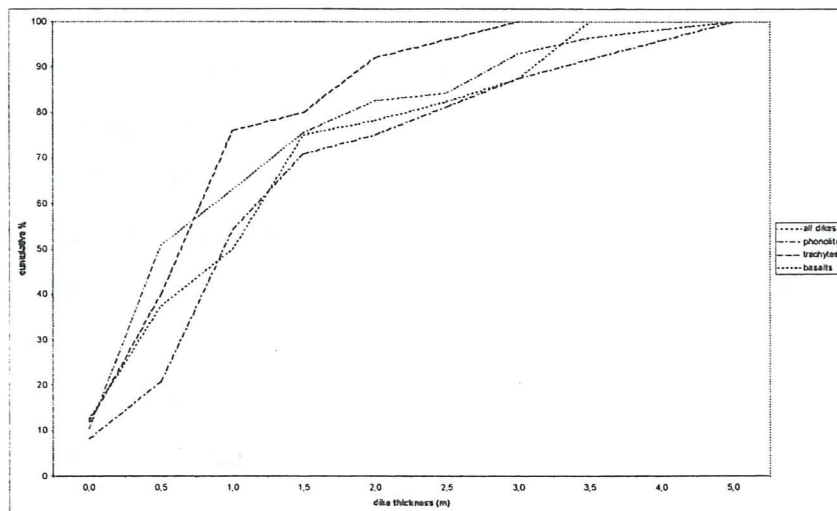


Fig 4.5 Cumulative dike thickness on the Portobello peninsula. Dikes with thickness of less than 0.25 m are grouped as 0.0 m.

The dike composition of the peninsula varies, as has been said before from basaltic to trachytic or phonolitic. Of the total amount of 62 dykes, 55 are rather silica-rich trachytes and phonolites. These generally silica-rich dike compositions contrast with the average composition of the dikes in the Lyttleton volcano, which are of a much more mafic (hawaiitic) composition.

The contacts of the dikes on the peninsula are often badly weathered, and consist either of a clay or a zone that has been eroded away. Some of the mafic and phonolitic dikes show chilled margins, with a more glassy composition towards the contact. Most of the dikes on the peninsula cut through volcanic sediments. According to Martin (2000), undulation of the contacts indicates emplacement into sediment, when it still was soft. Most dikes seem to vary in strike and dip, which could indicate that they are emplaced into the sediment when it was soft, i.e. early after the sediment deposition. A couple of dikes cut through lava flows, both trachytes and basalts, and they all have straight contacts, in contrast to the others.

To envisage the dike assemblage better, the dikes were plotted on a rose diagram. From the rose diagram (Fig. 4.6), two major strike directions seems to be prominent, one NNW-SSE and one NE-SW. No separation between dikes of different composition can be made. Among the phonolitic dikes there are a great number of dikes oriented NNW-SSE. This strike direction is also the prominent one for dikes of trachytic composition. The dips seem to be consistent within the dikes of similar strike. The dikes within the NNW-SSE assemblage dip to the east, whereas the dikes striking in a NE-SW fashion consistently dip to the south.

The crosscutting relationships indicate the relative age of the dikes. Outcrops showing crosscutting relationships between the two dike assemblages are found at five different places on the peninsula. At all five, the NE-SW dikes cut the NNW-SSE dikes. This behaviour is taken as evidence for the NE-SW dike assemblage being younger than the NNW-SSE dike assemblage.

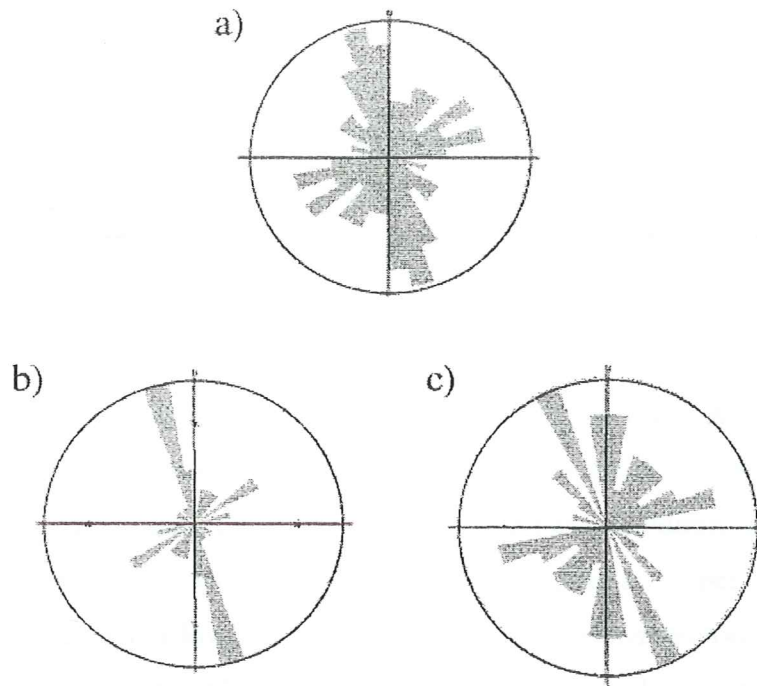


Fig. 4.6 Stereoplots of the dikes of Portobello Peninsula, (a) plot showing the total dike assemblage (b) phonolite dikes, (c) trachyte dikes

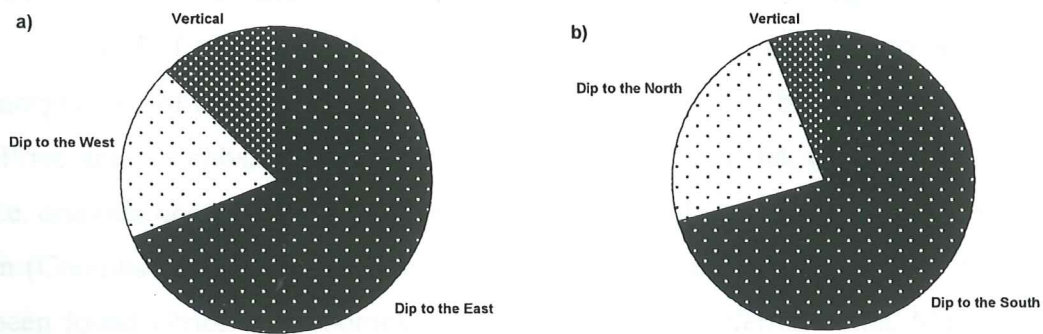


Fig. 4.7 Dips of dike assemblages, (a) NNW-SSE striking dikes, (b) NE-SW striking dikes.

4.4.2. Discussion

Dikes are generally thought to have their strike oriented perpendicular to the direction of minimal stress, σ_3 (Anderson, 1951; Pollard and Muller, 1976; Emerman and Marrett, 1990) and in this way give indications of the tectonic regime at the time of emplacement. As indicated by the dike studies of the Lyttleton volcano (Shelley, 1987), this may not be valid for areas in the very heart of a volcano. As a modern analogue of the dike behaviour in the Lyttleton Volcano, Shelley (1988) uses the Sicilian volcano, Etna. McGuire and Pullen (1989) studied dikes in the active volcano of Etna, Italy. At lower altitudes the dikes tend to be oriented parallel to each other, while the dikes at higher altitudes, closer to the summit, demonstrate a convincing degree of radial orientation. According to them, the volcano experienced two different tectonic regimes, an upper one controlled by gravitational forces and a lower one controlled by the regional tectonic forces. Shelley's studies are centered in the inferred crater of the Lyttleton volcano. Any comparisons to Etna must be to the dike pattern observed on the higher altitudes, in the gravitational regime.

An alternative dike behaviour to the ones seen at Mt Etna would be having intruding magma following preexisting cracks, and in that way having the dikes showing an older tectonic regime. Ziv et al. (2000) investigates this possibility and come to the conclusion that it is very difficult for dikes to follow preexisting fractures, unless they are subparallel to the stressfield. The forces exerted on the walls of the fracture often exceeds the tensile strength of the rock and the magma splays out of the crack, creating new cracks.

Both Lyttleton volcano and Etna represent cone shaped volcanoes. The morphology of the Dunedin volcanic complex is believed to be a more flat shield volcano (Price and Coombs, 1975), with eruption centres spread out, many being monogenetic, i.e. eruption occurring as a single event. The present day relief of Dunedin volcano is 700 m (Coombs et al., 1986). In the Dunedin area more than 40 domes and intrusives have been found (Price and Coombs, 1974). Close to the inferred vents, Martin (2000) has made observations of radial dike patterns. The largest inferred vent is situated in Hoopers Inlet, to the SSE of Portobello Peninsula. No material except for the dikes and sedimentation patterns of the lapilli tuffs in the area remains. Based on a few dikes situated around the inferred vent, Martin implies that a radial dike pattern exists several

kilometers from the vent site, extending into the present field area. On the Portobello Peninsula there are a large number of dikes that are roughly radial with respect to Hoopers Inlet (Fig. 4.6). However, Martin recognises a number of vent sites on the Otago Peninsula of which several can be possible sources for the Portobello dikes. Martin's work only deals with volcanics on Otago Peninsula, and almost all of the volcanics are thought to have been created before the end of Benson's initial phase. Many workers have suggested that the volcano had shield building phases as well as times of quiescence. The observations made at Etna, the lack of high relief of Dunedin Volcano, and the fact that there is no correlation between strike and chemical composition of the dikes, makes me conclude that the orientations of the dikes reflects, or partly reflects, the tectonic stress field at the time of emplacement. The radial dike pattern of the inferred vent in Hoopers Inlet (Martin, 2000) is only based on a few dikes and is considered to be purely coincidental to dike origins on Portobello Peninsula.

Otago is, as was mentioned in the introduction, dominated by the Otago fault-fold belt, comprising an eastward verging set of northeast-southwest striking reverse faults and folds (Litchfield and Norris, 2000). The belt extends from the Alpine Fault in the west, well to the east of the current coast line of eastern Otago (Carter, 1988). The faults are thought to be older, extensional faults from the late Cretaceous (Mutch and Wilson, 1952; Bishop and Laird, 1976), which have been reactivated during the Kaikoura orogeny, the uplifting of the Southern Alps (10 Ma to present). Exactly when this reactivation occurred is uncertain. Many workers model Otago as being in a compressional regime with active reverse faulting during the volcanic activity (Norris et al., 1978; Carter, 1988). Other workers have suggested having an extensional regime in the region from 38-10 Ma by showing that the relative motion between Australian plate and the Alpine fault was extensional, during this time period (Molnar et al., 1975; Walcott, 1979). Coombs et al. (1986) state that the volcano experienced an extensional regime while active. Clearly these opinions are contradictory, and the issue is far from resolved. The two dike assemblages on the Portobello Peninsula, striking NNW-SSE and NE-SW, and being of different age indicate that the tectonic stresses within the volcano have not been the same during the emplacement of the two assemblages. The younger set of dikes (NE-SW) are subparallel to the Otago fault-fold belt. Given that strikes of dikes

generally are considered to be perpendicular to σ_3 (Anderson, 1951), this indicates the maximum stress, σ_1 either to be vertical (extensional) or horizontal (transtensional). Sherwood (1988) suggests that the faults of the Taieri graben were active during the volcanism, which would be in accordance to the orientation of this dike assemblage. Subsequently **the stress regime during the emplacement of the NE-SW dikes, must have been extensional NW to SE.** This is supported by previous work (Coombs et al., 1986).

The older set of dikes (NNW-SSE), is subparallel to the NW-SE trending faults of the Otago region. Using the same arguments here as for the younger assemblage, **the older assemblage might reflect an extensional tectonic stress regime with σ_3 oriented ENE-WSW.** The age relations between the two dike sets put constraints on the stress regime in Otago in late middle Miocene. **From the two dike sets the minimum stress, σ_3 seems to have rotated clockwise from ENE-WSW into NW-SE (Fig.4.8).** Given the dextral movement on the Alpine Fault from the boundary oligocene-miocene to present and the increasing oblique extension of the region in the miocene (King, 2000), the most believable rotation direction of σ_3 is clockwise. From the dips of the dikes it seems as σ_3 has been slightly inclined, plunging towards to the west all through the sequence.

Portobello Peninsula is situated in the oldest units of the Dunedin Volcano, which makes it a good "recorder" of later dike behaviour. The two dike assemblages probably belong to two of the three major phases of volcanism in the Dunedin. More work is however needed to confirm this hypothesis.

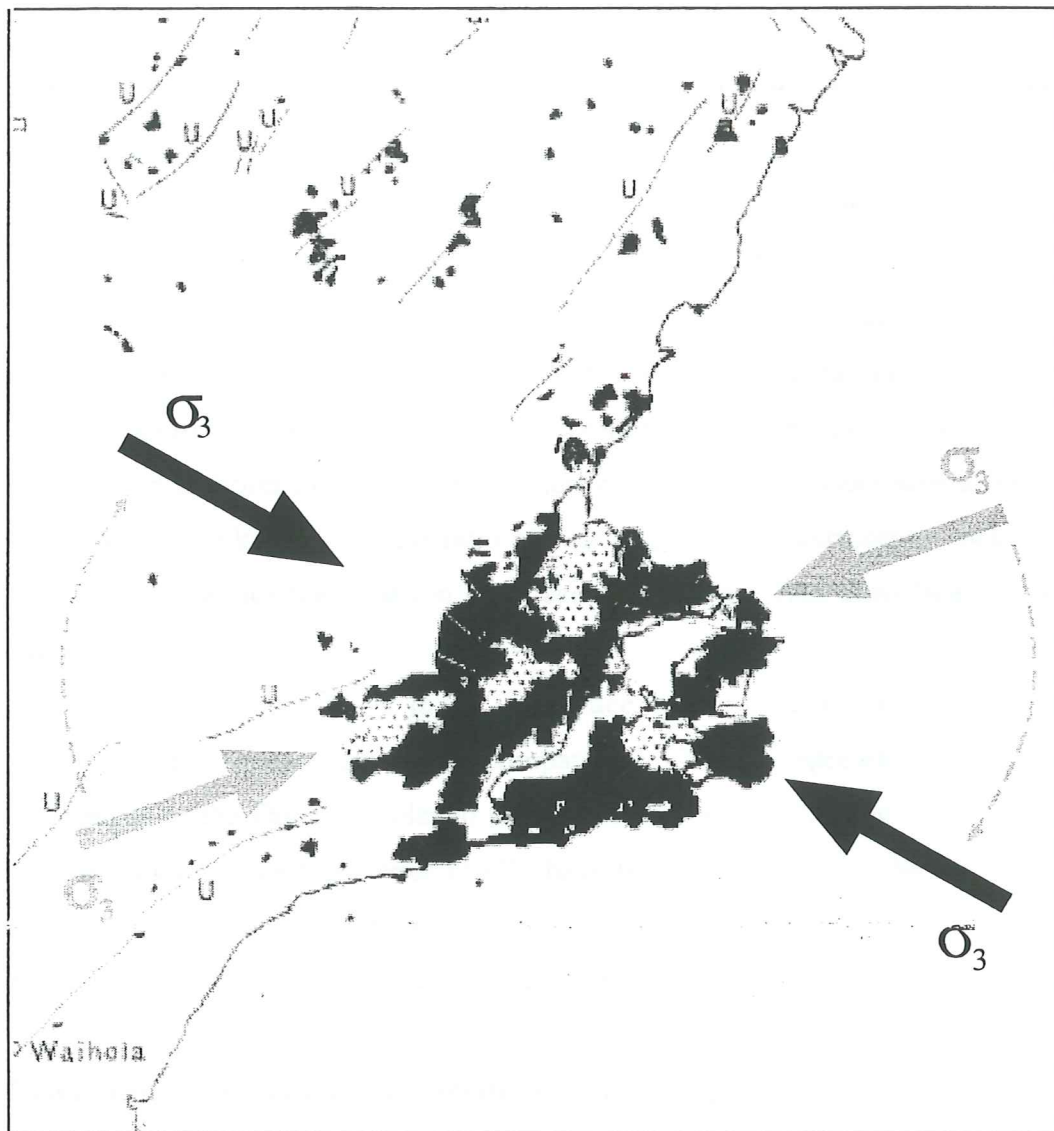


Fig. 4.8 Map showing the rotation of least compressive stress during the course of volcanic activity, from an ENE-WSW into a NW-SE orientation.

5. Classification from major elements

5.1 Introduction

The rocks of the Portobello Peninsula include members of both the lineages inferred to exist in the Dunedin volcano (see section 5.2). Two analyses of the anomalous quartz normative trachytes that previously have been encountered in the Otago Harbour (Allen, 1973; Price and Compston, 1973) are also included in the data set. In addition to undersaturated rocks, the peninsula have several units of hypersthene normative basaltic rocks (5 analyses). The hypersthene normative rocks have previously been disregarded, and these saturated rocks have been incorporated into the mildly undersaturated lineage. However, the lack of normative nepheline in these rocks, distinguish them from the rest of the rocks known in the Dunedin volcanic complex (Coombs and Wilkinson, 1969; Price, 1973). In addition to the degree of silica saturation, these rocks also differ in the percentage of total alkalis and in the ratio of $\text{Na}_2\text{O}:\text{K}_2\text{O}$ in the intermediate rocks, which put them in a (potassic) fractionation trend according to the TAS classification system (Le Bas et al., 1986).

The geochemistry (both major and trace element data) of rocks from the Portobello Peninsula (see chapter 6) is compared to 17 rocks representative of the two major lineages in the Dunedin volcano (Price and Chappell, 1975). In addition to this, another 24 rock analyses from Price (1973) have been used to define the more potassic variants of the two lineages. Analyses for this work, the data from Price and Chappell and the data taken from Price are tabulated in the Appendix.

5.2 Classification of rocks in the Dunedin volcanic complex

5.2.1. Coombs and Wilkinson (1969) classification

The rocks of the Dunedin volcanic complex were first classified by Coombs and Wilkinson in 1969. They divided the rocks into two major groups; a mildly undersaturated sodic lineage and a strongly undersaturated sodic lineage. The boundaries in the classification scheme are based upon normative compositions, but a general agreement between modal and normative composition should exist (Coombs and Wilkinson, 1969). The distinction between the two lineages is made by the normative content of nepheline, the strongly undersaturated lineage comprising basanite-nepheline

benmoreite-nepheline mugearite-nepheline benmoreite- phonolite, and the mildly undersaturated lineage comprising alkali basalt-hawaiiite-mugearite-benmoreite-trachyte (Fig. 5.4c). Rocks with normative ne greater than 5% are said to be strongly undersaturated. Within both lineages further distinctions are made, based upon the normative composition of plagioclase and the differentiation index, DI (sum of normative qz/ne + or + ab). Members with a normative anorthite content greater than An₅₀ (labradorite) are classified as alkali basalts while the slightly more evolved hawaiiite have an anorthite content between An₅₀-An₃₀ (andesine). Both mugearite and benmoreite have normative oligoclase (An₃₀-An₁₀). The distinction between them is made from differences in differentiation index. Benmoreites have a differentiation index between 65-75, whereas the mugearites have a lower differentiation index. Rocks with DI greater than 75 are said to be trachytes or phonolites. The distinction between them is made by phonolites having a normative ne geater than 8%, but this boundary is rather vague.

Both lineages also contain more potassic variants, generally being thought to represent rocks that have had a degree of alteration caused by wall rock alteration, during magma ascent.

To distinguish between different members of these lineages, normative Or vs. DI and An# vs. DI were used (Price, 1973) (see figure 5.1).

5.2.2 TAS classification

The presence in the field area of basaltic rocks with normative hypersthene and/or quartz and the consequent lack of normative nepheline, make the classification made by Coombs et al. inappropriate, in that it cannot fully describe the compositions of these rocks. The TAS classification system (Le Bas et al., 1986; Le Maitre et. al., 1989) might be considered better in that it does not take any account of the presence of ne, but instead only depends on the silica content, the total alkali content (Na₂O+ K₂O) and to a certain extent (among intermediate members) the ratio between the two alkali components (see figure 5.2). The ratio is important in intermediate rocks (trachybasalts-basaltic trachyandesites-trachyandesites) and, depending on the relationship between the two alkalic components, these fields are further subdivided into two parts (see figure 5.2b), sodic variants (Na₂O - 2.0 ≥ K₂O), and potassic variants (Na₂O - 2.0 ≤ K₂O). The sodic

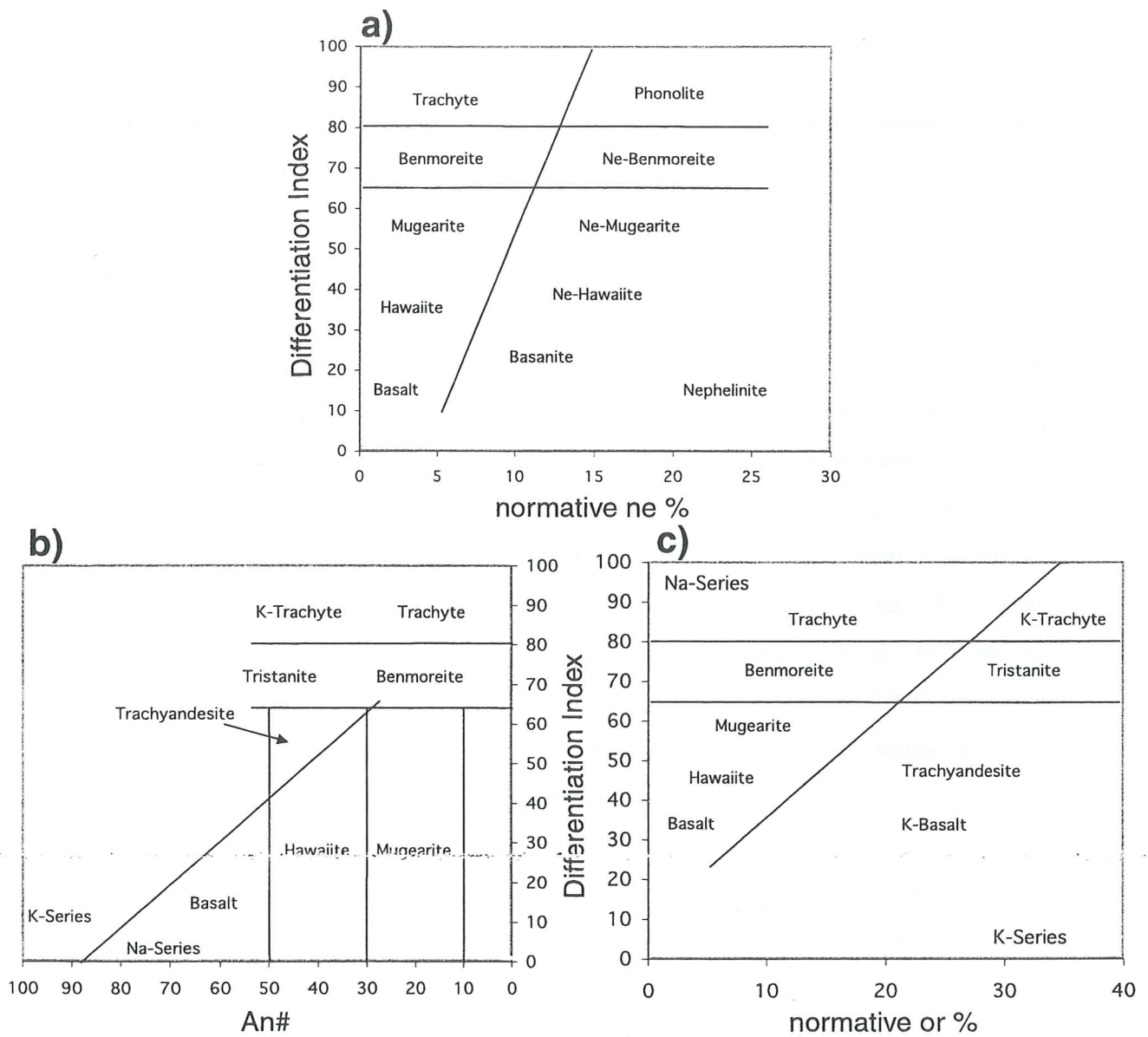


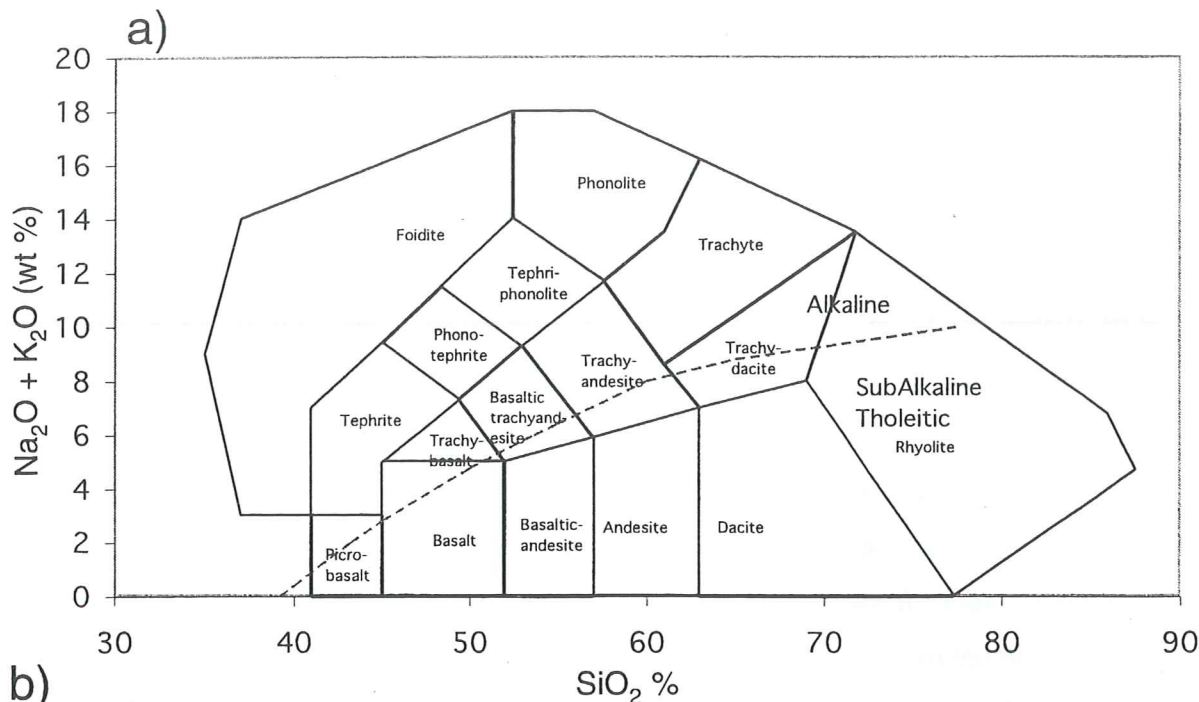
Fig. 5.1. Classification schemes of Price (1973). (a) norm. ne boundary between the mildly undersaturated lineage and the strongly undersaturated lineage, (b) scheme used to separate the potassic rocks from the sodic rocks in the lineages, (c) norm or-boundary between the two undersaturated lineages.

comprises hawaiite-mugearite-benmoreite, while the potassic variants are named potassic trachybasalt-shoshonite-latite respectively.

This classification scheme is solely geochemical and is not related to the tectonic environment in which they are created.

The alkalic Dunedin volcanic rocks plot in the upper half of the scheme (Fig. 5.2 & 5.3). The two trends proposed by Coombs and Wilkinson (1969) and refined by Price (1973) to also include potassic variants, plot along two reasonably well defined lines (Fig. 5.3); the variations are caused by fractional crystallization. Most of the basalts of the sodic lineage plot along the border between picrobasalts and basanites, having a SiO_2 -content between 43-45% and a total alkali content between 2.5-4.0 % (Fig. 5.3). The more evolved, mildly undersaturated rocks plot along the border between less undersaturated and strongly undersaturated rocks in the classification scheme (Fig. 5.3). However, most of the analyses made by Coombs and Wilkinson (1969) and Price (1973), plot in the less undersaturated field making the sodic variants hawaiite-mugearite-benmoreite (in accordance with the earlier classification scheme (Coombs and Wilkinson, 1969), and the potassic variants being shoshonites and latites (earlier classified as trachyandesites by Price(1973)). Despite the differences in ratio between Na_2O and K_2O , and increased total alkali content, the potassic undersaturated rocks plot along the same differentiation trend as the sodic, slightly undersaturated rocks.

The strongly undersaturated lineage plots within the the fields basanite-phonotephrite-tephriphonolite-phonolite. Most rocks within this lineage are strongly sodic, and only a few are potassic. The strongly sodic nature of this lineage is seen as larger percentage of normative nepheline, $\text{NaAlSi}_3\text{O}_8$ (between 10 and 25 %). Both the sodic and the potassic variants plot within the basanite-phonotephrite-tephriphonolite-phonolite fields roughly along the same trend.



b)

Further subdivision of intermediate fields	Trachybasalt	Basaltic trachyandesite	Trachyandesite
$\text{Na}_2\text{O} - 2.0 \geq \text{K}_2\text{O}$ (1)	Hawaiite	Mugearite	Benmoreite
$\text{Na}_2\text{O} - 2.0 \leq \text{K}_2\text{O}$ (2)	Potassic trachybasalt	Shoshonite	Latite

Fig. 5.2 a. and b. TAS classification system (Le Bas et al., 1986). (a) Total alkali vs. silica diagram. Dotted line marks boundary between alkaline and tholeiitic rocks. (b) further subdivision of intermediate rocks into a sodic (1) and a potassic (2) part.

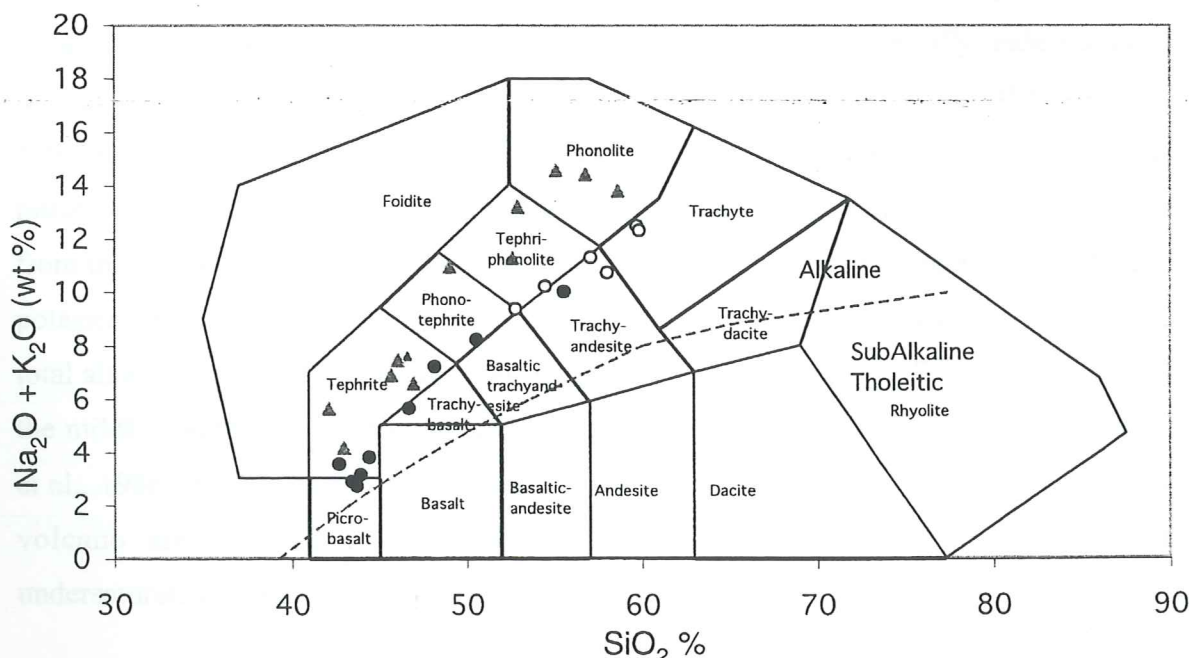


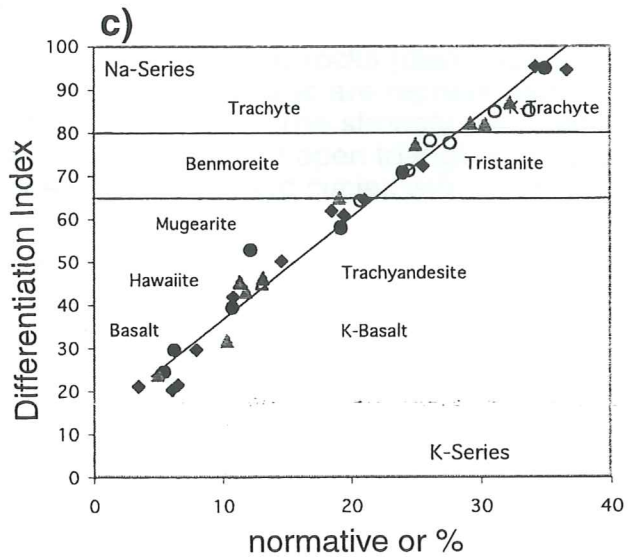
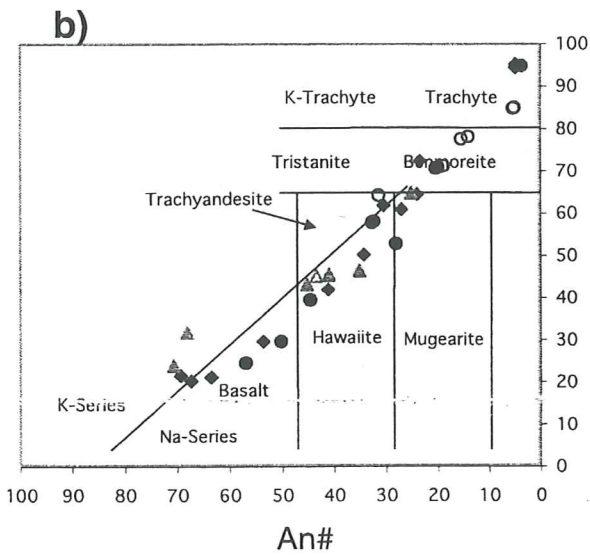
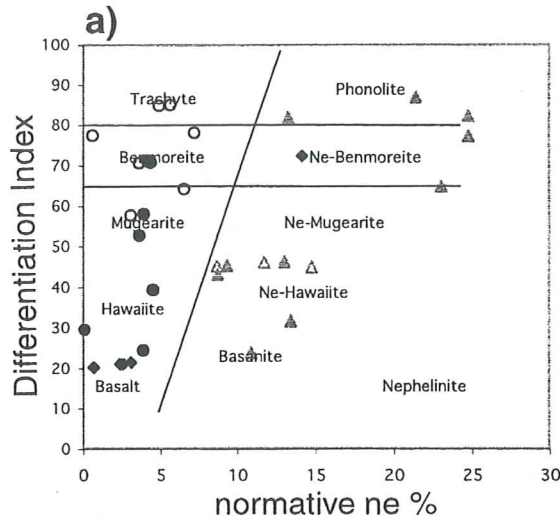
Fig. 5.3 Representative rocks of the Dunedin Volcano. Members of the strongly undersaturated lineage are shown by triangles. The mildly undersaturated lineage have members both from its sodic (filled circles) and from its potassic part (open circles).

5.3 Whole rock analyses of the Portobello Peninsula

The 13 whole rock analyses made of rocks from the peninsula were analysed using XRF (both major and trace elements) (see section 6.2). To be able to compare them with the other rock of the Dunedin Volcanic Complex the element oxides were normalized using the CIPW norm calculations. The analyses were plotted both on the TAS classification scheme and on the three major classification schemes used by Price (1973).

As can be seen from Price classification schemes, the rocks of Portobello Peninsula overlap with the rocks of the two lineages in the plot showing differentiation index, DI, vs. normative Or (Fig. 5.4c), and in the diagram comparing DI to normative An[#] (Fig. 5.4b). The third major diagram (Fig. 5.4a) is inadequate for eight of the rock analyses, since they lack normative nepheline. This will be dealt with in the next section. The remaining five rocks plot as members of the mildly undersaturated lineage (4 analyses) and as a member of the strongly undersaturated series (1 analysis).

For the five rocks containing normative nepheline four analyses plot along the mildly undersaturated trend, and one analysis plots along the strongly undersaturated trend in the TAS classification scheme (Fig. 5.5). The eight remaining analyses (of which only two are trachytes) don't plot along these trends. Instead they plot much closer to the boundary which separates the alkaline and the subalkaline trends. One analysis plots as a basalt, being a bit more silica rich (46 %) than the basalts of the mildly undersaturated lineage. According to the K₂O:Na₂O classification of Le Bas et al. (1986), shown in Fig. 5.2b, all of the Portobello evolved rocks lack normative nepheline and have potash:soda ratios which characterize them as potassic trachybasalt, shoshonite and latite. If rocks from the Portobello Peninsula and from the mildly undersaturated lineage (both sodic and potassic) with the same silica content are compared, the hy/qz normative rocks have a total alkali content 1-2% less than their undersaturated counterparts. The potassic parts of the mildly undersaturated lineage have previously been inferred to be saturated (Coombs et al., 1986), but the as fig. 5.4a combined with fig. 5.5 show many potassic rocks in the volcano are undersaturated. Thus, a distinction can be made, separating the undersaturated rocks from the saturated and oversaturated rocks.



Figures 5.4a, b and c. Schemes showing the distribution of rocks from Portobello Peninsula (diamonds) compared to representative rocks from the undersaturated lineages. The mildly undersaturated lineage is represented by filled circles (sodic) and open circles (potassic). The strongly undersaturated lineage is represented by filled triangles (sodic) and open triangles (potassic). (a). normative ne boundary clearly distinguish the strongly undersaturated from the mildly undersaturated lineages. (b). and (c). All the rocks plot along the same line. No separation between potassic and sodic types can be made from these schemes.

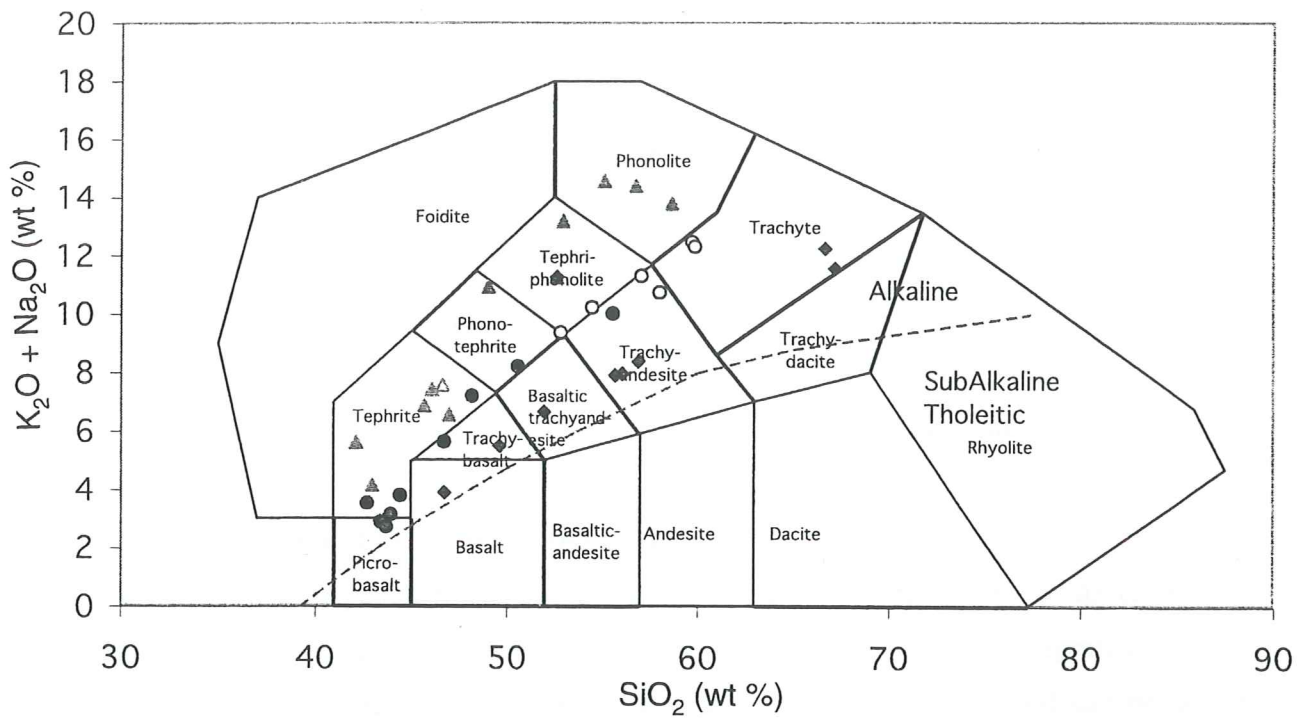


Fig. 5.5. TAS diagram showing distribution of Portobello volcanic rocks (diamonds), compared to the undersaturated lineages. The mildly undersaturated lineage are represented by filled circles (sodic members) and open circles (potassic members). The strongly undersaturated lineage are represented by filled triangles (sodic members) and open triangles (potassic members). The poobello picro basalts are shown as round filled circles with a thin darker edge.

The inadequacy of the TAS classification system (not having enough fields) is evident when the potassic variants of the mildly undersaturated lineage are compared to the qz/hy normative rocks. Despite them being chemically distinct, they still plot within the same field, and since they both have a similar K_2O and Na_2O distribution, they all get the rock names potassic trachybasalt, shoshonite and latite. Another inadequacy of this classification system, is the choice of the name for shoshonite. This rock name is traditionally thought to be related to arc volcanism and not to intra-plate settings. Usage of the name will cause more confusion than clarity; another name would be appropriate.

5.4 Classification of hy/qz normative rocks

The rocks with a geochemical composition containing normative hy or qz cannot, as mentioned above, readily be presented on the existing classification diagrams. To deal with this shortcoming, an extension of the diagram normative ne vs. DI can be added, containing normative qz + half the amount of normative hypersthene (D. Coombs, pers. comm.; Johnson et al., 1976). The addition of hypersthene onto the normative quartz content is done to take into account the amount of SiO_2 present as normative hy. This plotting technique has not been applied to the Dunedin volcano before, although silica saturated, hypersthene normative rocks, in addition to the trachytes were known (Coombs, pers. comm.), their status were considered uncertain because of the dominance of the ne-normative components. If plotted on this diagram, the analyses made for this thesis indicate increasing oversaturation as fractionation proceeds (see figure 5.6). The excess silica in the less evolved rocks (basalt, potassic trachybasalt and shoshonite) is all bound in normative hypersthene, while in the more evolved latites both normative hypersthene and quartz occur, giving them a $qz+hy/2 \approx 6\%$. The analysed trachytes have all the excess silica as normative quartz, one having 6.6% and the other having 12%. However the presence of normative corundum suggests that the trachytes are weathered, which if corrected for, would decrease the amount of excess quartz.

Among the Dunedin volcano rock data published in the thesis of Price (1973), 12 whole rock analyses matching the characteristics of the rocks from Portobello Peninsula, were found. If the TAS classification system is used, these data consist of 6 basalts, 1 mugearite, 3 latites and 2 trachytes. Just like the rocks on the Portobello Peninsula

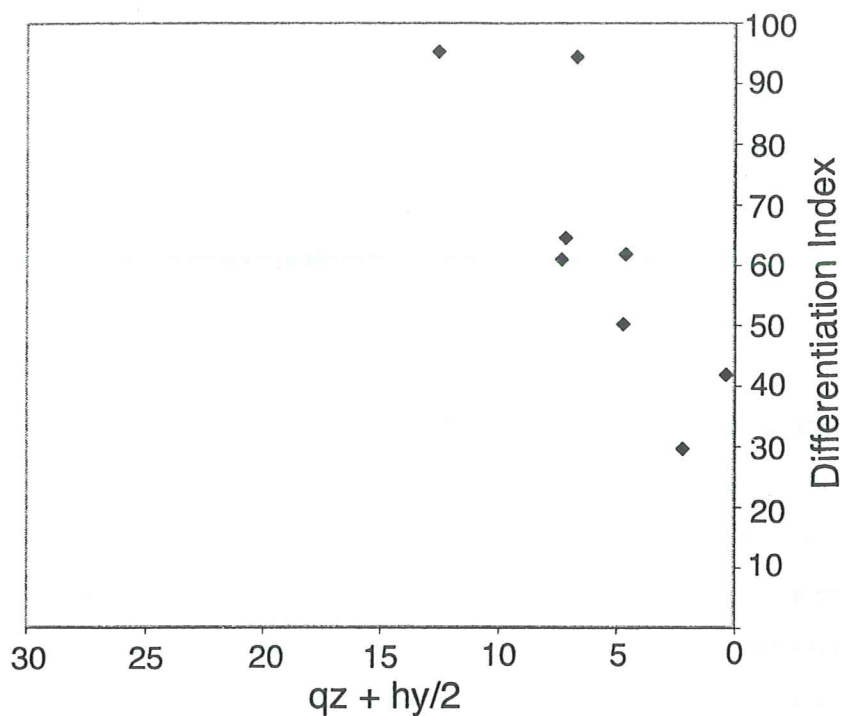


Fig. 5.6 Diagram showing the degree of oversaturation in eight samples from the Portobello Peninsula.

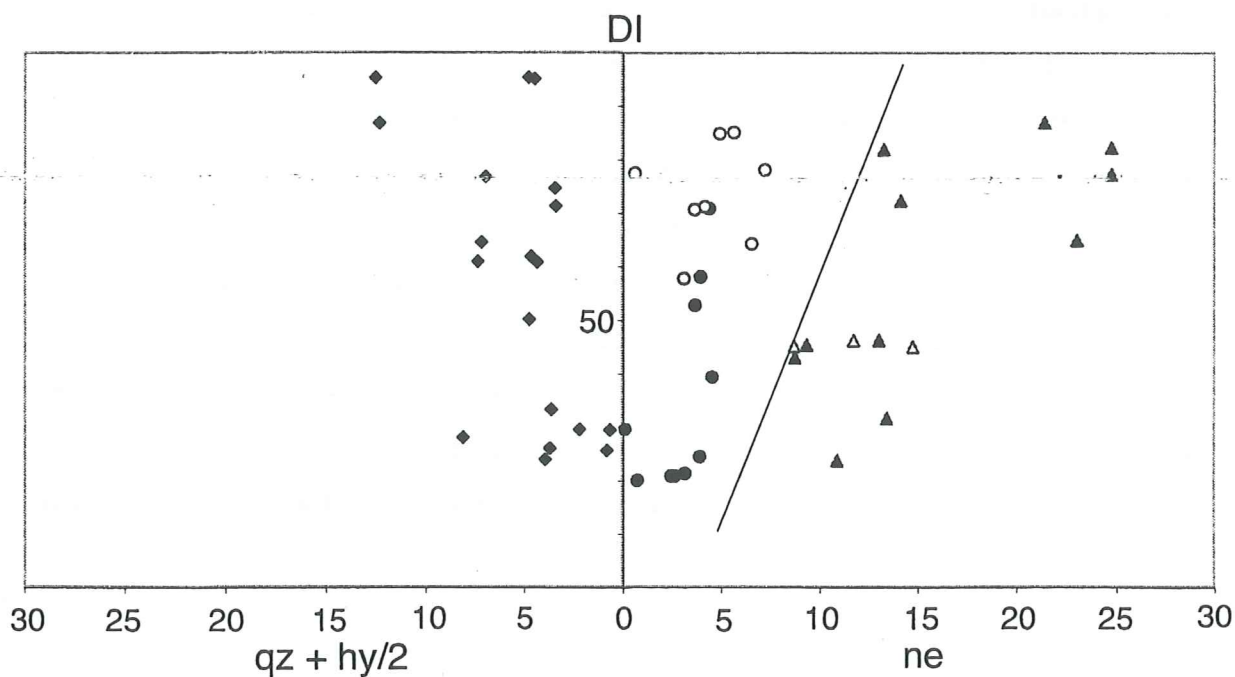


Fig. 5.7 Diagram showing Differentiation index versus either normative nepheline or qz+hy/2. The undersaturated rocks from Portobello Peninsula are shown as members of the undersaturated lineages.

analysed in this thesis, the basalts only contain normative hy, while all the others contain both hy and qz. If all the saturated and oversaturated rocks are plotted in the same diagram, together with the Portobello data, a less organized pattern results (see figure 5.7), but the distribution of rocks within the qz + hy/2 field is not more scattered than the rocks belonging to the two previously inferred lineages (Fig. 5.7).

5.5 Oxidation state

The XRF analyses made on the rocks only give the total amounts of iron in the rocks and not the actual Fe^{3+}/Fe^{2+} ratio in the rocks. The ratio of ferrous and ferric iron is computed using the standard procedure of Middlemost (1989). The ratio between the two oxidation states is related to the total alkali content and the silica content. Since the actual ratio of the rock isn't measured, the oxidation state of the magma is not considered in the normalization of the element oxides. Variations in this parameter will not show in the CIPW norms. Changes in oxidation state might cause ne-normative rocks to cross the line into the oversaturated field. To make sure that differences in oxidization state are not responsible for the shift from normative ne to qz, all the oversaturated rock analyses were normalized having all iron as either 2+ or 3+, simulating a strongly reducing and a strongly oxidizing environment. The result of this calculations can be seen in Fig. 5.8. All but one, the potassic trachybasalt, stays within the field of oversaturation irrespective of reducing or oxidizing environments. The effects of changes in oxidation state decrease with fractionation as the amount of total iron decreases. This test is taken as a proof of the existence of saturated to oversaturated magmas in the Dunedin volcano. The transfer of the potassic trachybasalt into the ne normative field, makes this rock an unsuitable representative of oversaturated rocks and is disregarded in further consideration. Plotting of the potassic trachybasalt in the TAS diagram indicates that this rock could represent a slightly evolved rock from an oversaturated magma.

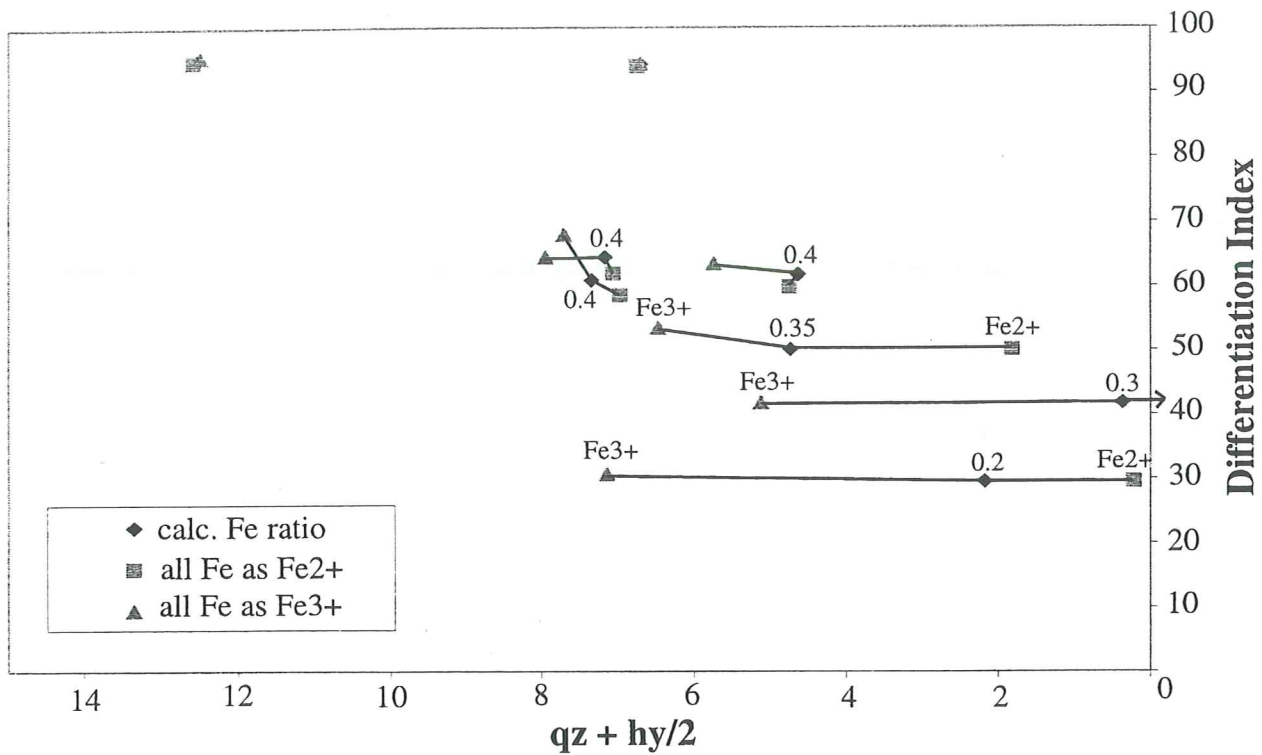


Fig. 5.8. Diagram showing the difference in normative quartz content with changing oxidation state. All but one of the oversaturated rocks (the potassic trachybasalt) from the Portobello Peninsula normative quartz and/or hypersthene irrespective of oxidation state.

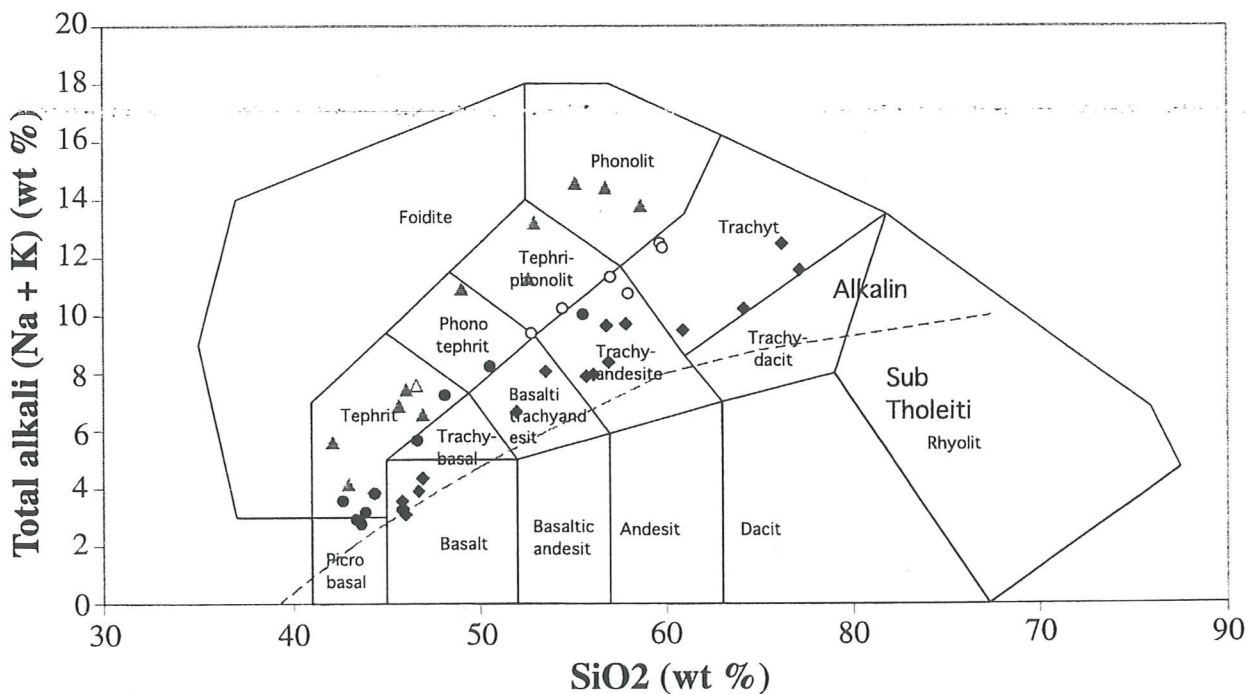


Fig. 5.9. TAS diagram showing the chemical variation of rocks within the Dunedin Volcano. The saturated to oversaturated rocks (diamonds) seem to make up a lineage of their own in addition to the mildly undersaturated lineage (sodic-filled circles, potassic-filled circles) and the strongly undersaturated lineage (sodic-filled triangles, potassic-open triangles).

5.6 Conclusion; Proposal of new lineage within the Dunedin Volcano

The differences discussed above make the existing classification of the rocks in the Dunedin volcano inadequate, in that it can't fully present all the rocks of the volcano. On the basis of the different distribution of the major elements (shown in figures 5.7 and 5.9) between the oversaturated rocks and the two existing lineages, I propose an extension of the variation of volcanic rocks of the Dunedin volcano into the hy-normative field. This third lineage contains the rock series (basalt-potassic trachybasalt-shoshonite-latitude-qz trachyte) as shown in figure 5.9. The characteristics for this lineage will be described in the next chapter, followed by a comparison with the existing lineages.

6. Geochemistry of the saturated to oversaturated lineage

6.1 Saturated to oversaturated lineage (basalt-potassic trachybasalt- shoshonite-latitude-qz trachyte)

Definition of the saturated to oversaturated lineage is based on major element data from 19 oversaturated rocks, and trace element data from 10 of them. The major and trace elements will be described in separate sections, followed by sections in which this new lineage is compared with the two earlier defined lineages.

6.2. Analyzing techniques

13 whole rock samples were taken for geochemical analysis. The analyses were performed in the geochemical laboratory at the University of Otago. The samples were prepared and crushed into a fine powder. All were analysed for major elements, and 9 of them were also analysed for trace elements. Both the major and trace element analyses were done by the XRF technique. The samples for the major analyses were prepared by mixing 0.64000 ± 0.00005 g of rock powder, 6.80000 ± 0.00010 g flux and 1.00 g NH_4NO_3 . This mixed was preignited, fused into a bead and analysed by XRF. The LOI value determined by weighing 2.0 g of rock powder, heating the rock powder in a furnace, and then reweighing it. From these weight differences the waterloss and be estimated. Trace element samples were analysed from a pressed powder pellet, prepared by mixing of rock powder and a binder.

6.3 Field relationship/aerial distribution

Hy/qz normative rocks are mostly confined to the Otago Harbour, but have been found all the way from Kaikorai Valley through the central parts of Dunedin to the outer parts of the Dunedin Harbour. This E-W pattern is, however, broken by one analysis performed by Price (1973), a basalt which is found at Swampy Summit, some 5 km northwest of Dunedin. This basalt makes up the basal layer with volcanics on top belonging to the third phase of Benson (1968). This basalt overlies the Abbotsford Mudstone, a unit preceding the volcanism. The samples taken from central Dunedin (D. Coombs, pers. comm.) were obtained in drill cores, during construction work on Cumberland Street in the late 1960's. The saturated to oversaturated rocks are quite widely distributed but,

where they occur outside of the harbour, they make up the basal layer, overlying non-volcanic, sedimentary units.

6.4 Major elements

6.4.1. Oversaturated lineage

Major element distribution is shown in Harker diagrams in figure 6.1 and in MgO variation diagrams in figure 6.2. Al_2O_3 , Na_2O and K_2O all increase with increasing SiO_2 content, consistent with production of more alkali feldspar as fractionation proceeds (Coombs et al., 1968). TiO_2 , Fe_{total} , MgO and CaO have a negative correlation with increasing SiO_2 content, since these elements mainly exist in major amounts in mafic minerals such as olivine, Ca-feldspar, magnetite and titanite (Coombs and Wilkinson, 1969). P_2O_5 show a random distribution with values spanning from 0.03 to 0.67 wt %. The maximum value attained is found in a shoshonite (SiO_2 -content 53%). The basalts of the lineage show large differences in the distribution of P_2O_5 from 0.2 to 0.6 wt %. When considered as a major element, no trend can be plotted for this element oxide, but it will be further considered under section spidergrams (6.4.1). The Mg numbers of the least evolved members are low indicating that even these rocks have gone through fractionation before emplacement. According to Reay and McIntosh (1991), magmas in the central area tend to be more evolved, with higher DI and lower Mg numbers, compared to the peripheral magmas. This feature is also well documented from several Cenozoic volcanoes in eastern Australia (Johnson, 1989).

6.4.2 Comparison to the undersaturated lineages

When compared to the other rocks of the volcano several differences are apparent. The total amount of alkalis in the oversaturated rocks are 1-2 wt% less than their potassic, mildly undersaturated counterparts. If compared to the mildly undersaturated sodic parts, the total alkali content is approximately the same but the silica content in the oversaturated rocks are much higher. The basalts of the different lineages plot in different areas in the TAS classification scheme, the undersaturated ones plot as picobasalts and tephrites whereas the oversaturated variants plot as basalt. The distribution of P between

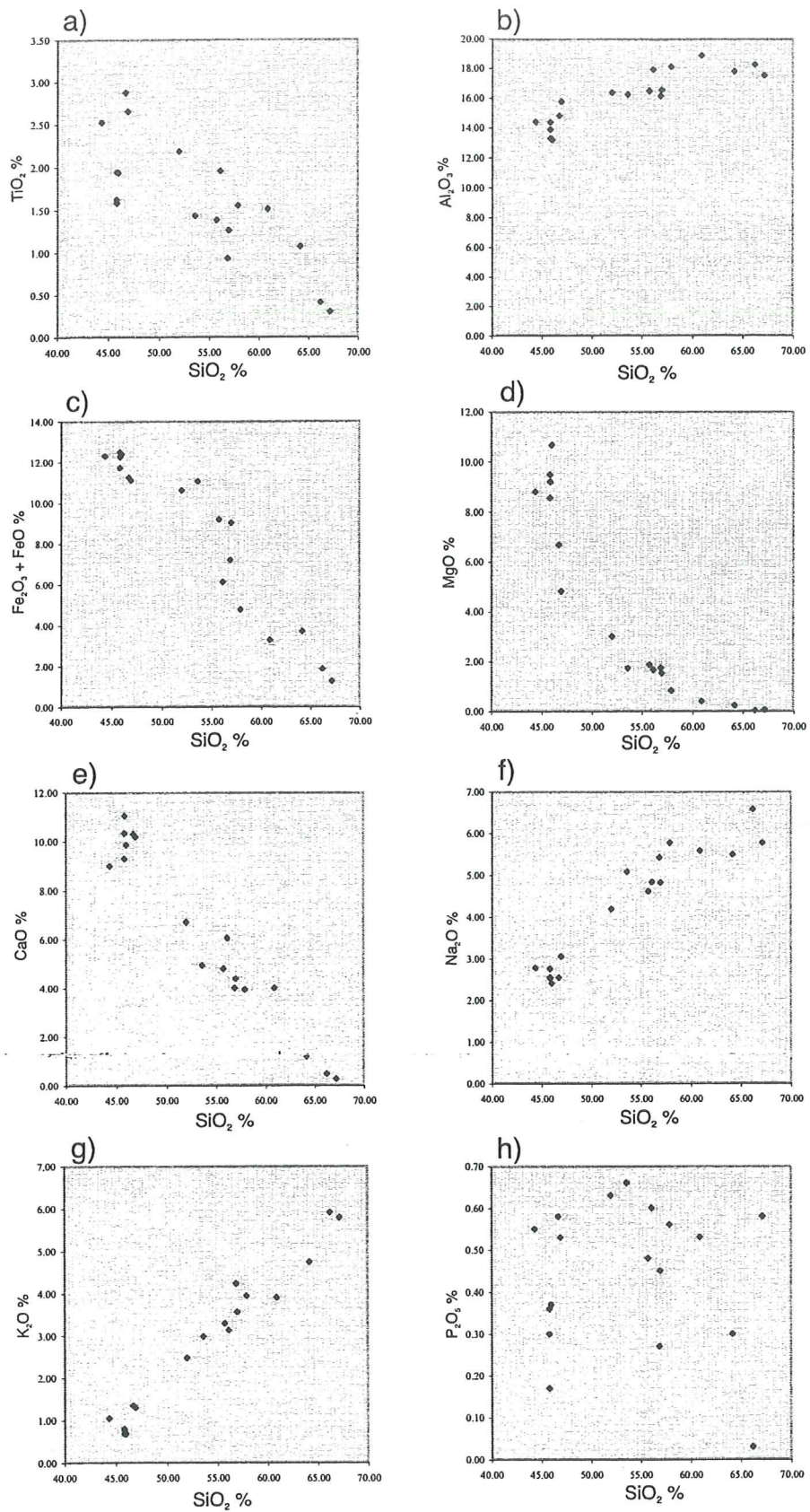


Fig. 6.1. a-h Harker diagrams showing element distribution in the oversaturated lineage

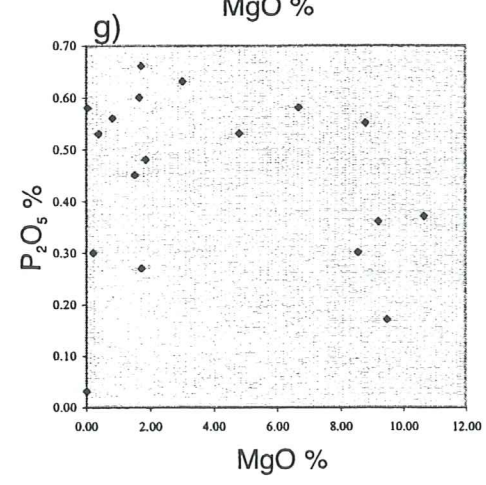
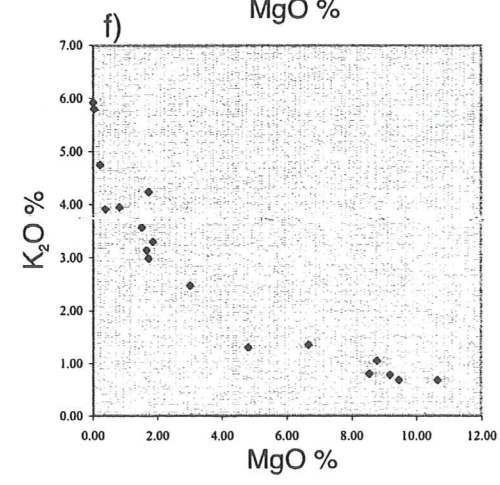
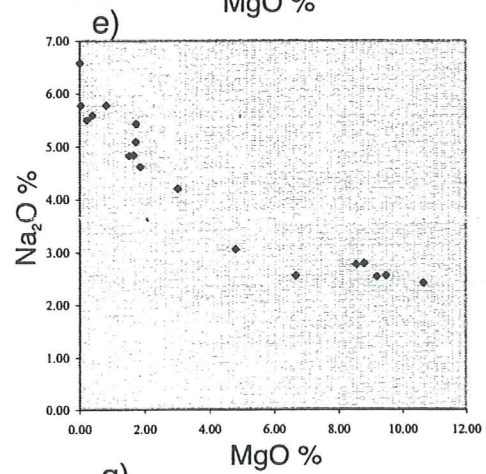
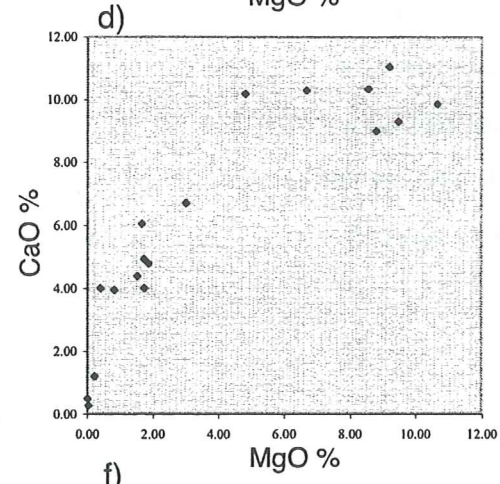
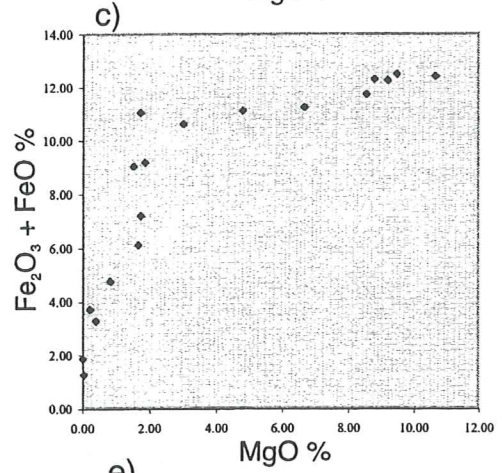
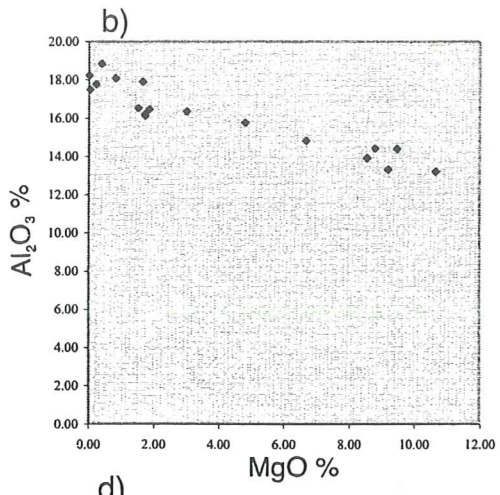
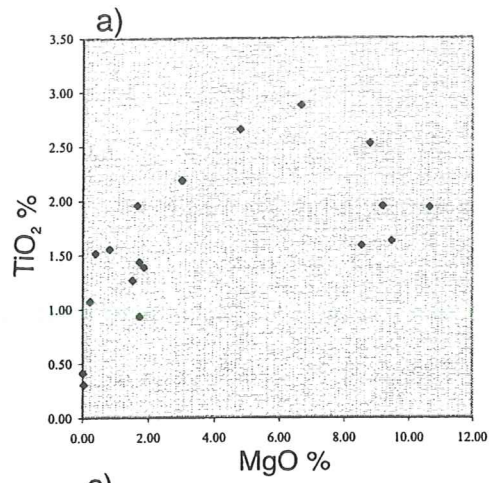


Fig. 6.2. a-g MgO variation diagrams showing element trends with decreasing MgO from right to left.

the saturated to oversaturated and the undersaturated lineages, is also somewhat different. Depletion of P does not seem to occur to the same extent as in the undersaturated lineages. Reasons for this behaviour will be discussed in the trace element section (6.5.1). Apart from these differences the general trends of the major oxides are the same in all of the three lineages.

The distribution of the alkalis in the intermediate rocks divides both the existing lineages into two parts, one potassic and one sodic part. The existence of the potassic parts have been explained by wall rock interaction, which has given the magma a larger potassium content (Coombs and Wilkinson, 1969) and at the same time also increased the silica content. In the oversaturated lineage, almost all the analysed rocks fall into the potassic field, having $K_2O \geq Na_2O - 2.0$ (Le Bas et al., 1986). The one analysis that plots as a sodic variant (mugearite) makes it likely that a sodic variant of this lineage possibly also exists within the volcano, but it is as yet, poorly characterized.

6.5 Trace elements

6.5.1. Oversaturated lineage

The trace elements Sc, V, Cr, Ni, Cu, Zn, Ga, As, Rb, Sr, Y, Zr, Nb, Ba, La, Ce, Nd, Pb, Th and U were analyzed. In the analysis (OU 30421) taken from Price (1973), Sc, As, La, Ce and Nd are not analyzed precluding comparisons of these element to the other lineages impossible.

The elements will be described in groups, depending on their geochemical behaviour. The groups described are high field strength elements (HFSE), large ion lithophile elements (LILE), chalcophiles and ferromagnesian elements. Y, La, Nd and Ce will be dealt with separately. As was only found in small concentration (1-2 ppm) and will not be discussed.

In summary, Rb, Pb, K, Nb, Zr, Th, U, Ga, La, Ce and Nd show continuous enrichment as fractionation proceeds, while Sr, Cu, V and Sc show continuous depletion throughout the lineage. The other elements show fluctuations in enrichment, most of them showing a breakage in trend between shoshonites and latites. All but one rock analysis, latite71, are taken from the Portobello Peninsula. The more evolved latite is from Deborah Bay, on the northern side of the harbour, some 2 km to the north of the peninsula.

HFSE (Nb, Zr)

Nb and Zr both show similar patterns being enriched throughout the lineage. Nb concentrations vary from 40 ppm in the basalts to 75 ppm in one of the latites (see figure 6.3a) while Zr occurs in much higher concentrations having values between 193-441 ppm (see figure 6.3b) in the same interval. The trachytes are enriched in both the elements compared to the less evolved rocks of the lineage (see figure 6.3c). The degree of enrichment between the two differs greatly, the more silica rich trachyte having almost double the amount of Nb (144 ppm compared to 78 ppm for latite64) and 25% more Zr (542 ppm compared to 425 ppm). Increasing amounts of these elements as fractionation proceeds are expected since both of them are incompatible to most mafic minerals. The mineral they most readily can enter is titanomagnetite. Both Nb and Zr are most compatible in environments of high temperature and/or low pressure. According to Nielsen and Beard (2000) the distribution coefficients, D_{Zr} and D_{Nb} , are above 2 in these conditions. Titanomagnetite is a common mineral in all the Dunedin volcanic rocks, and is thought to be one of the minerals crystallizing in basaltic magmas causing the fractionation trends of the same (Coombs and Wilkinson, 1969; Price, 1973). However, the increasing abundance of Zr and Nb throughout the lineage, and the presence of titanomagnetite only in the groundmass, indicate that no fractionation of titanomagnetite has occurred.

LILE (Ba, Rb, Sr, Pb, U and Th)

From mafic to intermediate compositions Ba, Rb, Pb, U and Th all show continuous enrichment. Ba, Rb and Pb show some signs of depletion in the more evolved latite compared to the other latite, while the other two show a continuous enrichment throughout the lineage (see figure 6.4). Sr shows anomalous behaviour being depleted throughout the fractionation process. The greater part of the depletion is, however, taking part in the more evolved rock, where concentrations drop from 425 to 221 ppm between latite64 (OU 63903) and latite71 (OU 30421).

Fig. 6.3 a-c

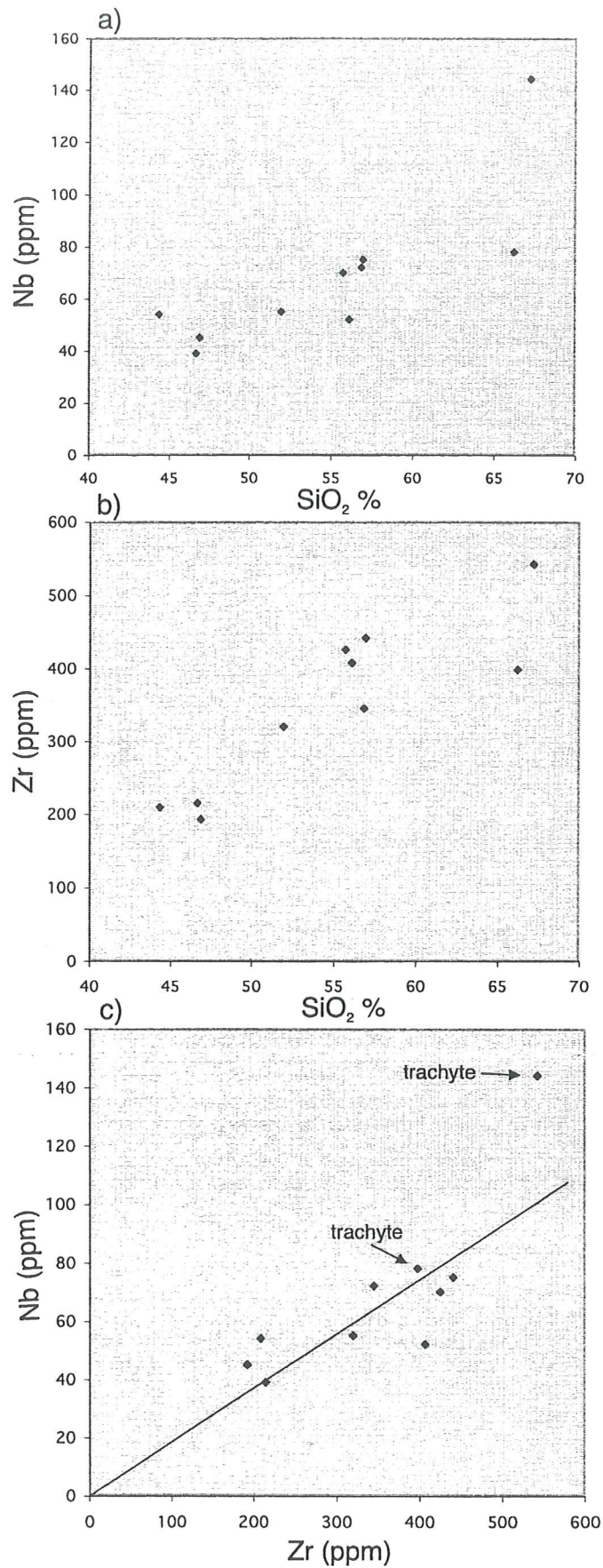


Fig. 6.3 a-c. HFSE elements (a) diagram showing Zr vs. silica (b) diagram showing Nb vs. silica (c) diagram showing difference in enrichment between the two trachytes.

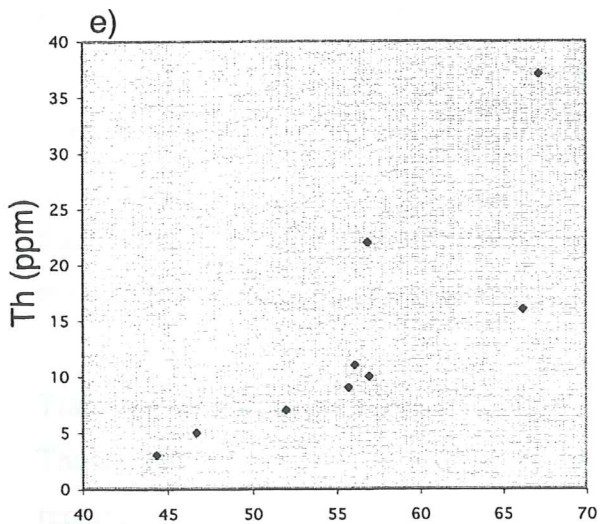
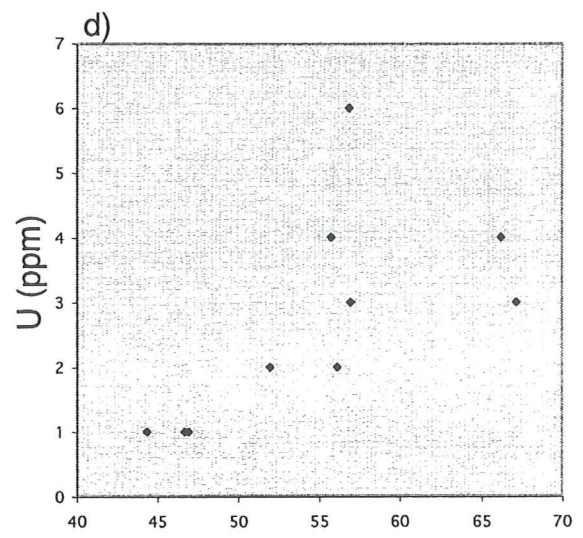
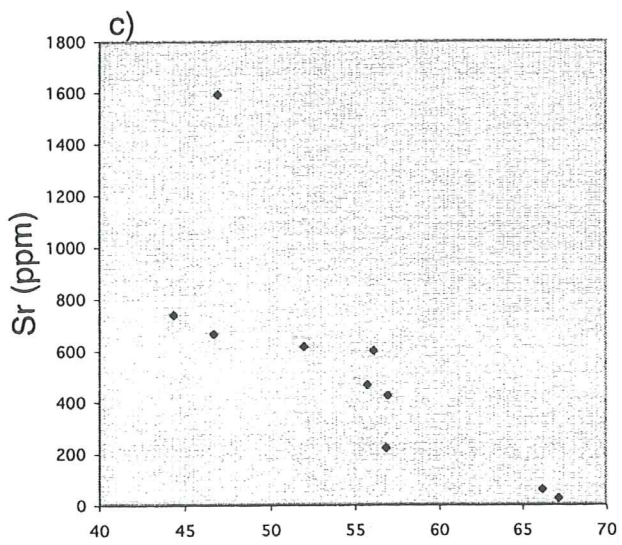
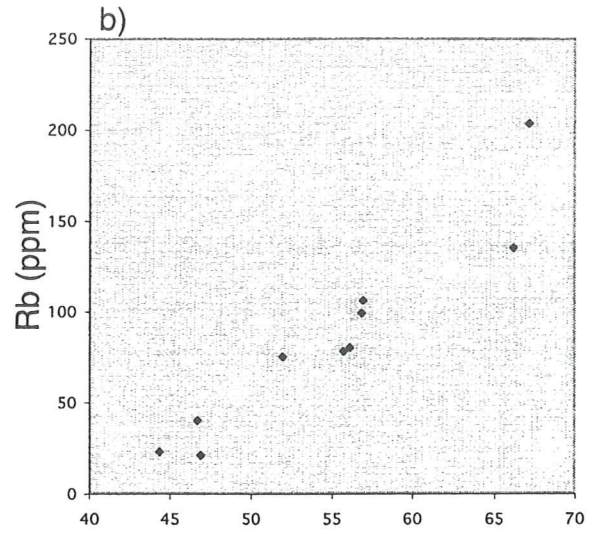
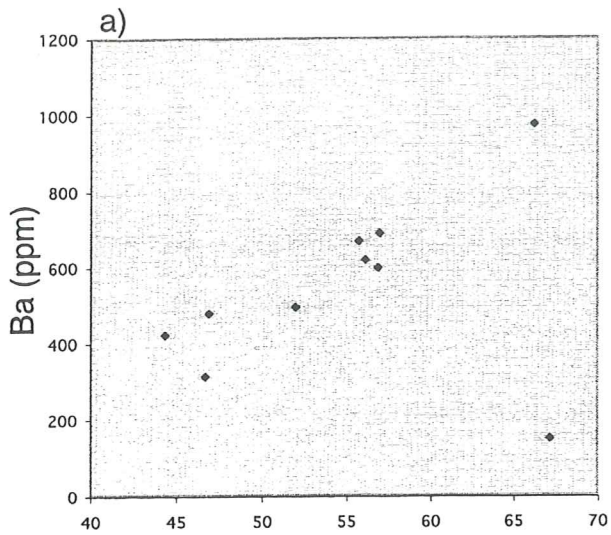


Fig. 6.4. a-e LILE variation with increasing silica content.

All LILE are incompatible in mafic melts (Green, 1994). The depletion of Sr early on in the fractionation process is best explained by fractionation of plagioclase in small amounts. The acceleration of Sr depletion is probably caused by the fractionation of plagioclase crystals from the melt. Sr has a higher partition coefficient, D_{Sr} in albite rich parts of the plagioclase (Blundy and Wood, 1991), which makes the depletion of Sr increase as the plagioclase composition evolves towards the albite component. Depletion in both Sr and Ba in the more evolved latite can be explained by fractionation of alkali feldspar (Guo and Green, 1989; Wilson et al., 1995; Blundy and Wood, 1991), something that is compatible with the phenocrysts of alkali feldspar in the latites. Lack of Ba depletion in early stages is probably a combination of a lower partition coefficient in plagioclase compared to Sr, smaller amount of plagioclase fractionated and the more anorthite-rich composition of the plagioclase.

Pb occurs in very small concentrations in the Dunedin volcano. The observed depletion with fractionation might be considered too small to be of any significance.

The large enrichment in Th is most likely caused by hydrothermal processes.

Chalcophile elements (Zn, Cu and Ga)

These elements show contrasting behaviour having Ga increasing throughout the lineage (see figure 6.5c), while Cu shows depletion throughout the same (see figure 6.5b). Zn has more or less the same concentration all through the lineage being around 100 ppm (see figure 6.5a). Gallium concentrations vary between 19-33 ppm, having its largest increase in the mafic part of the lineage. The only minerals present in this lineage Ga can enter are titanomagnetite and feldspar (Schroll, 1999). Ga mimics the behaviour of Al (Schroll, 1999). The increasing concentrations throughout the lineages, suggest that no fractionation of titanomagnetite has occurred. This is compatible with the observations of the HFSE, but contradict the concentration pattern of Sc (see section transition elements).

Transition elements (Sc, Cr, Ni and V)

These elements have also been called the ferromagnesian elements for their ability to replace magnesium and iron in olivine and clinopyroxene (Price 1973). All four show a negative correlation with fractionation (see figure 6.6), but anomalies occur in Cr and Ni.

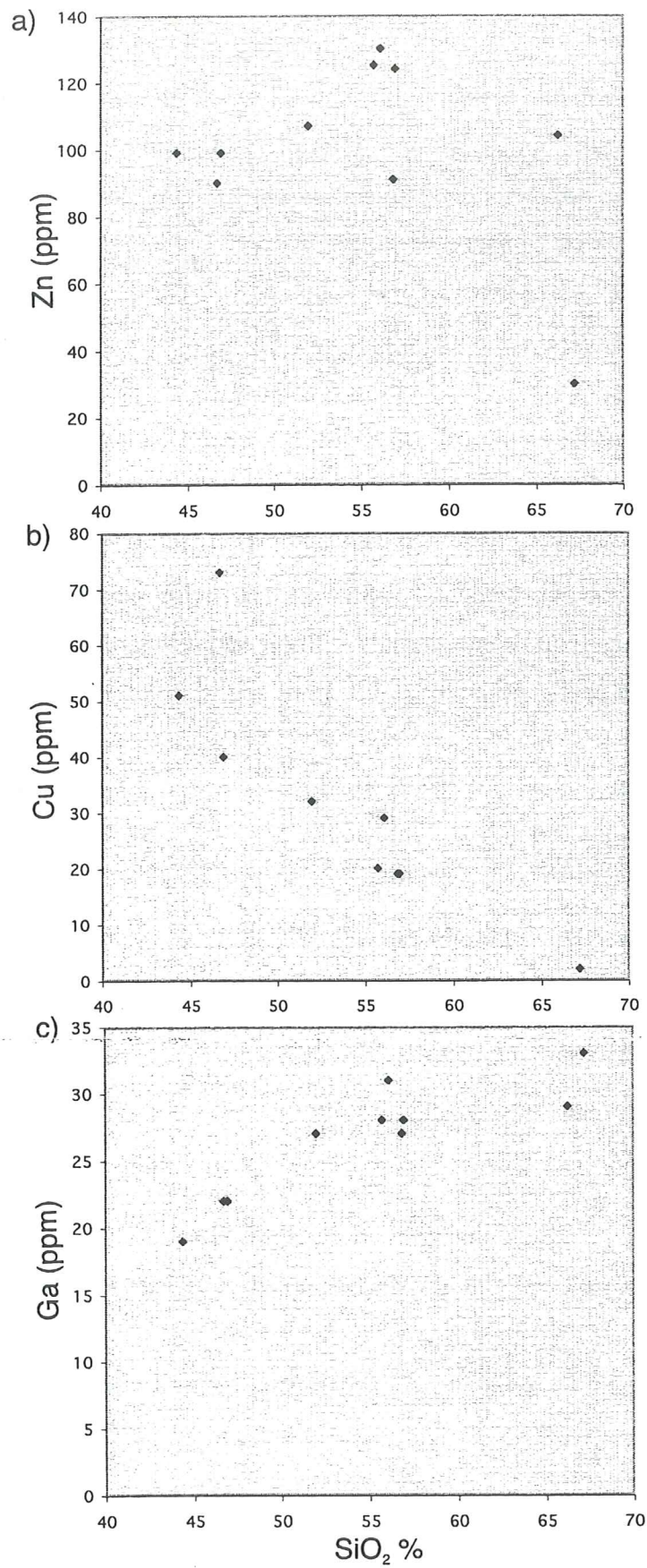


Fig. 6.5. a-c Chalcophile element distribution with increasing silica content.

Sc and V both show continuous depletion throughout the fractionation trend. Both elements most easily partition into clinopyroxene (Hart and Dunn, 1993; Green, 1994), suggesting a continuous fractionation of this mineral throughout the series. Cr shows a strong depletion dropping from 563 to 4 ppm, from basalt to the less evolved latite. In the latite71 there seems to be an enrichment (34 ppm) compared to latite64. Ni mimics the behaviour of Cr (103-5 ppm), being depleted in the less fractionated parts and showing an enrichment from latite64 (OU 63903) to latite71 (OU 30421). Nickel can partition into olivine, titanomagnetite (Nielsen et al. 1994) and clinopyroxene, but has a tendency to partition mostly into olivine (Green, 1994). Cr seems to prefer partitioning into clinopyroxenes (Hart and Dunn, 1993; Green, 1994), having $D_{Cr} \approx 3$. The sharp depletions in both these elements are most likely caused by the combined fractionation of olivine and clinopyroxene in the mafic to intermediate portions of the lineage. The apparent enrichment of Ni in the more evolved latite (23 ppm) might partially be explained by total depletion of olivine in the melt, making Ni incompatible to the remaining melt components, and subsequently causing enrichment in the residuum. The similar patterns of Cr are more difficult to explain. As the magma evolves it gets more water rich and gets a higher oxygen fugacity. This causes oxidation of Cr from Cr^{3+} to Cr^{6+} , the latter being strongly distributed into the melt phase. However, in order to get an enrichment from 4-34 ppm in the residuum you need to have 87.5% of the melt fractionated and transported away, which is an impossible scenario. The explanation must be that, either some other process is working as well, or the two members are coming from different magma chambers with different characteristics (A. Reay, pers. comm.). These factors have most likely also affected the enrichment in Ni.

The depletion of both Sc and V suggests a continuous fractionation of clinopyroxene throughout. The Cr pattern cannot entirely be explained by fractionation of only cpx. Comparisons of the depletion patterns between Sc, Ni, V and Cr shows two different patterns. Ni and Cr show a strong depletion in the mafic parts and a weakening depletion in the intermediate to highly evolved rocks while Sc and V show a steady state depletion throughout. The differences in depletion patterns suggest that D_{Cr} -olivine is larger than D_{Cr} -cpx during fractionation of this lineage, in the Dunedin volcano, and in this way more readily mimic the behaviour of Ni.

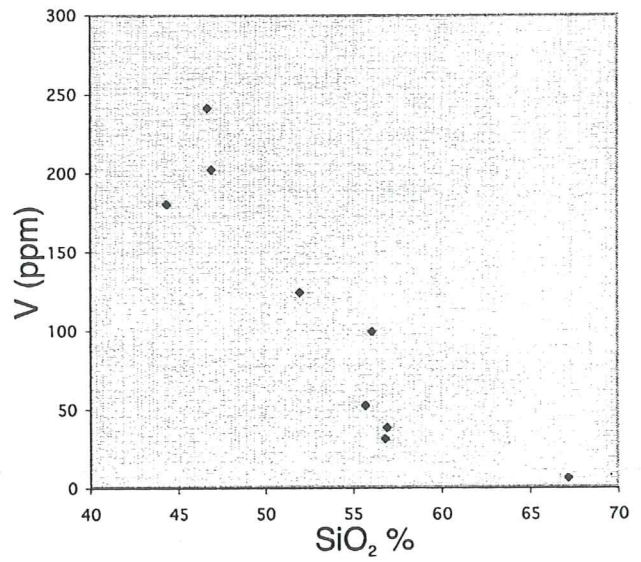
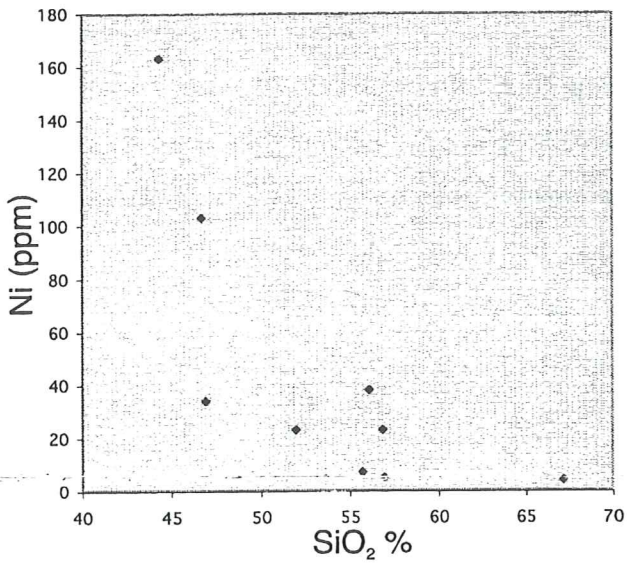
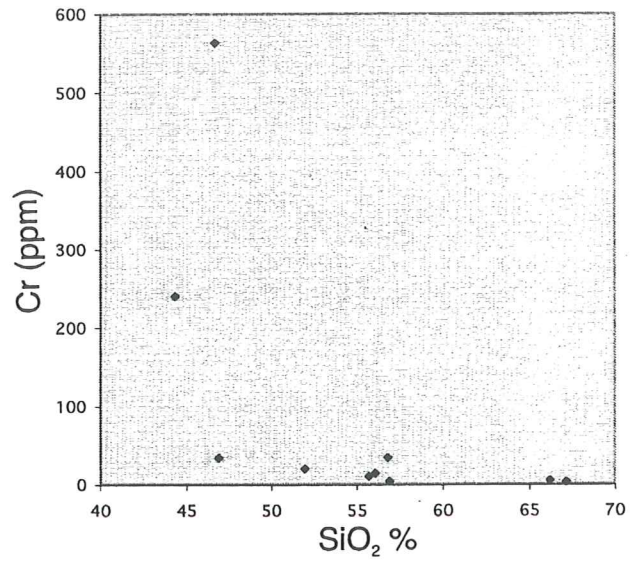
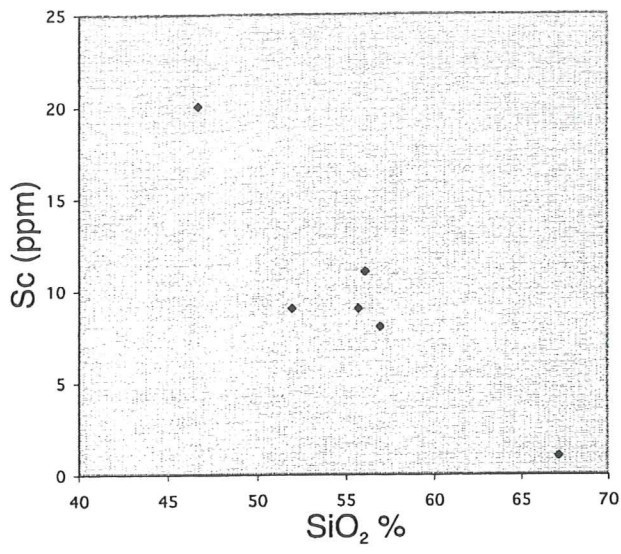


Fig. 6.6. a-d. Transition elements - all four show negative correlation with increasing silica content.

The trachytes of the saturated to oversaturated lineage are strongly depleted with values under 10 ppm for all the four elements. The observed values are consistent between the two trachyte samples, and best explained by continuing fractionation of clinopyroxene. Fractionation of titanomagnetite would best explain the continuous depletion in Sc (Nielsen et al., 1994). However, the lack of depletion of HFSE in the trachytes (see section HFSE), are suggesting that no fractionation of titanomagnetite has occurred and this process can therefore not be used as a solution for Sc depletion. No solution to this contrasting behaviour between Sc and HFSE can be found, only the recognition of the two indicating different behaviour of titanomagnetite in the highly evolved parts of the lineage.

La, Ce, Nd and Y (REE)

All these four can be inferred to belong to the REE. La and Ce are LREE, Nd is to be found in the middle and Y can be seen to represent the HREE. All the four elements show an enrichment as fractionation proceeds (see figure 6.7a). In Y there is a breakage in this trend from latite64 (OU 63903) to latite71 (OU 30421) something that cannot be correlated with the other three elements since no data exist for these samples. The trend of Y is in accordance with observations made on REE patterns of the mildly ne-normative lineage where a depletion of all REE occurs between mugearite and benmoreite (Price and Taylor, 1973). The LREE (La and Ce) show strong enrichment from mafic to intermediate compositions, increasing from 44-108 (Ce 40-85) times the value of primitive mantle. Nd show a similar but smaller enrichment from 22-41 times primitive mantle. The depletion of Y can be explained by the existence of apatite as a phenocryst phase, which can readily incorporate REE in its lattice (Green, 1994).

The trachytes all show enrichment in REE compared to the basaltic rocks of the lineage, something to be expected with continuous fractionation.

Spidergrams

Figures 6.7a and 6.7b show the elements distribution of the members (basalt, potassic trachybasalt, shoshonite, latite and qz trachyte) of the oversaturated lineage. All but the more evolved latite (OU 30421) are rocks found on Portobello Peninsula. The general

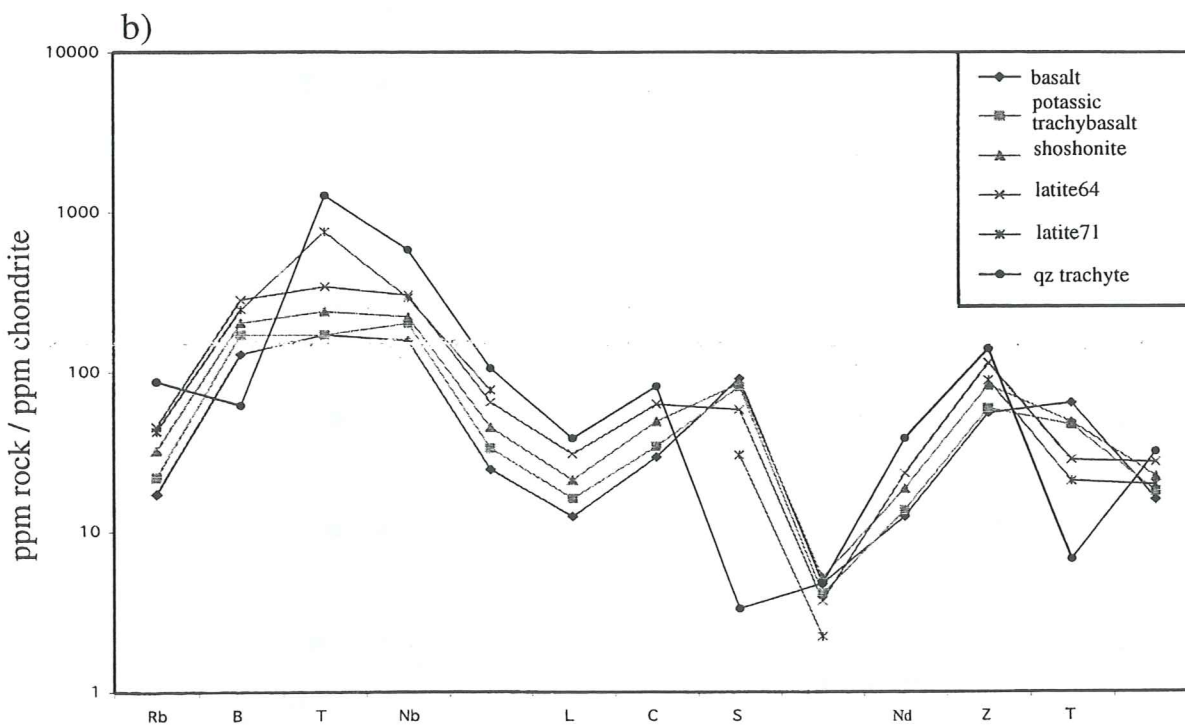
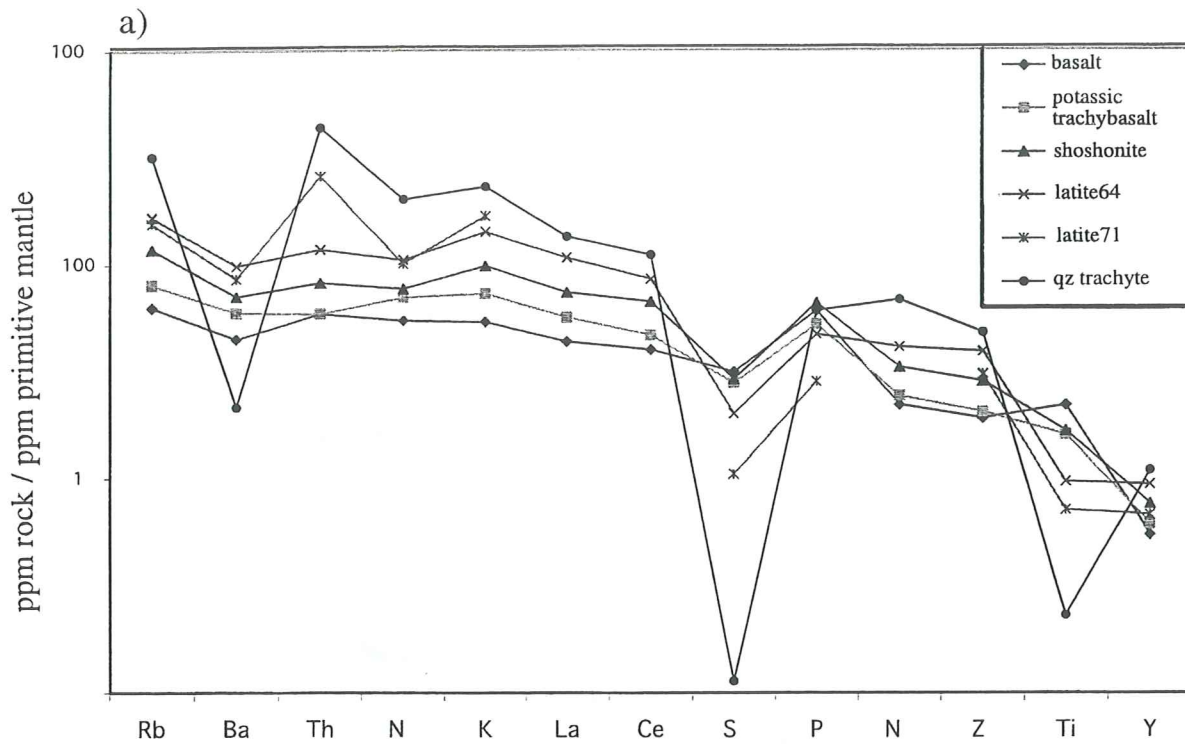


Fig. 6.7 a-b. spidergrams of the oversaturated lineage (a) values normalised against primitive mantle (Sun and McDonough, 1989) (b) values normalised against chondrite (Sun and McDonough, 1989).

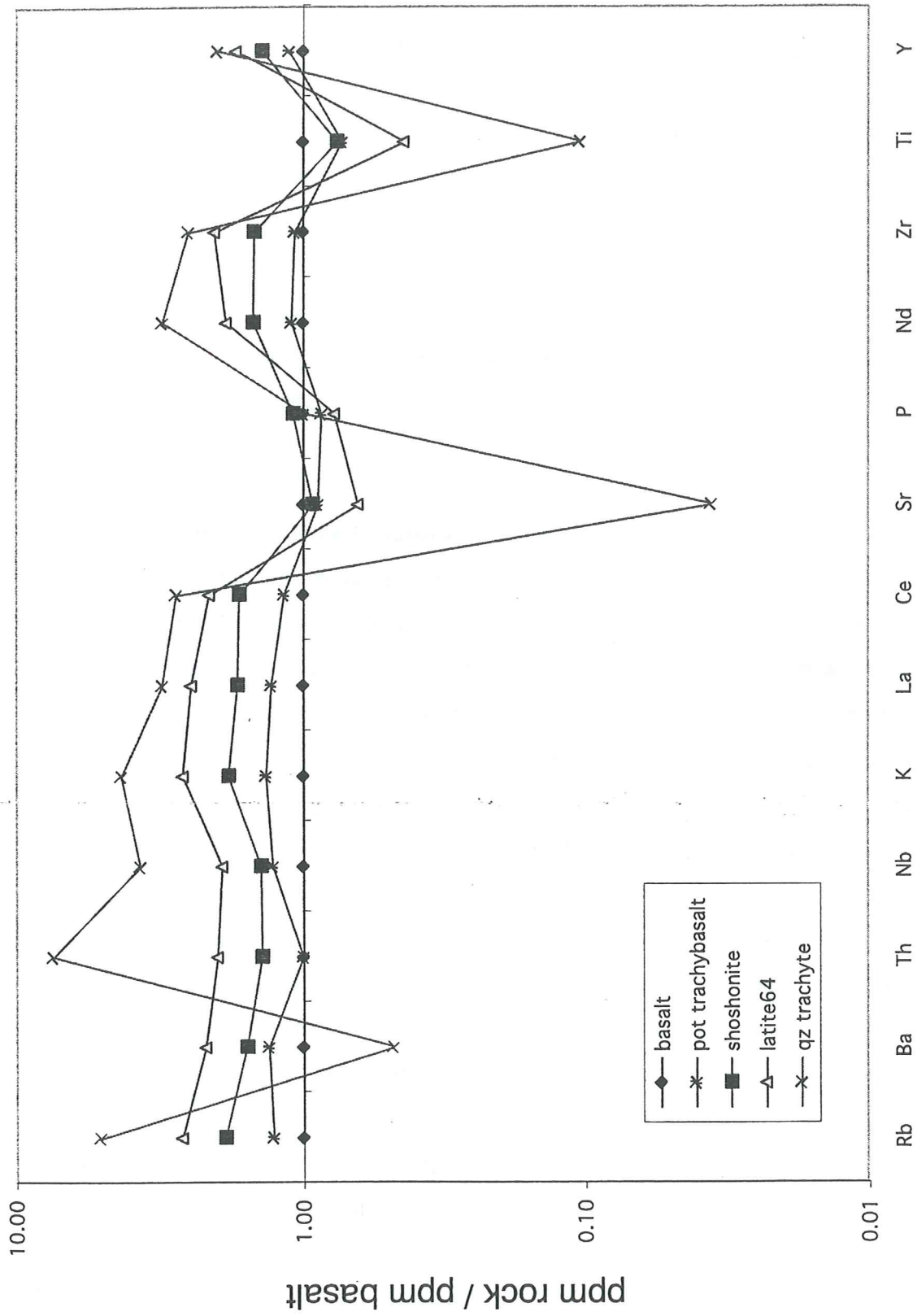


Fig. 6.8 Spidergrams normalised against least evolved member, basalt. Notice the strong depletions of Ba and Sr in the qz trachyte caused by fractionation of alkali feldspar

appearance of the spidergram indicates, as expected, a large enrichment of the incompatibles (a bit less than 100 times that of a primitive mantle) decreasing to the right in the diagram, something characterising intra plate, alkaline rocks. Figure 6.8 shows the differences between different members and the least evolved member, basalt. The most striking feature of this spidergram is the increasing Sr depletion as the magma evolves, which as mentioned above, is caused by feldspar fractionation. K shows a continuous enrichment, while Ti is being depleted throughout. The Ti behaviour is best explained by partition into mainly titanomagnetite, but also into clinopyroxene. P shows a random distribution. From basalt to qz trachyte P is displaying minor fluctuations, having approximately the same concentration throughout the series. The consistent concentration of P throughout, suggests that apatite have played a minor role during fractionation of these magmas.

6.5.2. Comparison to the undersaturated lineages

When the oversaturated lineage is compared to its ne-normative counterparts (diagrams of all trace elements are to be found in the back.) a number of trace elements (P, Sr, Ni and Cr) differ in behaviour. The most obvious is Sr which, in the ne normative lineages, shows an enrichment in rocks of mafic to intermediate compositions. Depletion is first recognizable in the benmoreites. In the oversaturated lineage, Sr is depleted throughout, which may point to differences in feldspar involvement. The most plausible explanation for this is a more intense Ca-feldspar fractionation in the mafic part of the lineage, removing Sr more readily from the melt. A lesser degree of apatite involvement, compared to the ne-normative rocks, also seems likely due to the much smaller depletion of P. Ni enrichment in more evolved rocks might indicate that magmas belonging to this assemblage are totally depleted in Mg and Fe causing disappearance of olivine as a liquidus phase, enabling Ni to become incompatible and subsequently enriched. The degree of enrichment in both Ni and in Cr might more likely be due to heterogeneities in the magma supply, most likely envisaging the magmas coming from two different magma chambers. The latite from Deborah Bay is probably derived from a different source.

Comparison of the least evolved rocks of the three different lineages is shown in Fig. 6.9a. The spidergrams for the basanite, the ne-normative basalt and the hy-normative

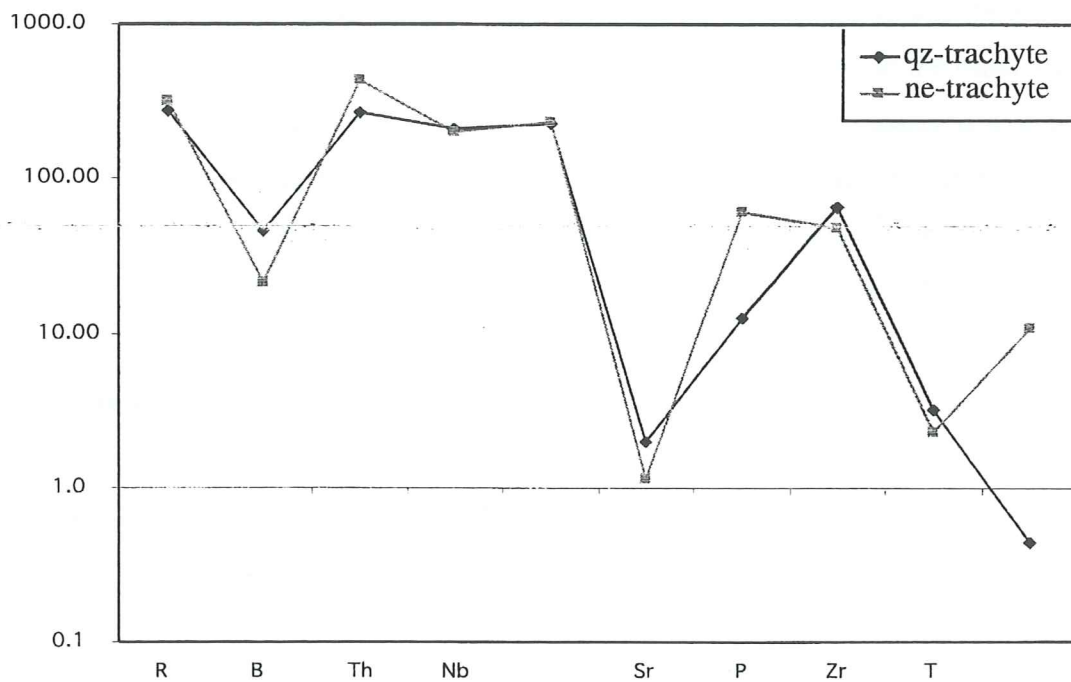
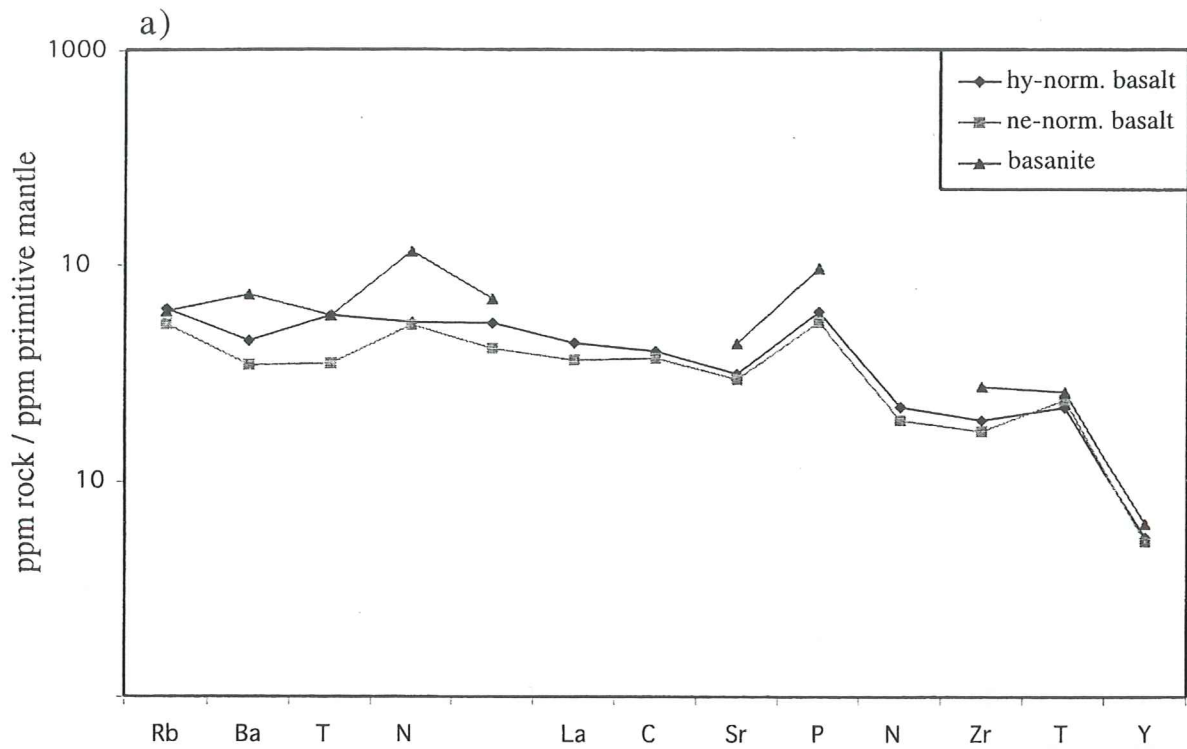


Fig. 6.9 a-b. (a) Spidergram comparing the least evolved members of the three lineages (b) spidergram comparing an oversaturated trachyte to an undersaturated trachyte.

basalt all have the same general appearance when compared to a primitive mantle. All the rocks show a P enrichment. The ne-normative basalt and the hy-normative basalt show a small Sr depletion coupled with a Rb enrichment. The REE have a ratio of 8:1 between LREE and HREE. These two features indicate fractionation prior to emplacement, even of the most mafic members. The basanite has higher REE vs. mantle/chondrite ratios, something that is generally thought to originate from higher depth of origin or lesser degree of partial melting of the strongly undersaturated rocks (Price, 1973; Hirose and Kushiro, 1993).

Figure 6.9b shows the element distribution of a feldspathoidal trachyte (OU 30408, Price 1973) and the quartz normative trachyte from Portobello Peninsula. The feldspathoidal trachyte is not analysed for La, Ce and Nd, but comparison for the other ten elements can be made. The two trachytes have very similar distribution with strong depletion in both Ba and Sr, caused by fractionation of alkali feldspar. Both rocks are depleted in Ti, something that probably is caused by fractionation of clinopyroxene (titanaugite). The undersaturated trachyte is depleted in P, indicating involvement of apatite, something lacking in the quartz normative trachyte. The Y value of the rocks are very different with the ne-normative rock having a Y concentration of 2 ppm. By looking at the other values this value seems to be way too low. Confirmation of the value and comparison with other analyses has been made in the thesis of Price (1973), and the anomalous value can only be explained by a printing error. A more appropriate value should be in the '20's, something that would make the normalized Y ratios of the two rocks close to one another.

6.6 Discussion

The presence of normative minerals indicating oversaturation in the rocks, is nothing new to the Dunedin volcanic complex. Coombs and Wilkinson (1969) mention hy normative basaltic rocks, and Price (1973) mentions the possibility of an oversaturated lineage existing within the volcano. The lava flows on the Portobello peninsula are the first example described geochemically, of a larger coherent area consisting of oversaturated volcanics, with different degrees of fractionation. As described earlier, the occurrence of oversaturated rocks is mostly confined to an area within Otago Harbour, but can also be found to the west and to the north of it. In the outermost parts of Dunedin Harbour, at

North Head, Price (1973) describes a quartz trachyte and a kaiwekite occurring in the same outcrop. The kaiwekite is thought to be the result of magma mixing between a quartz trachyte and a ne normative basalt (Coombs et al., 1968; Gurney, 1993). The quartz trachyte and the kaiwekite are separated by extensive flows of nepheline normative basalts and trachytes. The interlayering of over- and undersaturated flows suggests different magma chambers and magma characteristics. The easiest way of creating these differences is to have extrusion of magma from several vents. This is compatible with the current understandings on the volcano (Price and Coombs, 1975; Martin, 2000) and with the field mapping of the sediments on Portobello Peninsula reported in this thesis.

Coexisting undersaturated and oversaturated basalts are known from places such as the Cameroon line (Fitton, 1987), the Atlantic island of Ascension (Weaver et al., 1987) and the Cantal volcano in Massif Central, France (Wilson et al., 1995). In the latter two, both under- and oversaturated rocks have been found within the same volcano. Previously, existence of cogenetic under- and oversaturation in volcanic trends has been constrained by phase equilibria conditions (Foland et al., 1993). In classical experimental studies made by Bowen (1937), the albite-orthoclase join has acted as a thermal boundary in the petrogeny's residua system, PRS, making magmas evolve either to the granitic or the phonolitic side, but not to both. In Yoder and Tilley's (1962) basalt classification, the scheme is set up somewhat differently, but again the plane separating the oversaturated and the undersaturated volume is described as a thermal divide. In 1978, Miyashiro made another attempt to classify the alkalic basalts. In his paper he suggests that at pressures above 10 kbar, or at hydrous or oxidizing conditions possibly also at lower pressures, the olivine-plagioclase-diopside plane no longer acts as a thermal divide. This removal makes it possible for undersaturated magmas to cross into the oversaturated field, as fractionation proceeds. This hypothesis needs testing before being accepted. No evidence for this process was presented in the article (Miyashiro, 1978), only the suggestion of the process coupled with a number of places where it might have happened. More recent hypotheses on the subject suggest potential processes, that can be divided into two categories; special cases of fractionation and processes of intracrustal magma alteration, also called open system processes (Foland et al., 1993). Combinations of the two have also been suggested. Among the fractionation hypotheses, effects of volatiles, change in

water pressure and amphibole fractionation are mentioned as possible processes. In later years, however, magma-crust interaction seems to be the process that has received most attention.

The first example of open system process, which fulfills requirements from phase equilibria (Petrogeny's Residua System, Bowen (1937)), was described by Foland et al. (1993). In this model, oversaturated magma is produced by crustal contamination of an undersaturated parent magma. At pressures of 1 kbar this process must occur at temperatures over 865° C due to the division of the under- and oversaturated liquidus fields that exist at lower temperatures (the albite-orthoclase join). The degree of crustal contamination needed is dependant on factors such as initial magma composition and temperature. This process would be possible, saturating an undersaturated magma via magma-crust interactions beneath the Dunedin Volcano. As shown in fig. 5.9 the differences displayed between the sodic and potassic parts of the mildly undersaturated lineage, cannot be caused by crustal contamination. The potassic rocks are not less undersaturated than the sodic rocks of the mildly undersaturated lineage. A distinct difference can also be seen between the crustal contaminated undersaturated rocks and the saturated to oversaturated rocks (Fig. 6.9). Thus crustal contamination as a linking agent between the two lineages is considered less likely. In Massif Central, Wilson et al. (1995) argued that the differences in silica, alkali and in trace element distribution in the Cantal volcano are caused by different degree of partial melting, with the alkali basalts representing the higher degree of partial melting compared to the basanites. Their data suggest that the chemical differences observed, both in major and trace elements, are established at the earliest stages of magmatic differentiation. These two examples illustrate the wide spectrum of possible depths of origin of different lineages. Foland et al. (1993) suggest an intracrustal setting (1kbar \approx 3 km depth in continental crust), whereas Wilson et al. (1995) have an asthenospheric source of their different lineages. Subsequently, oversaturation can be explained by several processes, operating at different depths in the crust and upper mantle.

6.7 Genesis of hy-normative melts

In the Dunedin volcano the hy-normative rocks seem to be confined to the lower, early parts of the volcanic edifice. This suggests that the **oversaturated rocks were extruded early**, which would make crustal interaction between the ascending magma and the crust likely. In the underlying schist, potassium is held in the micas, whereas sodium is held in albite. When the ascending magmas come in contact with the basement schist, the micas are more easily broken down and assimilated into the magma than the feldspar. Subsequently a contaminated magma should have a higher K:Na ratio compared to an unaltered magma. Thus **the potassic nature of the oversaturated rocks supports the idea of crustal contamination** (Price, 1973). According to Hirose and Kushiro (1993) differences in silica content don't reflect differences in source composition. Elements such as Al, Ca and incompatible elements are controlled by the composition of the source. Within the Dunedin Volcano only small differences in distribution of Al_2O_3 , CaO and incompatible elements can be found. The CaO-content is somewhat lower and the enrichment of REE is higher in the strongly undersaturated lineage compared to the other two lineages. No differences in distribution of CaO, Al_2O_3 and REE can be found between the mildly undersaturated and the oversaturated lineages.

As described by Foland et al. (1993), a process involving crustal contamination of an undersaturated magma could potentially lead to oversaturation of the magma. **Intra-crystal processes as a mean of saturation of magma is considered unlikely in the Dunedin volcanic complex**, given the lack of deviation from the fractionation trend in crustally contaminated mildly undersaturated rocks (see section 5.6). The fractionation of a silica poor phase could possibly explain the differences in SiO_2 . The aluminous amphibole kaersutite has long since been considered to be a stable phase in the upper mantle (Price, 1973; Sen et al., 1996). **Removal of kaersutite would theoretically lead to increase in silica, resulting in saturation of the magma** (A. F. Cooper, pers. comm., 2001; Tiepolo et al., 2000). Kaersutite is readily recognized in the Dunedin Volcanic Complex, mostly in the strongly undersaturated rocks, in the oversaturated kaiwekite but most importantly in a qz-normative trachyandesite (latite) (Price, 1973). The rocks of Portobello Peninsula do not contain any kaersutite or even remnants of it. The lack of kaersutite can be interpreted two ways. Either it was never present during formation, or it

Strongly undersaturated
lineage

Mildly undersaturated
lineage

Oversaturated lineage

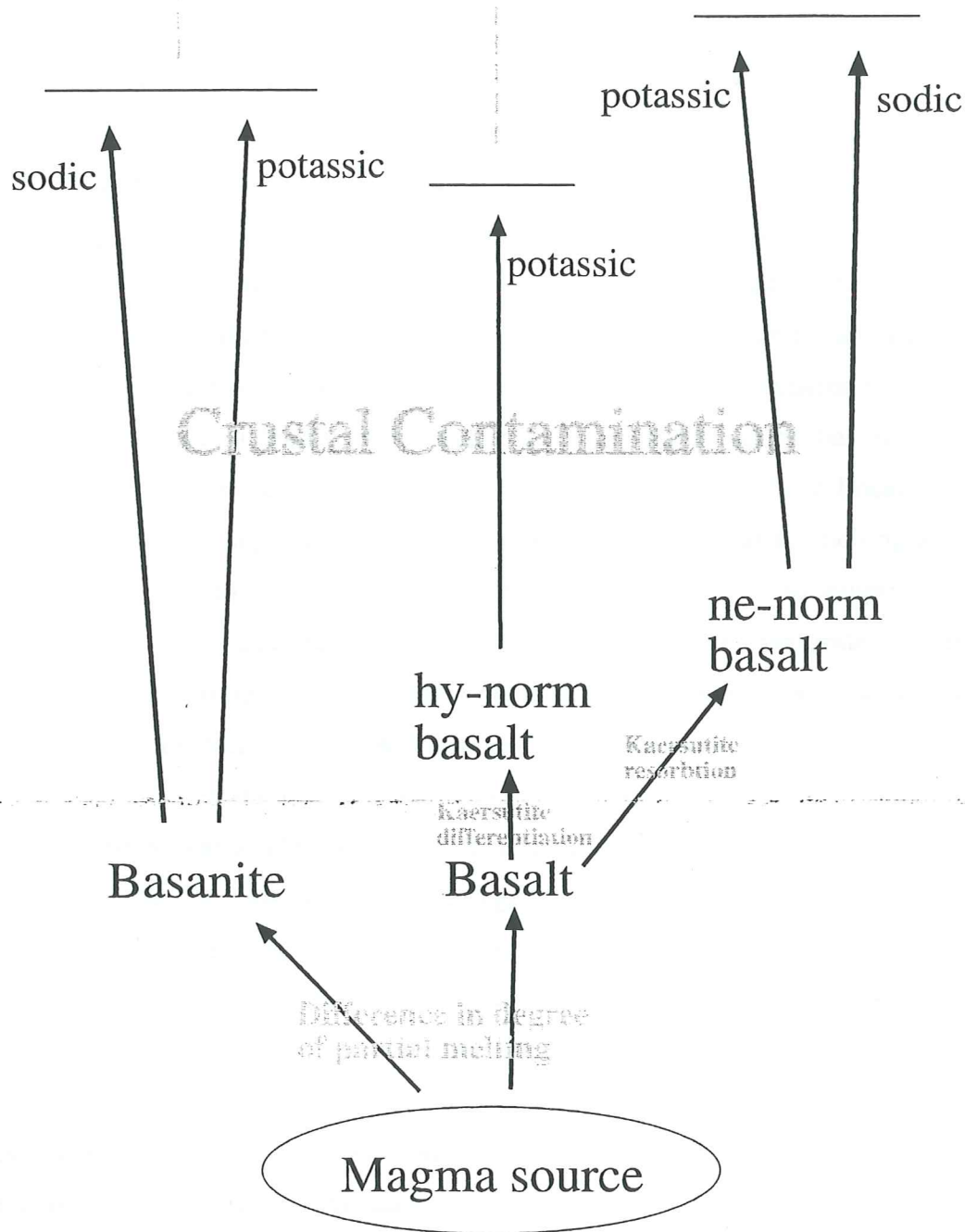


Fig. 6.10 Schematic model showing possible evolution paths of magmas in the Dunedin Volcano. Differences between and within the three lineages are explained by a combination of difference in degree of partial melting, differentiation time within lower crust/upper mantle and crustal contamination.

was present but was totally removed by fractionation. The presence of aluminous amphibole in a qz-normative latite might point to the latter interpretation. This explanation would readily explain the differences in silica compared to the undersaturated lineages.

6.8 Implications for magma generation in the Dunedin Volcano

A model involving differences in depth of origin, degree of melting and fractionation involving the amphibole kaersutite could possibly explain the large difference in volcanic products, in the Dunedin Volcano (Fig. 6.10). It has long since been known that increasing partial melting of the mantle causes changes in composition from nephelinite to basanite to alkali basalt to tholeiite (Green, 1970). The strongly undersaturated lineage shows a higher degree of enrichment in incompatible elements compared to the others, caused by derivation at greater depth and/or at lesser degrees of partial melting. No difference in REE can be detected between the mildly undersaturated lineage and the oversaturated lineage suggesting that differences in degree of partial melting are not a satisfactory explanation for this. Transport time from source to eruption is one alternative, having fractionation times decreasing from oversaturated to mildly undersaturated to strongly undersaturated magmas. Involvement of kaersutite suggests fractionation of the magma at an early stage of development. This fractionation has not occurred in the undersaturated lineages. The oversaturated rocks are early in the history of the Dunedin volcano. This means that these rocks had to 'build the road' which later magmas only had to follow. Maybe storage of the magma deep in the crust, as it ascended, would cause fractionation of kaersutite and subsequent silica saturation. This process haven't occurred in the undersaturated rocks, since they have not been stored for longer times in the lower crust. Thus kaersutite can have occurred in all of the lineages in the Dunedin volcano, but is only preserved in the strongly undersaturated ones. The kaersutite within the mildly undersaturated magmas, has not been fractionated out but has been resorbed completely as the magma has got out of the stability field of kaersutite. This is only a possible hypothesis which would need much testing of both the crystal formation, the fractionation and the importance of the time factor before accepted.

7. Conclusions

The field mapping and the following geochemical and petrographic evaluation have led to a number of conclusions regarding the lava flows on the Portobello Peninsula. Eight of the rocks from Portobello Peninsula are saturated to oversaturated, having normative hypersthene and/or normative quartz. The rocks are believed to make up a third oversaturated lineage in addition to the two preexisting, undersaturated lineages in the Dunedin Volcano (Cooms and Wilkinson, 1969). The oversaturated lineage comprises the rock series basalt-potassic trachybasalt-shoshonite-latitude-qz trachyte. The oversaturated lineage differs from the other lineage in SiO_2 content and alkali content. All but one of the oversaturated rocks studied had a potassic nature suggesting crustal contamination as the magmas ascended through the crust. The high frequency of contamination in these rocks are explained by their emplacement very early in the history of the Dunedin Volcano. Being the first magmas to ascend to higher levels in the crust they encountered meta sedimentary rock (Otago schist), from which micas could be assimilated into the magma and subsequently changing the potash:soda ratio. The oversaturation can be explained by fractionation of the amphibole kaersutite. Residence times of these magmas have been longer in the lower parts of the crust, compared to the undersaturated magmas, causing fractionation of kaersutite. The result of the kaersutite fractionation is a silica enriched and to a limited extent also alkali depleted magma.

The possible involvement of kaersutite within the oversaturated lineage would have ramifications for magma evolution of all inferred lineages in the Dunedin Volcano. If kaersutite have been present in the rocks from Portobello Peninsula, it is likely that kaersutite has been present in all the magmas of the Dunedin Volcano, early on in the magma evolution. Kaersutite is a common mineral in rocks from the strongly undersaturated lineage, and has been found in one rock from the saturated to oversaturated lineage, but has still not been found in the slightly undersaturated lineage. The presence of kaersutite within the strongly undersaturated rocks have previously been interpreted as a result of greater depth of origin compared to the other lineages (Price 1973). The behaviour of this mineral can also be explained by difference in storage times in the lower crust/upper mantle between the three different lineages, having differentiation times decreasing from oversaturated lineage through mildly undersaturated

lineage to strongly undersaturated lineage. The longer evolution times in the oversaturated and the mildly undersaturated lineages, lead to resorption of kaersutite within the magma, as the magma gets outside of the stability field of kaersutite higher up in the crust.

Two prominent dike assemblages were found on the Portobello Peninsula, one oriented NNW-SSE and one oriented NE-SW. From the crosscutting relationships a clear age difference seem to exist, the NNW-SSE assemblage being older. The different orientation of the dikes are explained by differences in the tectonic stress field. It seems as the minimum stress, σ_3 have rotated clockwise from a ENE-WSW into a SE-NW orientation in the later parts of the volcanic activity.

The gravimetric anomaly centred on Portobello Peninsula (Reilly, 1972) is not visible in the geology. The major part is made up of (light) volcanic sedimentary rocks. Most of the layers are felsic but some mafic components can also be found. The sedimentary regime in which they have been emplaced cannot be determined from the outcrops on Portobello Peninsula. However, some of the sediments may have the same genesis as the pyroclastic flow deposits mapped to the south of the field area (Martin, 2000).

7.1. Future research

The placing of Portobello Peninsula in the centre of an old eroded volcano makes it a perfect place to study dike behaviour. The peninsula belongs to the older units in the Dunedin and has subsequently been able to register later phases in the evolution of the volcano. The two dike assemblages found on the Portobello Peninsula probably represent the stress field during two of the three major basaltic phases. All around the Otago Harbour volcanic units are well exposed probably making a large area excessable to further dike studies in the very centre of a volcano. Emplacement of dikes require space, i.e. extension. By studying the dike behaviour on a larger scale within the Dunedin volcano, it could be possible to quantify a minimum of the crustal extension rate exerted by the Dunedin Volcano in the middle late Miocene, given that the life time of the volcano is reasonably well known (Marinoni, 2000). If this study is accompanied by studies of the dike behaviour of the latest volcanics, age constraints could probably also

put on the inferred rotation of the least compressive stress recorded on the Portobello Peninsula (see 4.4.2).

The anomalous geochemistry of the lava flows on Portobello Peninsula give rise to a new group of magmas. Oversaturated magmas is thought to have existed in the very start of volcanic evolution, and possibly also later on, being the first volcanic products being extruded after long periods of quiescence. Within the Dunedin volcano large parts of the initial volcanism is situated on the Otago Peninsula. Martin (2000) mapped a large number of lava flows during her study of the volcanic sediments on the Otago Peninsula. Among these lava flows is most likely that some are oversaturated. If studied geochemically, these could would be valuable to improve the understanding of the oversaturated lineage, and its relation to the undersaturated lineages within the Dunedin Volcano.

BIBLIOGRAPHY

- Adams C. J., C. A. F. 1996. K-Ar age of lamprophyre dike swarm near Wanaka, west Otago, South Island, New Zealand. *New Zealand Journal of Geology and Geophysics* **39**, 17-23.
- Adams, C. J. 1981. Migration of the late Cenozoic volcanism in the South Island of New Zealand and the Campbell Plateau. *Nature* **294**, 153-155.
- Allen, J. M. 1974. Port Chalmers Breccia and adjacent early flows of the Dunedin Volcanic Complex at Port Chalmers. *New Zealand Journal of Geology and Geophysics* **17**, 209-223.
- Benson, W. N. 1942. The basic igneous rocks of eastern Otago and their tectonic environment. *Transactions Roy. Soc. N.Z.* **72**, 85-118.
- Benson, W. N. 1968. Dunedin district. N. Z. Geological Survey Miscellaneous Series.
- Bishop D.G., L. M. G. 1976. Stratigraphy and depositional environment of the Kyeburn Formation (Cretaceous), a wedge of coarse terrestrial sediment in central Otago. *Journal of Royal Society of N.Z.* **6**, 55-71
- Blundy J. D., W. B. J. 1991. Crystal-chemical controls on the partitioning of Sr and Ba between plagioclase feldspar, silicate melts, and hydrothermal solutions. *Geochimica et Cosmochimica Acta* **55**, 193-209.
- Carter R.M., N. R. J. 1975. Cainozoic history of southern New Zealand: an accord between geological observations and plate-tectonic predictions. *Earth and Planetary Science Letters* **31**, 85-94.
- Carter, R. M. 1988. Post-breakup stratigraphy of the Kaikoura Synthem (Cretaceous-Cenozoic), continental margin, southeastern New Zealand. *New Zealand Journal of Geology and Geophysics* **31**, 405-429.
- Chen J. F., H. C. M. B., Foland K. A. 1994. Open-system, sub-volcanic magmatic evolution - constraints of the petrogenesis of the Mount Brome Alkaline Complex, Canada. *Journal of Petrology* **35**, 1127-1153.
- Coombs D. S., C. R. A., Kawachi Y., Landis C. A., McDonough W. F., Reay A. 1986. Cenozoic volcanism in north, east and central Otago. *Royal Society of N. Z. Bulletin* **23**, 278-312.
- Coombs D.S., W. J. F. G. 1969. Lineages and fractionation trends in undersaturated volcanic rocks from the Otago volcanic province (New Zealand) and related rocks. *Journal of Petrology* **10**, 440-501.

- Davidson, J. 1999. Strontium in igneous rocks.
- Emerman S. H., M. R. 1990. Why dikes? *Geology* **18**, 231-233.
- Farrar E, D. J. M. 1984. Overriding of the Indian-Antarctic Ridge: origin of Emerald Basin and migration of late Cenozoic volcanism in southern New Zealand and Campbell Plateau. *Tectonophysics* **104**, 243-256.
- Fitton, J. G. 1987. *The Cameroon line, West Africa: a comparison between oceanic and continental alkaline volcanism*. Geological Society Special Publication.
- Foland K. A., L. J. D., Henderson C. M. B, Jiangfeng C. 1993. Formation of cogenetic quartz and nepheline syenites. *Geochimica et Cosmochimica Acta* **57**, 697-704.
- Galoisy, L. 1999. Nickel. In: *Encyclopedia of Geochemistry*.
- Green, D. H. 1970. A review of experiential evidence of the origin of basaltic and nephelinitic magmas. *Physical Earth Planetary Interactions* **3**, 221-235.
- Green, T. H. 1994. Experimental studies of trace-element partitioning applicable to igneous prtogenesis - Sedona 16 years later. *Chemical Geology* **117**, 1-36.
- Guo J., G. T. H. 1989. Barium partitioning between alkali feldspar and silicate liquid at high temperature and pressure. *Contributions to Mineralogy and Petrology* **102**, 328-335.
- Gurney, P. 1993. Geochemistry of the Kaiwekite flow, East Otago, New Zealand. Unpublished B. Sc. (hons.) thesis, University of Otago.
- Hart S. R., D. T. 1993. Experimental cpx/melt partitioning of 24 trace elements. *Contributions to Mineralogy and Petrology* **113**, 1-8.
- Hill, D. P. 1977. A Model for Earthquake Swarms. *Journal of geophysical research* **82**, 1347-1352.
- Hirose K., K. I. 1993. Partial melting of dry peridotites at high-pressures - determinations of composition of melts segregated from peridotite using aggregates of diamond. *Earth and Planetary Science Letters* **114**, 477-489.
- Ilton, E. S. 1999. Chromium. In: *Encyclopedia of Geochemistry*.
- Johnson, R. W. 1989. *Intraplate volcanism in eastern Australia and New Zealand*. Cambridge University Press.
- King, P. R. 2000. Tectonic reconstructions of New Zealand: 40 Ma to the present. *New Zealand Journal of Geology and Geophysics* **43**, 611-638.

- Kogiso T., H. K., Takahashi E. 1998. Melting experiments on homogeneous mixtures of peridotite and basalt: application to the genesis of ocean island basalts. *Earth and Planetary Science Letters* **162**, 45-61.
- Le Bas M. J., L. M. R. W., Streckeisen A., Zanettin B. 1986. A Chemical Classification of Volcanic Rocks Based on the Total Alkali diagram. *Journal of Petrology* **27**, 745-750.
- Litchfield N. J., N. R. J. 2000. Holocene motion on the Akatore Fault, south Otago coast, New Zealand. *New Zealand Journal of Geology and Geophysics* **43**, 405-418.
- Marinoni, L. B. 2001. Crustal extension from exposed sheet intrusions: review and method proposal. *Journal of Volcanology and Geothermal Research* **107**, 27-46.
- Martin, U. 2000. Dunedin Volcanic Complex. Unpublished Ph. D. thesis, University of Otago.
- McDougall I., C. D. S. 1973. Potassium-Argon ages fro the Dunedin volcano and oulying volcanics. *New Zealand Journal of Geology and Geophysics* **16**, 179-188.
- McGuire W. J., P. A. D. 1989. Location and orientation of eruptive fissures and feeder dykes at Mount Etna; influence of gravitational and regional tectonic stress regimes. *Journal of Volcanology and Geothermal Research* **38**, 325-344.
- Miyashiro, A. 1978. Nature of Alkalic Volcanic Rock Series. *Contributions to Mineralogy and Petrology* **66**, 91-104.
- Mutch A.R., W. D. D. 1952. Reversal of movement of the Titri fault. *N.Z. journal of Science Technology* **33**, 398-403.
- N.L., B. 1937. Recent high-temperature research on silicates and its significance in igneous petrology. *American Journal of Science* **33**, 1-21.
- Nekvasil H., S. A., Lindsley D. H. 2000. Crystal Fractionation and the Evolution of Intra-plate *hy*-normative Igneous Suites: Insights from their Feldspars. *Journal of Petrology* **41**, 1743-1757.
- Nielsen R. L., B. J. S. 2000. Magnetite-melt HFSE partitioning. *Chemical Geology* **164**, 21-34.
- Nielsen R. L., F. L. M., Gallahan W. E., Fiske M. R. 1994. Major-element amd trace-element magnetite-melt equilibria. *Chemical Geology* **117**, 167-191.
- Norris R. J., C. R. M., Turnbull I.M. 1978. Cainozoic sedimentation in basins adject to a major continental transform boundary in southern New Zealand. *Journal of the*

Geological Society London **135**, 191-205.

- Panter K. S., K. P. R., Smellie J. L. 1997. Petrogenesis of a Phonolite-Trachyte Succession at Mount Sidley, Mary Byrd Land, Antarctica. *Journal of Petrology* **38**, 1225-1253.
- Price R. C., C. B. W. 1975. Fractional Crystallisation and the Petrology of Dunedin Volcano. *Contributions to Mineralogy and Petrology* **53**, 157-182.
- Price R. C., C. D. S. 1975. Phonolitic lava domes and other features of the Dunedin volcano, east Otago. *Journal of the Royal Society of N.Z.* **5**, 133-152.
- Price R. C., C. W. 1973. The geochemistry of the Dunedin volcano: strontium isotope chemistry. *Contributions to Mineralogy and Petrology* **42**, 55-61.
- Price R. C., T. S. R. 1980. Petrology and Geochemistry of the Banks Peninsula Volcanoes, South Island, New Zealand. *Contributions to Mineralogy and Petrology* **72**, 1-18.
- Price R.C., T. S. R. 1973. The geochemistry of the Dunedin volcano east Otago, New Zealand: rare earth elements. *Contributions to Mineralogy and Petrology* **40**, 195-205.
- Price, R. C. 1973. Geochemistry of the Dunedin Volcano. Unpublished Ph. D. thesis, University of Otago.
- Reay A., M. P. E., Gibson I. L. 1991. Lherzolite xenolith bearing flows from the east Otago province: crystal fractionation of upper mantle magmas. *New Zealand Journal of Geology and Geophysics* **34**, 317-327.
- Reilley, W. I. 1972. Gravitational expression of the Dunedin volcano. *New Zealand Journal of Geology and Geophysics* **15**, 16-21.
- Rubin, A. M. 1995. Propagation of magma filled cracks. *Annual Review of Earth Planetary Science* **23**, 287-336.
- Schroll, E. 1999. Gallium. In: *Encyclopedia of geochemistry*.
- Sen G., M. A., Srimal N. 1996. Significance of rare hydrous alkaline melts in Hawaiian xenoliths. *Contributions to Mineralogy and Petrology* **122**, 415-427.
- Shelley, D. 1987. Lyttleton 1 and Lyttleton 2, the two centres of Lyttleton Volcano. *New Zealand Journal of Geology and Geophysics* **30**, 159-168.
- Shelley, D. 1988. Radial dikes of Lyttleton Volcano - their structure, form, and petrography. *New Zealand Journal of Geology and Geophysics* **31**, 65-75.

- Sherwood, G. J. 1988. Paleomagnetism and Magnetostratigraphy of Miocene volcanics in Eastern Otago and Banks Peninsula, New Zealand. *New Zealand Journal of Geology and Geophysics* **31**, 207-224.
- Sun S-S., M. W. F. 1989. Chemical and isotopic systematics of oceanic basalts: implications for mantle composition and processes. In: *Magmatism in the Ocean Basins* (edited by Saunders A. D., N. M. J.) **42**. Geological Society of London, Special Publication, 313-345.
- Tiepolo M., V. R., Oberti R., Foley S., Bottazzi P., Zanetti A. 2000. Nb and Ta incorporation and fractionation in titanium pargasite and kaersutite: crystal-chemical constraints and implications for natural systems. *Earth and Planetary Science Letters* **176**, 185-201.
- Weaver B. L. 1991. Trace element evidence for the origin of ocean-island basalts. *Geology* **19**, 123-126.
- Weaver B. L., W. D. A., Tarney J., Joron J. L. 1987. *Geochemistry of ocean island basalts from the South Atlantic: Ascension, Bouvet, St. Helena, Gough and Tristan da Cunha*. Geological Society Special Publication.
- Wilson M., D. H., Cebria J-M. 1995. Contrasting Fractionation Trends in Coexisting Continental Alkaline Magma Series; Cantal, Massif Central, France. *Journal of Petrology* **36**, 1729-1753.
- Yoder H. S., T. C. E. 1962. Origin of Basalt magmas; an experimental study of natural and synthetic rock systems. *Journal of Petrology* **3**, 342-532.

Appendix I

TRACHYTIC DIKES			PHONOLITIC DIKES			BASALTIC DIKES		
strike	dip	direction	strike	dip	direction	strike	dip	direction
	72	73 S	332	78	78 SW	284	82	82 S
	280	83 N	76	74	74 N	80	76	76 SE
	39	82 SE	343	80	80 NE	278	82	82 N
	310	76 NE	341	82	82 NE	314	90	90
	1	86 E	10	86	86 W	301	53	53 SW
	8	77 W	58	83	83 SE	60	83	83 NW
	84	69 S	348	70	70 NE	325	69	69 SW
	300	73 S	343	72	72 NE			
	334	90	82	56	56 S			
	17	90	343	80	80 NE			
	68	65 NW	358	83	83 E			
	38	79 SE	55	78	78 SE			
	46	78 SE	348	85	85 W			
	330	77 NE	56	86	86 SE			
	4	90	77	84	84 S			
	40	78 W	21	87	87 SE			
	28	90	348	90	90			
	336	90	350	90	90			
	354	70 E	354	72	72 E			
	354	72 E	50	90	90			
	20	90	19	88	88 E			
	50	73 S	28	58	58 E			
	74	64 S	290	80	80 S			
	75	75 S	38	75	75 E			
	357	58 W	36	80	80 W			
	310	88 E	322	82	82 E			
	336	68 E	306	90	90			
	60	90						

Appendix II

Geochemical analysis of rocks from the Portobello Peninsula

1. Hatchery basalt (OU 63911) – on top of northern hill (I44,J44/269-841)
2. Portobello Potassic trachybasalt (OU 63905) – on top of southern hill (I44,J44/274-834)
3. Hatchery shoshonite (OU 63910) – on southern slope of northern hill (I44,J44/271-838)
4. Hatchery latite (OU 63902) – around the northern hill (I44,J44/269-843), sample from weathered nodule.
5. Hatchery latite (OU 63903) – around the northern hill (I44,J44/269-843), fresh sample.
6. Hatchery latite (OU 63913) – around the northern hill (I44,J44/269-839), fresh sample
7. Quartz trachyte (OU 63904) – at Quarantine Point, tip of peninsula (I44,J44/267-845)
8. Quartz trachyte (OU 63909) – dike within basalt intrusive (I44,J44/275-837)
9. ne-normative plagioclase-titanaugite-olivine basalt (OU 63906) – outcrop on southern slope of southern hill (I44,J44/277-835), sample from block.
10. ne-normative plagioclase-titanaugite-olivine basalt (OU 63907) – outcrop along shoreline, eastern part of peninsula (I44,J44/276-837)
11. ne-normative plagioclase-titanaugite-olivine basalt (OU 63908) – outcrop along shoreline, eastern part of peninsula (I44,J44/274-837)
12. ne-normative plagioclase-titanaugite-olivine basalt (OU 63912) – on the southern slopes of northern hill (I44,J44/271-837)
13. Nepheline benmoreite (“ulrichite”) (OU 63901) - 150 m north of aquarium (I44,J44/267-841)

	1	2	3	4	5	6	7	8	9	10	11	12	13
Oxide wt%													
SiO2	46.7	49.61	51.98	56.11	56.95	55.73	67.17	66.66	43.87	43.37	43.55	43.65	52.65
TiO2	2.87	2.09	2.18	1.95	1.26	1.38	0.3	0.3	3.08	3.06	3.07	3.11	0.81
Al2O3	14.77	15.9	16.32	17.88	16.5	16.43	17.48	18.21	14.32	13.96	14	14.01	19.72
Fe2O3	1.87	2.37	2.75	1.75	2.58	2.62	0.42	0.21	1.67	1.67	1.66	1.67	1.76
FeO	9.37	7.89	7.86	4.37	6.45	6.56	0.84	0.42	11.12	11.13	11.08	11.11	4.39
MnO	0.17	0.19	0.19	0.19	0.15	0.16	0	0	0.18	0.19	0.19	0.19	0.13
MgO	6.67	5.85	3.01	1.67	1.53	1.87	0.05	0.05	8.72	8.58	8.55	9.06	1.43
CaO	10.29	8.3	6.7	6.05	4.38	4.79	0.27	0.57	11.66	11.43	11.53	11.44	2.98
Na2O	2.55	3.66	4.19	4.83	4.82	4.61	5.77	6.04	2.07	2.33	2.31	1.73	6.92
K2O	1.35	1.83	2.47	3.13	3.56	3.29	5.79	6.2	1.11	0.59	0.59	1.03	4.34
P2O5	0.58	0.5	0.63	0.6	0.45	0.48	0.58	0.04	0.53	0.5	0.5	0.52	0.2
Loi	1.67	0.57	0.5	0.54	0.55	0.92	0.91	0.57	0.6	1.28	1.25	1.18	3.76
Total	98.86	98.76	98.78	99.07	99.18	98.84	99.58	99.27	98.93	98.09	98.28	98.7	99.09
CIPW norm													
Q				2.36	2.57	2.37	12.11	6.57					
C							2.62	0.62					
or	7.98	10.81	14.6	18.5	21.04	19.44	34.22	36.64	6.56	3.49	3.49	6.09	25.65
ab	21.58	30.97	35.45	40.87	40.79	39.01	48.82	51.11	11.73	14.89	15.07	13.34	32.44
an	24.87	21.55	18.43	17.86	12.87	14.42	2.45	2.57	26.5	25.89	26.09	27.42	9.93
ne									3.13	2.62	2.43	0.71	14.15
di	18.29	13.35	8.9	6.79	5.02	5.23			22.76	22.5	22.74	21.14	2.98
wo	9.35	6.83	4.47	3.44	2.47	2.59			11.64	11.5	11.63	10.83	1.48
en	5.33	3.96	2.03	1.77	0.83	0.98			6.7	6.58	6.66	6.32	0.59
fs	3.61	2.56	2.41	1.58	1.72	1.66			4.41	4.42	4.46	3.99	0.91
wo													
hy	4.34	0.74	9.44	4.52	9.17	9.92	0.82	0.23					
en	2.59	0.45	4.31	2.39	2.98	3.68	0.12	0.12					
fs	1.75	0.29	5.12	2.13	6.19	6.25	0.7	0.1					
ol	10.62	12.2	1.88		8.65				18.15	18.04	17.83	19.3	5.64
fo	6.09	7.12	0.81		6.24				10.52	10.37	10.26	11.38	2.08
fa	4.54	5.08	1.06		2.41				7.63	7.67	7.57	7.91	3.55
mt	2.71	3.44	3.99	2.54	3.74	3.8	0.61	0.3	2.42	2.42	2.41	2.42	2.55
li	5.45	3.97	4.14	3.7	2.39	2.62	0.57	0.57	5.85	5.81	5.83	5.91	1.54
ap	1.34	1.16	1.46	1.39	1.04	1.11	1.34	0.09	1.23	1.16	1.16	1.2	0.46
Total	97.19	98.19	98.28	98.53	98.63	97.92	98.67	98.7	98.33	96.81	97.03	97.52	95.33
DI	29.56	41.78	50.05	61.73	64.4	60.82	95.15	94.32	21.42	21	20.99	20.14	72.24
An#	53.54	41.03	34.21	30.41	23.98	26.99	4.78	4.79	69.32	63.49	63.39	67.27	23.44

	1	2	3	4	5	6	7	8	9	10	11	12	13
Sc	20	16	9	11	8	9	1				26	23	
V	241	158	124	99	38	52	6				297	305	
Cr	563*	183	20	14	4	10	3				226	502	
Ni	103	89	23	38	5	7	4				108	120	
Cu	73	45	32	29	19	20	2				34	50	
Zn	90	90	107	130	124	125	30				93	99	
Ca	22	22	27	31	28	28	33				21	22	
As	1	2	2	1	2	2	2						
Pb	40	51	75	80	106	78	203				22	34	
Sr	664	589	615	599	425	466	24				761	626	
Y	25	28	35	44	43	42	50				24	24	
Zr	215	230	320	407	441	425	542				189	191	
Nb	39	50	55	52	75	70	144				35	38	
Ba	313	414	494	619	689	668	150				226	242	
La	30	39	51	65	74	68	93				26	25	
Ca	71	83	119	158	152	144	197				61	66	
Nd	30	33	45	57	56	52	93				23	26	
Pb	6	7	11	16	13	17	18				4	4	
Th	5	5	7	11	10	9	37				3	3	
U	1	2	2	2	3	4	3				0.029	0.054	
	0.060	0.087	0.122	0.134	0.249	0.167	8.458						

**Geochemical analysis of oversaturated rocks from the Dunedin Volcano
(analyses taken from Price, 1973)**

1. Basalt (OU 30436) – Swampy summit, base of section (164/126-820)
2. Olivine basalt – 2,5 km south of Trig. C Swinburn S.D. (Benson, 1942) Seelye
3. Doleritic olivine basalt – 1 km west of Trig. A on Haughton Hill (Williamson, 1939) Dominion analyst
4. Doleritic olivine basalt – Trig. L. (Flat cap) Rock & Pillar S.D. (Williamson, 1939) Dominion analyst
5. Basalt (OU 30417) – Quarry in Kaikorai Valley (“Roslyn Dolerite”) (164/134-721)
6. Basalt (OU 30433) – Quarry on Green Island, Bush Road (163/ 091-662)
7. Trachyandesite (OU 00631) – Quarry on spur between Broad Bay and Macandrew Bay Seelye
8. Benmoreite (OU 30421) – Careys Bay, Otago Harbour (164/257-802)
9. Trachyandesite – Bell Hill, core-depth 250’ cr. Castle & Stuart Streets, (Benson & Turner, 1939) Seelye
10. Trachyandesite (OU 20642) – Dowling Street drill holes. Bore 4. 7’ 6’’. (164/156-714) Reay
11. Trachyandesite (OU 20642A) – segregation vein (see 30) Reay
12. Trachyte (OU 24023) – North Head training wall quarry (164/300-823)

	1	2	3	4	5	6	7	8	9	10	11	12
Oxide wt%												
SiO2	44.36	45.83	45.83	45.85	46.00	46.92	53.59	56.85	57.88	60.90	64.16	66.22
TiO2	2.52	1.62	1.58	1.94	1.93	2.65	1.43	0.93	1.55	1.51	1.07	0.41
Al2O3	14.37	14.35	13.86	13.27	13.17	15.73	16.19	16.09	18.07	18.82	17.75	18.21
Fe2O3	3.99	1.71	1.95	5.06	3.76	2.80	4.29	2.22	2.22	2.24	1.98	1.70
FeO	8.30	10.76	9.76	7.18	8.63	8.31	6.76	4.26	2.54	1.04	1.72	0.16
MnO	0.18	0.18	0.17	0.18	0.20	0.19	0.18	0.16	0.11	0.05	0.04	0.01
MgO	8.79	9.47	8.55	9.19	10.66	4.81	1.73	1.74	0.83	0.40	0.23	0.02
CaO	8.99	9.29	10.33	11.04	9.85	10.17	4.93	4.00	3.94	4.00	1.19	0.48
Na2O	2.78	2.55	2.76	2.53	2.41	3.05	5.08	5.42	5.77	5.58	5.49	6.57
K2O	1.05	0.68	0.80	0.78	0.68	1.30	2.98	4.23	3.94	3.90	4.74	5.91
P2O5	0.55	0.17	0.30	0.36	0.37	0.53	0.66	0.27	0.56	0.53	0.30	0.03
LoI	3.31	3.48	3.93	2.68	2.05	2.86	1.87	2.69	2.22	1.12	1.42	0.28
Total	99.19	100.09	99.82	100.06	99.71	99.32	99.69	99.58	99.63	100.09	100.09	100.00
CIPW norm												
Q												
C												
or	6.20	4.02	4.73	4.62	3.55	7.68	0.11	0.32	2.40	6.43	12.04	4.72
ab	23.23	21.58	23.35	21.39	20.39	25.59	17.61	25.00	0.00	0.79	2.14	0.60
an	23.79	25.70	23.07	22.56	23.35	25.51	42.99	45.86	23.38	23.05	28.01	34.92
ne							12.57	7.08	11.77	47.22	46.65	55.59
hl	0.07					0.05						1.10
dl	13.27	15.54	7.06	19.93	17.90	14.66	5.46	4.86	1.11			
wo	6.90	7.94	3.61		9.30	7.47	2.71	2.45	0.58			
en	4.65	4.53	2.08		6.26	4.12	1.06	1.23	0.43			
fs	1.72	3.07	1.37		2.34	3.07	1.69	1.18	0.10			
wo	1.25	1.58	16.19	7.34	7.79	7.19	8.41	6.09	2.02	1.00	0.57	0.05
hy	0.91	0.94	9.76		5.67	4.12	3.25	3.11	1.84			
en	0.34	0.64	6.43		2.12	3.07	5.16	2.98	0.38			
fs	16.13	22.18	11.43	8.70	14.47	4.79						
ol	11.45	12.69	6.62		10.25	2.63						
fo	4.68	9.49	4.81		4.22	2.16						
fa	5.79	2.48	2.83	7.34	5.45	4.06	6.22	4.26	3.22		2.57	
mt	4.79	3.08	3.00	3.69	3.67	5.03	2.72	1.77	2.94	2.30	2.03	0.36
ll												
ru												
hm												
ap	1.30	0.39	0.70	0.84	0.86	1.23	1.53	0.63	1.30	2.24	0.21	1.70
cc	0.25	0.09	6.32	1.77	0.30	1.30	0.39	1.84	0.98	1.23	0.70	0.07
H2O	3.03	3.44	1.06	1.90	1.90	2.16	1.71	1.87	1.79	0.98	1.42	0.11
Total	99.07	100.08	99.74	100.08	99.63	99.25	99.72	99.58	99.63	99.29	100.08	99.44
DI	29.43	25.60	28.08	26.01	23.94	33.27	60.71	71.18	74.60	76.70	86.70	95.23
An#	50.60	54.36	49.70	51.33	53.38	49.92	22.62	13.37	19.43	21.10	7.79	1.94

	1	2	3	4	5	6	7	8	9	10	11	12
Sc	180											
V	240					202		31				5.00
Cr	163					34		34				
Ni	51					34		23				
Cu	99					40		19				
Zn	19					99		91				104.00
Ga						19		27				29.00
As												
Pb	23					21		99				135.00
Sr	738					1591		221				60.00
Y	22					26		31				27.00
Zr	209					193		345				398.00
Nb	54					45		72				78.00
Ba	422					478		598				973.00
La												20.10
Ce												43.00
Nd	4					5		11				6.10
Pb	3							22				13.00
Th	1					1		6				16.00
U	0.04					0.01		0.448				4.00
Rb/Sr												2.25

Geochemical analyses of mildly undersaturated rock from the Dunedin Volcano (data taken from Price (1973) and Price and Chappel (1975))

1. Basalt (OU 30435) – Swampy Summit section (164/126-820)
2. Hawaiiite (OU 30441) – St. Clair-Black Head Road (164/105-665)
3. Mugearite (OU 30426) – Scroggs Hill (163/992-661)
4. Benmoreite (OU 30412) – Highcliff, 200m west of Cadzow Monument (164/203-701)
5. Trachyandesite (OU 20694) – Boulders and slump material at north end of Sandy Beach (164/271-869)
6. Trachyandesite (OU 30410) – Stone Hill, North Otago Harbour (164/293-833)
7. hfg hfg ???
8. Benmoreite (OU 30419) – Taylors Pt. Quarry, Otago Harbour (164/291-819)
9. Benmoreite (OU 30409) – Hare Hill (164/265-826)
10. Feltspathoidal trachyte (OU 30408) – small quarry on Purakanui – Pt. Chalmers Road (164/243-803)

	1	2	3	4	5	6	7	8	9	10
Oxide wt%										
SiO2	42.65	46.63	48.11	55.55	50.54	52.79	54.47	57.05	57.98	59.82
TiO2	2.90	2.43	2.17	0.99	1.87	1.03	0.94	0.28	0.70	0.42
Al2O3	12.78	15.46	16.07	18.15	17.90	19.59	17.93	18.80	18.20	18.01
Fe2O3	4.97	3.38	4.03	3.16	2.57	3.08	3.57	2.89	2.84	2.03
FeO	8.48	8.38	9.03	4.14	6.37	4.32	4.43	3.51	3.33	2.87
MnO	0.18	0.22	0.24	0.19	0.19	0.19	0.28	0.20	0.18	0.15
MgO	10.39	5.43	2.90	1.31	2.11	2.11	1.32	0.61	0.92	1.00
CaO	10.40	8.92	6.43	3.91	5.54	4.79	3.36	2.76	2.47	1.66
Na2O	2.65	3.85	5.18	5.98	5.00	5.89	6.11	6.91	6.08	6.64
K2O	0.92	1.81	2.05	4.06	3.24	3.50	4.14	4.42	4.68	5.70
P2O5	0.59	0.67	1.49	0.16	0.70	0.21	0.33	0.14	0.18	0.12
LoI	2.24	2.45	1.93	1.99	2.97	2.26	2.65	2.75	1.61	1.42
Total	99.15	99.63	99.63	99.59	99.00	99.76	99.53	100.32	99.17	99.84
CIPW norm										
Q										
C	5.44	10.70	12.11	23.99	19.15	20.68	24.46	26.12	27.66	33.68
or	15.27	24.25	37.11	42.54	35.60	37.10	42.67	44.87	49.34	45.82
ab	20.26	19.56	14.54	10.69	17.38	17.07	10.02	7.42	9.10	2.50
an	3.88	4.51	3.64	4.37	3.07	6.50	4.13	7.17	0.58	5.61
hi					0.23	0.16	0.31	0.08	0.23	
dl	21.92	16.59	6.38	6.37	4.46	3.69	3.33	4.36	1.60	4.07
wo	11.48	8.48	3.18	3.20	2.23	2.18	1.67	1.88	0.80	2.04
en	8.22	4.87	1.33	1.48	0.97	1.02	0.73	0.63	0.35	0.89
fs	2.23	3.24	1.86	1.69	1.26	0.79	0.93	1.65	0.45	1.14
wo										
hy										
en										
fs										
ol	16.07	10.51	10.50	2.81	7.31	5.47	4.18	2.41	2.99	2.69
fo	12.37	6.07	4.13	1.25	3.00	2.96	1.79	0.62	1.36	1.12
fa	3.69	4.44	6.37	1.56	4.31	2.51	2.49	1.79	0.93	1.57
mt	7.21	4.90	5.84	4.58	3.73	4.47	5.18	4.19	4.12	2.94
ll	5.51	4.61	4.12	1.88	3.55	1.96	1.79	0.53	1.33	0.80
ap	1.37	1.55	3.45	0.37	1.62	0.49	0.76	0.32	0.42	0.28
cc					0.07	0.30	0.18	0.05	0.02	0.02
Total	96.91	97.18	97.70	97.60	96.17	97.89	97.01	97.52	97.39	98.41
DI	24.59	39.46	52.86	70.90	57.82	64.28	71.26	78.16	77.58	85.11
An#	57.02	44.65	28.15	20.08	32.80	31.51	19.02	14.19	15.57	5.17

	1	2	3	4	5	6	7	8	9	10
Sc	235	147	37		22	16	158	1		
V	320	146				2	261			
Cr	234	69			2	2	116			
Ni	64	43	20	7	27	12	47	7	8	6
Cu	101	98	112	104	131	107	107	125	98	112
Zn	18	19	21	25	24	23	22	26	27	27
Ga										
As										
Rb	22	43	44	113	95	108	49	150	141	173
Sr	617	733	818	503	847	757	1036	221	271	42
Y	22	26	37	35	35	27	24	29	39	2
Zr	180	269	365	525	442	447	316	643	629	733
Nb	46	69	70	108	121	99	87	119	129	149
Ba	295	510	503	870	793	684	696	741	1028	316
La										
Ce										
Nd										
Pb	2	5	5	11	10	9	7	11	17	16
Th	3	6	4	16	15	17	10	22	25	23
U	1	2	2	3	4	5	3	6	5	6
Rb/Sr	0.036	0.059	0.054	0.225	0.112	0.143	0.05	0.679	0.520	4.119

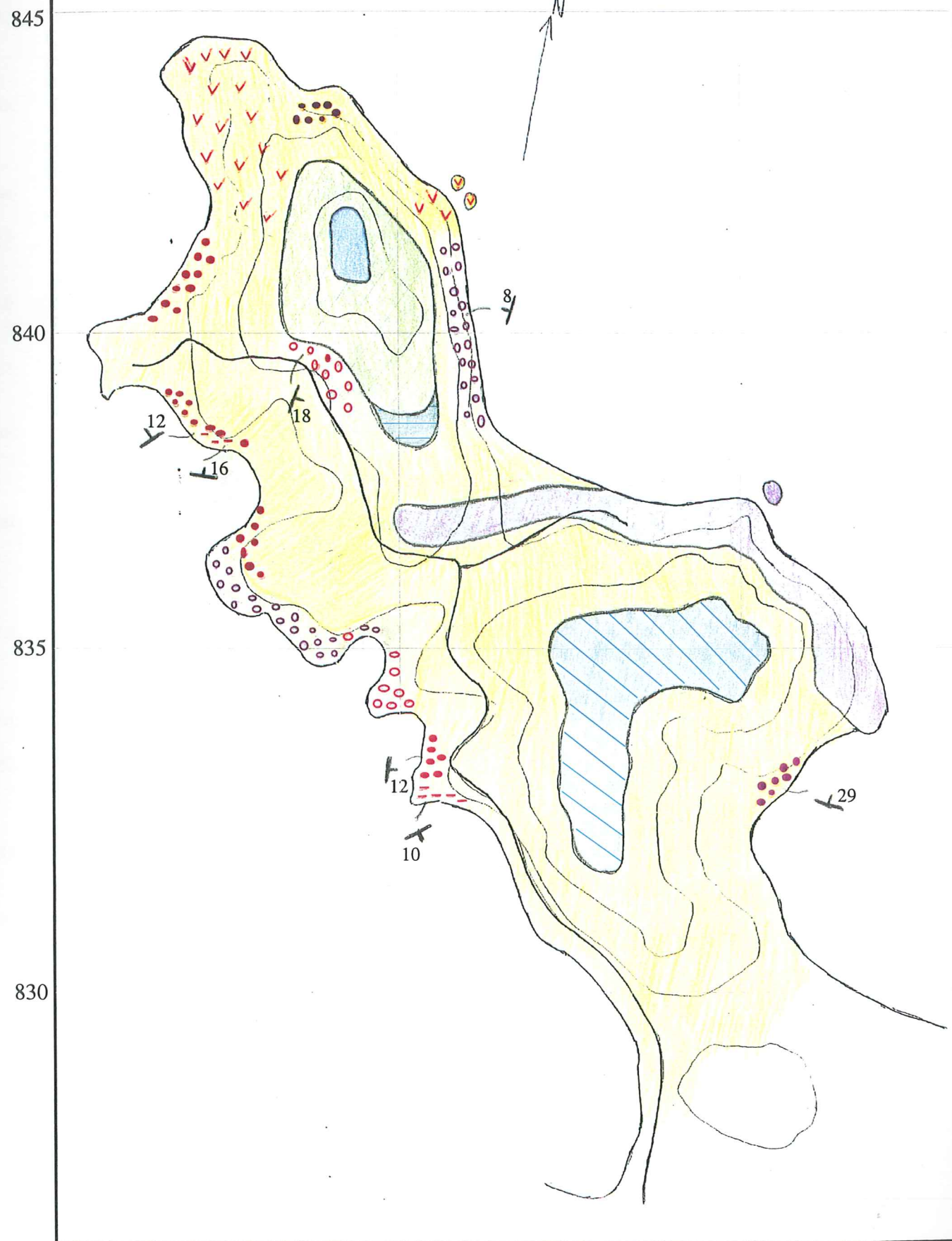
Geochemical analyses of strongly undersaturated rocks from the Dunedin Volcano (Price and Chappell, 1975)













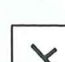
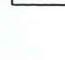
1. Basanite (OU 30442) – Quarry on Black Head (163/093-649)
2. Basanite (OU 30430) – Saddle Hill (163/031-673)
3. Nepheline hawaiiite (OU 22515) – Trench on north slopes of Jeffreys Hill (163/021-668)
4. Nepheline trachyandesite (OU 30447) – North side of Hautai Hill, Otago Peninsula (164/345-828)
5. Nepheline hawaiiite (OU 22523) – Stoney Hill (163/051-656)
6. Nepheline benmoreite (OU 22636) – Small road cut on ridge crest, S-W flank of Mt. Cargill (164/185-784)
7. Phonolite (OU 30451) – Cutting highway 1, west of Mt. Cargill (164/162-779)
8. Phonolite (OU 22639) – West end of summit ridge, Mt Cargill (164/195-789)
9. Phonolite (OU 30458) – Mt Zion quarry (164/211-791)
10. Phonolite (OU 22553) – Summit Ridge, Mt. Kettle (164/225-822)

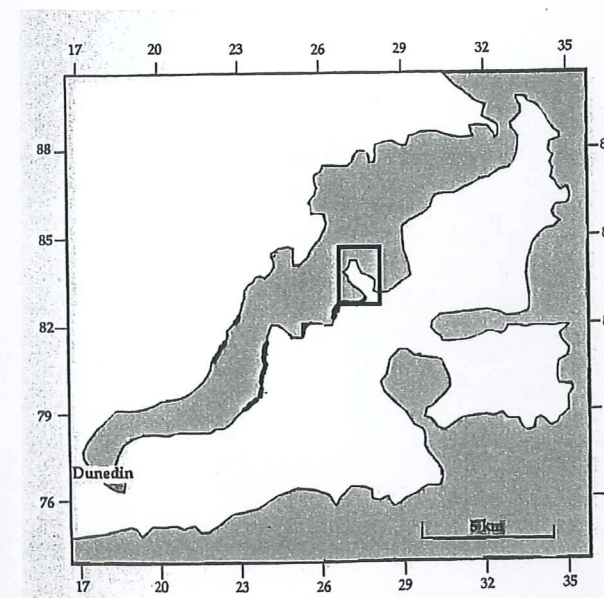
	1	2	3	4	5	6	7	8	9	10
Oxide wt%										
SiO2	42.12	42.96	45.66	46.04	46.94	49.03	52.97	55.16	56.81	58.66
TiO2	3.38	2.91	3.17	1.92	2.43	1.28	0.58	0.19	0.19	0.15
Al2O3	14.38	13.33	16.47	14.94	16.43	18.95	18.79	19.71	20.04	17.75
Fe2O3	4.44	3.08	3.72	5.49	3.33	3.34	3.46	3.83	2.86	4.25
FeO	8.71	9.36	8.96	5.88	8.35	4.34	3.36	2.03	2.29	1.67
MnO	0.22	0.22	0.21	0.21	0.21	0.18	0.20	0.22	0.17	0.20
MgO	6.71	10.60	4.12	6.82	4.33	2.36	1.57	0.40	0.22	0.14
CaO	11.10	11.56	7.84	8.12	8.96	5.60	2.96	1.38	1.28	1.18
Na2O	3.86	3.31	4.95	5.21	4.56	7.70	8.95	9.61	8.95	8.66
K2O	1.75	0.84	1.92	2.22	2.00	3.23	4.24	4.95	5.45	5.13
P2O5	0.92	0.55	0.96	0.87	0.71	0.59	0.22	0.06	0.05	0.11
LoI	1.45	1.83	1.17	1.56	1.03	2.48	2.23	2.33	1.54	1.81
Total	99.04	100.55	99.15	99.28	99.28	99.68	99.53	99.87	99.85	99.71
CIPW norm										
Q										
C	10.34	4.96	11.35	13.12	11.82	15.09	25.06	29.25	32.21	30.32
or	7.87	7.91	24.64	20.05	22.45	22.64	27.36	28.14	33.18	38.23
ab	16.74	19.03	17.05	10.82	18.45	7.60	0.00	0.00	0.00	0.00
an	13.43	10.89	9.34	13.02	8.74	22.03	24.75	24.75	21.43	13.27
hl								6.60	2.64	9.29
dl	26.05	27.93	12.81	18.87	17.56	13.39	10.91	5.51	5.22	4.48
wo	13.49	14.50	6.50	9.93	8.92	6.82	5.53	2.69	2.52	2.14
en	8.80	9.67	3.44	7.42	4.72	3.71	2.88	0.79	0.47	0.30
fs	3.76	3.75	2.86	1.52	3.92	2.86	2.50	2.02	2.24	2.03
wo										
hy										
en										
fs	8.16	16.74	9.16	8.22	8.14	2.81	1.42	0.55	0.33	0.26
fo	5.55	11.72	4.78	6.70	4.25	1.52	0.72	0.14	0.05	0.03
fa	2.62	5.01	4.38	1.51	3.89	1.29	0.69	0.40	0.28	0.23
mt	6.44	4.47	5.39	7.96	4.83	4.84	3.83	2.24	2.82	1.51
ll	6.42	5.53	6.02	3.65	4.61	2.43	1.10	0.36	0.36	0.28
hm										
ap	2.13	1.27	2.22	2.02	1.65	1.37	0.51	0.14	0.12	0.25
cc										
Total	97.59	98.72	97.98	97.72	98.25	97.20	97.30	97.54	98.31	97.90
DI	31.64	23.76	45.33	46.19	43.01	64.76	77.17	82.14	86.82	81.82
An#	68.02	70.64	40.90	35.05	45.11	25.13				

	1	2	3	4	5	6	7	8	9	10
Sc	214.00	253.00	122.00	126.00	162.00	65.00	27.00	7.00		
V	114.00	270.00	6.00	190.00	54.00	32.00	36.00	8.00		
Cr	85.00	212.00	11.00	137.00	32.00	24.00	26.00	4.00		
Ni	47.00	73.00	26.00	36.00	43.00	25.00	14.00	5.00	4.00	4.00
Cu	117.00	102.00	118.00	105.00	112.00	104.00	191.00	216.00	159.00	231.00
Zn	20.00	19.00	23.00	18.00	21.00	23.00	30.00	32.00	30.00	36.00
Ga										
As	39.00	12.00	40.00	50.00	49.00	79.00	163.00	184.00	173.00	269.00
Rb	922.00	658.00	963.00	1022.00	739.00	1507.00	563.00	227.00	30.00	9.00
Sr	29.00	25.00	29.00	28.00	29.00	27.00	37.00	40.00	38.00	66.00
Y	308.00	214.00	367.00	342.00	281.00	477.00	849.00	998.00	802.00	1175.00
Zr	83.00	67.00	77.00	88.00	75.00	75.00	137.00	149.00	181.00	262.00
Nb	512.00	388.00	500.00	727.00	588.00	1103.00	379.00	139.00	185.00	
Ba										
La										
Ce										
Nd	4.00	4.00	3.00	7.00	6.00	9.00	18.00	21.00	17.00	34.00
Pb	5.00	3.00	4.00	8.00	6.00	11.00	33.00	42.00	32.00	51.00
Th	2.00	2.00	2.00	2.00	2.00	4.00	9.00	10.00	7.00	11.00
U	0.042	0.018	0.042	0.049	0.067	0.052	0.289	0.811	5.767	29.899
Rb/Sr										

Scale 1:7000



-  Ne-norm. plag-ol-ti aug basalt
-  Portobello potassic trachybasalt
-  Hatchery basalt
-  Hatchery latite
-  Hatchery shoshonite
-  Mafic lapilli tuffs and tuff breccias containing clasts of mafic origin
-  Mafic lapilli tuffs and tuff breccias containing clasts of felsic origin
-  Undifferentiated trachytic sediments
-  Trachytic lapilli tuffs and lapilli tuff breccias with clasts of basalt
-  Trachytic lapilli tuffs and lapilli tuff breccias with clasts of trachytic material
-  Trachytic tuffs
-  Quarantine Point trachyte
-  bedding plane
-  road



Numbers on the sides of map refer to gridmap (260 & I44, J44)

Tidigare skrifter i serien "Examensarbeten i Geologi vid Lunds Universitet":

82. Meyerson, Jacob, 1997: Uppermost Lower Cambrian - Middle Cambrian stratigraphy and sedimentary petrography of the Almbacken drill-core, Scania, southern Sweden.
83. Åkesson, Mats, 1997: Moränsedimentologisk undersökning och bestämning av postglacialt bildade järn- och manganmineral i en drumlinformad rygg.
84. Ahlgren, Charlotte, 1997: Late Ordovician communities from North America.
85. Strömberg, Caroline, 1997: The conodont genus *Ctenognathodus* in the Silurian of Gotland, Sweden.
86. Borgenlöv, Camilla, 1997: Vätskeinklusioner som ledtrådar till bildningsmiljön för Bölets manganmalm, Västergötland, södra Sverige.
87. Mårtensson, Thomas, 1997: En petrografisk och geokemisk undersökning av inneslutningar i Nordingrågraniten.
88. Gunnemyr, Lisa, 1997: Spårämnesförsök i konstgjort infiltrerat vatten - en geologisk och hydrogeologisk studie av Strömsholmsåsen, Hallstahammar, Västmanland.
89. Antonsson, Christina, 1997: Inventering, hydrologisk klassificering samt bedömning av hydrogeologisk påverkan av våtmarksområden i samband med järnvägstunnelbyggnation genom Hallandsåsen, NV Skåne.
90. Nordborg, Fredrik, 1997: Granens markpåverkan - en studie av markkemi, jordmänsbildning och lermineralogi i gran- och lövskogsbestånd i södra Småland.
91. Dobos, Felicia, 1997: Pollen-stratigraphic position of the last Baltic Ice Lake drainage.
92. Nilsson, Johan, 1997: The Brennvinsfjorden Group of southern Botniahalvøya, Nordaustlandet, Svalbard - structure, stratigraphy and depositional environment.
93. Tagesson, Esbjörn, 1998: Hydrogeologisk studie av grundvattnets kloridhalter på östra Listerlandet, Blekinge.
94. Eriksson, Saskia, 1998: Morängenetiska undersökningar i klintar vid Greifswalder Boddens södra kust, NÖ Tyskland.
95. Lindgren, Johan, 1998: Early Campanian mosasaurs (Reptilia; Mosasauridae) from the Kristianstad Basin, southern Sweden.
96. Ahnesjö, Jonas, B., 1998: Lower Ordovician conodonts from Köpings klint, central Öland, and the feeding apparatuses of *Oistodus lanceolatus* Pander and *Acodus deltatus* Lindström.
97. Rehnström, Emma, 1998: Tectonic stratigraphy and structural geology of the Ålkatj-Tielma massif, northern Swedish Caledonides.
98. Modin, Anna-Karin, 1998: Distributionen av kadmium i moränmark kring St. Olof, SÖ Skåne.
99. Stockfors, Martin, 1998: High-resolution methods for study of carbonate rock: a tool for correlating the sedimentary record.
100. Zillén, Lovisa, 1998: Late Holocene dune activity at Sandhammaren, southern Sweden - chronology and the role of climate, vegetation, and human impact.
101. Bernhard, Maria, 1998: En paleoekologisk -paleohydrologisk undersökning av våtmarks-komplexet Rolands hav, Blekinge.
102. Carlemalm, Gunnar, 1999: En glacialgeologisk studie av morän och moränfyllda sprickor i underliggande sandersediment, Örsjö, Skåne.
103. Blomstrand, Malou, 1999: 1992-1998 Seismicity and Deformation at Mt. Eyjafjallajökull volcano, South Iceland.
104. Dahlqvist, Peter, 1999: A Lower Silurian (Llandoveryan) halysitid fauna from the Berge Limestone Formation, Norderön, Jämtland, central Sweden.
105. Svensson, Magnus A., 1999: Phosphatized echinoderm remains from upper Lower Ordovician strata of northern Öland, Sweden - preservation, taxonomy and evolution.
106. Bengtsson, Anders, 1999: Trilobites and bradoriid arthropods from the Middle and Upper Cambrian at Gudhem in Västergötland, Sweden.
107. Persson, Christian, 1999: Silurian graptolites from Bohemia, Czech Republic.
108. Jacobson, Mattias, 1999: Five new cephalopod species from the Silurian of Gotland.
109. Augustsson, Carita, 1999: Lapillituff som bevis för underjurassisk vulkanism av stromboli-karaktär i Skåne.
110. Jensen, Sigfinn J., 1999: En silurisk transgressiv karbonatlagerföljd vid S:t Olofsholms stenbrott, Gotland.
111. Lund, Mats G., 1999: En strukturgeologisk modell för berggrunden i Sarvesvage - Luottalako-området, Sareks Nationalpark, Lappland.
112. Magnusson, Jakob, 1999: Exploration of submarine fans along the Coffee Soil Fault in the Danish Central Graben.
113. Wickström, Jenny, 1999: Conodont biostratigraphy in Volkhovian sediments from the Mäekalda section, north-central Estonia.
114. Sjögren, Per, 1999: Utmarkens vegetationsutveckling vid Ire i Blekinge, från forntid till nutid - en pollenanalytisk studie.

115. Sälgeback, Jenny, 1999: Trace fossils from the Permian of western Dronning Maud Land, Antarctica.
116. Söderlund, Pia, 1999: Från gabbro till granat-amfibolit. En studie av metamorfos i Åkermetabasiten väster om Protoginzonen, Småland.
117. Jönsson, Karl-Magnus, 2000: Sedimentologiska och litostratigrafiska undersökningar i södra Malmös kvartära avlagringar, södra Sverige.
118. Romberg, Ewa, 2000: En sediment- och biostratigrafisk undersökning av den tidigare Littorina-lagunen vid Barsebäck, SV Skåne, med beskrivning av en Preboreal klimatoscillation.
119. Bergman, Jonas, 2000: Skogshistoria i Söderåsens nationalpark. En pollenanalytisk studie i Söderåsens nationalpark, Skåne.
120. Lindahl, Anna, 2000: En paleoekologisk och paleohydrologisk studie av fuktängar i Bräkneåns dalgång, Bräkne-Hoby, Blekinge.
121. Eneroth, Erik, 2000: En paleomagnetisk detaljstudie av Sarekgångsvärmen.
122. Terfelt, Fredrik, 2000: Upper Cambrian trilobite faunas and biostratigraphy at Kakeled on Kinnekulle, Västergötland, Sweden.
123. Sundberg, Sven Birger, 2000: Vattenrening genom komplexbildning mellan järn och humusämnen - en litteraturstudie med försök.
124. Sundberg, Sven Birger, 2000: Sedimentationsprocesser och avlagringsmiljö för en kantrygg kring platåleran vid Rydsgårds gods i backlandskapet söder om Romeleåsen, Skåne.
125. Kjällerström, Anders, 2000: En geokemisk studie av bergartsvariationen på Bullberget i västra Dalarna.
126. Cinthio, Kajsa, 2000: Senglacial och tidig-holocen etablering och expansion av lövträd på en lokal i nordvästra Rumänien.
127. Lamme, Sara, 2000: Klimat- och miljöförändringar under holocen i Sylarnaområdet, södra svenska Skanderna, baserat på analys av makrofossil och klyvöppningar.
128. Jönsson, Charlotte, 2000: Geologisk och hydrogeologisk modellering av området mellan Bjuv och Söderåsen, nordvästra Skåne.
129. Kleman, Johan, 2001: Utvärdering av den underkambriska litostratigrafin på Österlen, södra Sverige.
130. Sundler, Malin, 2001: En jämförande studie mellan uppmätt och MACRO-simulerad pesticidutlakning på ett odlingsfält i Skåne.
131. Grönholm, Anna, 2001: Högtrycksmetabasiter i den södra delen av Mylonitzonen: fältgeologi, petrografi och metamorf utveckling.
132. Ekdahl, Magnus, 2001: En studie av Källsjögranitens deformationsmönster och kinematiska indikatorer inom Ullaredszonen.
133. Axheimer, Niklas, 2001: Middle Cambrian trilobites and biostratigraphy of the Almbacken drill core, Scania, Sweden.
134. Lindén, Mattias, 2001: Proglacial deformation of glaciofluvial sediments during the Pomeranian deglaciation in the Neubrandenburg area, NE Germany.
135. Warnhag, Jon, 2001: A geochemical study of the zoned Pan-African Mon Repos intrusion, Central Namibia.
136. Lundmark, Mattias, 2001: Zirkonstudie av Norra Hortens bergarter, SV Sverige.
137. Gunnarson, Rebecka, 2001: Sedimentologisk undersökning av en moränksärning i en djupvittrad sprickdal på Romeleåsen, Skåne.
138. Karlsson, Christine, 2001: Diagenetic and petrophysical properties of deeply versus moderately buried Cambrian sandstones of the Caledonian foreland, southern Sweden.
139. Eriksson, Märten, 2001: Bedömning av förorenings spridning kring en nedlagd bensinstation i Karlaby, sydöstra Skåne.
140. Ljung, Karl, 2001: A paleoecological study of the Pleistocene-Holocene transition in the Kap Farvel area, South Greenland.
141. Åkesson, Cecilia, 2001: Undersökning av grundvattenförhållanden i området kring Östra Vemmerlöv, Simrishamns kommun, sydöstra Skåne.
142. Bermin, Jonas, 2001: Modelling Mössbauer spectra of biotite.
143. Mansurbeg, Howri, 2001: Modelling of reservoir quality in quartz-rich sandstones of the Lower Cretaceous Bentheim sandstones, Lower Saxony Basin, NW Germany.
144. Hermansson, Tobias, 2001: Sierggaväggeskollans strukturgeologiska utveckling; nyckeln till Sareks berggrundsgeologi.
145. Veres, Daniel-Stefan, 2001: A comparative study between loss on ignition and total carbon analysis on Late Glacial sediments from Atteköps mosse, southwestern Sweden, and their tentative correlation with the GRIP event stratigraphy.
146. Ahlberg, Tomas, 2001: Hydrogeologisk undersökning samt sårbarhetskartering av området kring tre bergborrade grundvattenanläggningar i Simrishamns kommun.
147. Boman, Daniel, 2001: Tektonostratigrafi och deformationsrelaterad metamorfos i norra Kebnekaisefjällen, Skandinaviska Kaledoniderna.
148. Olsson, Stefan, 2002: The geology of the Portobello Peninsula; proposal of a saturated to oversaturated lineage within the Dunedin Volcano, New Zealand.